The Dissertation Committee for Cristian Rene Carvajal certifies that this is the approved version of the following dissertation:

SEDIMENT VOLUME PARTITIONING, TOPSET PROCESSES AND CLINOFORM ARCHITECTURE –UNDERSTANDING THE ROLE OF SEDIMENT SUPPLY, SEA LEVEL AND DELTA TYPES IN SHELF MARGIN BUILDING AND DEEPWATER SAND BYPASS: THE LANCE-FOX HILLS-LEWIS SYSTEM IN S. WYOMING

Committee:

Ronald J. Steel, Supervisor

Craig S. Fulthorpe

William L. Fisher

Lesli J. Wood

David C. Mohrig

SEDIMENT VOLUME PARTITIONING, TOPSET PROCESSES AND CLINOFORM ARCHITECTURE –UNDERSTANDING THE ROLE OF SEDIMENT SUPPLY, SEA LEVEL AND DELTA TYPES IN SHELF MARGIN BUILDING AND DEEPWATER SAND BYPASS: THE LANCE-FOX HILLS-LEWIS SYSTEM IN S. WYOMING

by

Cristian Rene Carvajal, B. Sc., M. Sc.

Dissertation

Presented to the Faculty of the Graduate School of

The University of Texas at Austin

in Partial Fulfillment

of the Requirements

for the Degree of

Doctor of Philosophy

The University of Texas at Austin

May, 2007

Dedication

To my parents Carlos and Delfina

Acknowledgements

Support for this research has been provided by Devon Energy Corporation (Dale Reitz), A2D technologies (John French and Bill Ross), the Jackson School of Geosciences (Geology Foundation), the Geological Society of America, the Wyoming Geological Association and Chevron Corporation (Rebecca Latimer, Dave Mercer and Erik Davidsen). I thank Carlos Uroza and Andy Petter for assistance with well log interpretation; Jennifer Aschoff for insightful conversations regarding foreland basin tectonics and sedimentation; Rick Petters for field assistant; and Andy Petter, Carlos Uroza and Cornell Olariu for sharing their knowledge about delta and deepwater processes. I also thank the members of my dissertation committee Drs. Ron Steel, Craig Fulthorpe, William Fisher, Leslie Wood and David Mohrig for their critical review of earlier versions of this manuscript and suggestions for improvement. David Piper, Peter Burgess and William Helland-Hansen reviewed already published portions of this dissertation (mainly chapter 3). John Espy and his family, and the personnel at Black Buttes Mining Company kindly provided permission to access their properties and do outcrop field work in southern Wyoming.

Finally I am most thankful to my parents Carlos and Delfina who taught me through their example to persevere and work hard to achieve my goals in life.

SEDIMENT VOLUME PARTITIONING, TOPSET PROCESSES AND CLINOFORM ARCHITECTURE –UNDERSTANDING THE ROLE OF SEDIMENT SUPPLY, SEA LEVEL AND DELTA TYPES IN SHELF MARGIN BUILDING AND DEEPWATER SAND BYPASS: THE LANCE-FOX HILLS-LEWIS SYSTEM IN S. WYOMING

Publication No._____

Cristian Rene Carvajal, Ph.D.

The University of Texas at Austin, 2007

Supervisor: Ronald J. Steel

This research focuses on how sediment supply, sea level and delta processes control the partitioning of the sediment budget across and into the topset, slope and basin-floor compartments of deepwater basins. Addressing this problem provides significant insight to characterize source-to-sink systems, improve tectono-stratigraphic models and predict sand bypass to deepwater areas. The research was carried out in the Lance-Fox Hills-Lewis shelf margin formed during the Maastrichtian in the Washakie-Great Divide basin of southern Wyoming. I use a database with approximately 520 wells integrated with outcrops to develop a high resolution, dynamic stratigraphy approach for shelf-margin characterization.

The results emphasize the driving role of sediment supply in rapid shelf-margin building and deepwater sand emplacement. On the study margin, high sediment supply was able to outpace shelf accommodation even at times of relatively high and rising sea level. At these times, shelf margin clinoforms developed a more aggradational architecture with relatively thick and more marine influenced topsets formed in response to basin deepening due to rapid subsidence. The high supply and subsidence are interpreted to have resulted from crustal loading and significant erosion during prominent Laramide thrust-driven source uplift. The high supply caused the formation of highstand shelf-edge deltas with strong wave and river influences. These deltas resulted in extensive coastal sand belts at the shelf margin, and bypass of significant volumes of sand to deepwater areas. In contrast, during times of stable to very low rates of sea level rise, the basin developed more progradational clinoforms with more terrestrial and generally thinner topsets. More of the sediment was funneled to the basin floor and shelf-edge deltas were under strong river and tidal influence. Stable or even falling sea level resulted from decreased subsidence or slight basin uplift, interpreted to have resulted from decreasing uplift, tectonic quiescence or possibly slight tectonic rebound in the basin. The Lewis-Fox Hills margin is considered supply-dominated, a term to denote moderately deep shelf margins (< 1000 m) that prograde at high rates (several tens of km/my) and deliver sand to deepwater areas recurrently and in large volumes even at sea level highstand.

Table of Contents

List of Tables

List of Figures

CHAPTER 1: INTRODUCTION

PROBLEM AND SIGNIFICANCE

The source-to-sink problem to be addressed by this research refers to the relationship between sediment budget partitioning, shelf margin architecture and topset regime. In siliciclastic systems, sediment budget partitioning refers mainly to the relative storage of sand and mud (and to their ratio) in the topset, slope and basin-floor compartments of shelf margin clinoforms (i.e. clinoforms hundreds of meters high). Shelf margin architecture is used to characterize the aggradational and progradational geometry of the clinoforms as well as to characterize their amplitude and slope angle. Shelf regime (Swift and Thorne, 1991) refers to the combined effects that caliber and volume of sediment supply, relative sea level and wave, tidal and river currents exert on the sedimentation in the topset, especially in its marine segment or shelf. The clinoform topset also includes environments at the shoreline such as deltas, estuaries and strandplains, and the coastal and alluvial plains landward from the shoreline. Relative sea level (or simply sea level as used in the text) corresponds to the sea level position respect to a local datum which may be mobile (e.g. a datum below the sea floor) (Posamentier and Allen, 1999). Relative sea level therefore includes the changes in sea level due to eustasy and basin subsidence.

Understanding the relationships between sediment partitioning, shelf margin architecture and topset regime is important to develop better tectono-stratigraphic models and to develop a more predictive and dynamic stratigraphy. Sediment volumes are intimately related to basin tectonic setting through its influence on catchment area and

relief (Hovius, 1998; Milliman and Syvitski, 1992; Syvitski et al., 2003; Syvitski et al., 2004). Properly interpreted, therefore, volumes ought to provide insight into source-area tectonics, denudation and relief. On the marine segments of the sink, relative sea level and sediment supply will exert the main controls on the relative volumes of sediment stored on the shelf, slope and basin-floor. Therefore the sediment volumes in each of these compartments and the associated margin architecture ought to reveal the interplay between realative sea level and sediment supply. In addition, the relative interaction between waves, tides and rivers on the clinoform topset will influence the pattern of sediment dispersal and so further influence the more detailed architecture of the shelf margin stratigraphy. In ancient successions, emphasis has been placed on the importance of sea-level falls and on the importance of rivers to bypass sand to deepwater areas (Posamentier and Allen, 1999). Nonetheless, as developed in this investigation, sediment supply does play the dominant role in building the overall shelf margin and in the absolute volumes of sediment in the slope and basin floor (especially in margins with < 1000 clinoform amplitude). In addition, waves and tides will interact with rivers at the shelf edge and significantly influence the delivery of sand to deepwater. In general, therefore, sediment partitioning and its relationship to tectonics, sea level, sediment supply and basin processes, and its reflection in shelf margin architecture provide the most significant and best characterization of source-to-sink systems, and assist greatly in developing predictive stratigraphy.

The Maastrichtian Lance-Fox Hills-Lewis shelf margin in the Washakie and Great Divide basins of southern Wyoming provides an excellent opportunity to address the problem. The basin contains good exposures and an excellent subsurface database. In the

subsurface ~520 wells give a good coverage of the basin allowing a close tracking of the three-dimensional architecture of the shelf margin and its evolution through time. The logs also make possible a reasonable discrimination between sandstone and shale which along with the three dimensional coverage permit the calculation of rock volumes and their partitioning into compartments. In the basin, outcrops contain good exposures of shelf-edge deltas in which it is possible to study processes and their role in deepwater bypass. Furthermore, the sediment source is in close proximity to the 'sink' and source and sink display intimate tectono-stratigraphic relationships, decipherable with the assistance of basin architecture, processes, volumes and the history of uplift and subsidence.

OBJECTIVES

The objectives of this research are:

1. To quantify the partitioning of the preserved sediment budget into the topset, slope and basin-floor compartments of the Lance-Fox Hills-Lewis shelf margin. Such quantification ought to discriminate among the main lithologies in the margin and as far as possible ought to differentiate the regressive and transgressive volumes in the topset. In addition, such quantification has to be done at a large enough scale to adequately characterize sediment supply to the basin. The three chosen compartments together form large-scale clinoforms, the key morphologic unit that, by its lateral movement through time, infills basins.
2. To interpret how sediment supply, sea level, basin processes and tectonics contribute to produce such partitioning.

3. To characterize how partitioning and its driving variables are reflected in the shelf-margin stratigraphy, especially as it refers to shelf margin geometry, topset depositional environments, abundance and recurrence of sand delivery to deepwater areas and accretion rates.
4. To compare and contrast the Lance-Fox Hills-Lewis shelf margin pattern of sediment partitioning with other shelf margins around the world especially as regards sediment supply and accretion rate.

METHODOLOGY

The backbone of the methodology consists of the identification of regressive-transgressive cycles on the clinoform topsets and the correlation these cycles to the slope and basin floor to produce a high-resolution stratigraphic framework. The correlation is based on about 520 wells providing a good coverage of the Washakie and Great Divide basins. The stratigraphic framework is used to reproduce clinoform architecture, to map cycles from the topset to the basin floor and to track the three-dimensional variability of these cycles. This framework marks the main subdivisions of the basin stratigraphy which, in conjunction with well log normalization, permits volume calculation through Petra software. The stratigraphic framework is also integrated with outcrop study. The outcrops allow facies and architectural analysis and enable the interpretation of shelf-edge delta processes, sea level and the influence of these processes on sediment storage.

The integrated subsurface-outcrop database is then used to answer more specific problems. These problems constitute research subjects with their own methodology, results and conclusions and are presented as chapters, which provide a more detail review

of the methodology in each case. These research subjects are thematically linked to one and other, and as whole contribute to answer the larger scale problem of this investigation, and to achieve the described objectives.

OVERVIEW OF THE CHAPTERS

Chapter 2

Chapter 2 presents the results of sediment volume partitioning in the Lance-Fox Hills-Lewis shelf margin, and the interpretation of these results in terms of clinoform architecture, sea level and tectonics. As such, chapter 2 serves as an excellent description of the geologic setting. Also, chapter 2 demonstrates how sediment volumes can help to characterize variables typically unknown in ancient source-to-sink systems such as hinterland relief, river load and sediment supply rate. These variables, in turn, and the basin architecture and depositional environments lead to a tectono-stratigraphic model to describe basin stratigraphy, and its relationship to sea level, subsidence and uplift. Prior to this work, no tectono-stratigraphic model for the basin existed and the presented model represents a contribution of new ideas to the development and infilling of Laramide basins.

Chapter 3

Chapter 3 is a manuscript already published (Carvajal and Steel, 2006). It highlights some interesting and challenging elements of the Lewis-Fox Hills shelf margin stratigraphy. These elements include: 1) high abundance and recurrent presence of relatively high volumes of deepwater sandstones in each of 15 fourth- to fifth-order cycles of shelf-margin accretion (on average ~110 ky duration for each cycle), 2) the

presence of these sandstones in clinoforms that show both rising and flatter shelf-edge trajectories, and 3) the very high progradation rate of the Lewis-Fox Hills shelf margin. As developed in the chapter, these elements strongly point to a shelf margin that received very large volumes of sediment relative to its dimensions. The large supply caused abundant delivery of sand to deepwater areas at lowstand, but also during the highstand limb of 4^{th}-5^{th} order basin-infill cycles (also referred as clinothems or genetic sequences). As in Chapter 1, these ideas are new in terms of understanding the study shelf margin. More importantly however these ideas document the importance of sediment supply for shelf-margin accretion and sand bypass to deepwater areas, and call for caution in assuming that bypass to the slope and basin floor is restricted to times of low sea level only.

Chapter 4

Chapter 4 characterizes the highstand and lowstand types of deepwater delivery regarding shelf-edge delta processes and morphology, and their linked deepwater fans. Outcrops are the basis for shelf-edge delta processes characterization and subsurface data serve to map sand distribution at basin scale from the topset to the basin floor, which in turn assist in characterizing coastal morphology and deepwater fan geometry. Chapter 4 emphasizes that despite the importance of rivers in delivery of sand to deepwater areas, waves and tides are important elements of the highstand and lowstand shelf-edge coasts respectively. Waves and tides thus can complexly interact with river processes and result in understudied modes of sediment delivery to the basin floor with quite different scenarios of sediment dispersal along the shelf-edge coast.

Chapter 5

One of the main lessons that emerges from the analysis in Chapters 2 through 4 is that in the study-margin sediment supply was relatively high, and represents the principal driver for 1) rapid shelf margin accretion 2) abundant and recurrent sand delivery to slope and basin floor and 3) the potential of such delivery to take place at highstand. In addition, the volume analysis in Chapter 2 indicates that shelf-edge progradation and aggradation rates may serve as a proxy for sediment supply. In this context, Chapter 5 documents these rates for a number of selected margins around the world to investigate whether they correlate with sediment supply and with abundance/recurrence of sand delivery to deepwater areas. The results of the analysis are promising and it seems that in margins of moderate water depth (i.e. water depth < 1000m) accretion rates correlate with sediment supply and with deepwater sand abundance. This implies, in turn, that sediment supply may be the key limiting variable controlling the accretion and partitioning of sediment across these shelf margins.

CHAPTER 2: SOURCE-TO-SINK SEDIMENT VOLUMES IN A WYOMING DEEPWATER LARAMIDE BASIN: IMPLICATIONS FOR LARAMIDE RELIEF, SEDIMENT LOAD AND TECTONICS

ABSTRACT

Sediment volumes and their storage in shelf-margin compartments are used to decipher the tectonics and accretion of a Laramide source-to-sink system. Logs from some 520 wells were used to quantify volumes stored in the accreting, early Maastrichtian shelf margin in southern Wyoming during a ~1.8 my time interval. Basin development was monitored through the analysis of 15 clinothems; an approach suitable for the greenhouse, high subsidence and high sediment supply conditions under which the Washakie-Great Divide Basin filled.

Volume partitioning into topset, slope and basin-floor compartments averages 1.1:1.1:1.0 respectively. The topset is the sandiest compartment reflecting deposition from fluvial and shorelines systems. The basin floor, where sand is concentrated in submarine fans has the next largest sand volume, whereas the slope, which traps turbiditic sand in channels, tends to be mud-prone. However, the slope contains the largest volumes per compartment area reflecting its progradational nature. Topset and slope volumes combined represents at least 2 thirds of total volume, and therefore they serve as a reasonable proxy for total volume. Consequently, shelf-edge accretion rate, as an indirect measure of topset and slope volumes, may serve as a reasonable proxy for sediment supply in ancient margins where volumes are not available.

Volumes and clinothem architecture suggest a two-stage tectono-stratigraphic model for basin development and infill. During stage 1, clinothems become aggradational and thick with increasing volume and average rate of sediment supply; these clinothems

have more marine topsets and prograde into deepening basinal-waters. This indicates a high and rising rate of relative sea level interpreted to result from increasing rates of tectonic subsidence. Greater supply and subsidence in stage 1 suggest increasing thrust-driven uplift and crustal loading. In stage 2, clinothems are progradational and thinner, with decreasing volume, but high average supply rate; they developed more terrestrial topsets and prograded into a basin of relatively stable to slightly deepening water depth. This indicates lower rates of sea level rise due to lower tectonic subsidence rates, which points to diminishing thrust loading. In addition, in the stage 2 supply rates are markedly high and sea-level falls are also present suggesting continued mountain uplift and possibly basin uplift through isostatic rebounding.

Through stages 1 and 2, average source uplift rate is estimated to have been high, few mm/y. Uplift resulted in exposure and erosion of sandier rocks through time accordingly rising the sand/mud ratio in basin deposits. Average catchment is estimated at ~23,200 km^2 and from this catchment, average river load to the ocean is estimated at ~9 x 10^9 kg/y resulting in a yield of ~400 ton/km^2/y and denudation rate of 0.15 mm/y. These values suggest an average of ~1800 m for maximum hinterland relief, but at stage 1 climax, maximum relief likely was probably 2000-3000 m.

INTRODUCTION

Sediment volumes, their changing sand to mud ratio and their distribution into shelf margin compartments are the result of short- and long-term geologic processes driving source-to-sink systems. As such, these volumes provide key information that can help glean the relationships between tectonics, sea level, climate and basin processes at different time scales. Total volume of sediment is a reflection mainly of drainage area, relief, surface hydrology, bedrock lithology and climate, and so total volume quantification can assist in deciphering source tectonics and climate. In addition, the

relative storage of sediment in topset, slope and basin floor compartments is strongly influenced by the nature of the transport system, by base level behavior, and by sediment flux and therefore compartment volumes can assist on interpreting these variables in the past.

Unfortunately volume estimation and storage is a problem that has largely been ignored in basin studies probably due to the difficulty in reasonably quantifying the volumes, though there are some notable exceptions (Liu and Galloway, 1997; Cross and Lessenger, 1998). Source-to-sink systems can be of sub-continental scale such those on passive margins (e.g. those of the Amazon and Mississippi rivers) making the task of quantifying volumes monumental. In smaller basins, the database needs to provide enough coverage of the sink and a reasonable distinction between lithologies. Moreover the basin fill needs to be adequately subdivided into time slices, if possible at a high resolution, to allow detailed monitoring of basin development and infill.

In this chapter, I address the problem of quantifying sediment volumes in the topset, slope and basin floor compartments of a neritic to bathyal shelf margin. I use a data set from the Washakie and Great Divide basins in southern Wyoming. During the lower Maastrichtian, these basins formed a sediment sink in response to Laramide orogenic movements mainly in the adjacent Wind River Range, Granite Mountains and Rawlins Uplift. The results show that an evaluation of the volume partitioning of the sediment budget plus an understanding of source tectonics/lithology, and basin-fill stratigraphy provide a holistic view of this Maastrichtian source-to-sink system.

GEOLOGIC SETTING

The Wind River Range, Granite Mountains and Rawlins Uplift, and adjacent depocenters in the Washakie and Great Divide basins are major structural elements in south-central Wyoming (Figure 2.1). Thick-skin deformation from Maastrichtian times

led to the uplift of these mountains (Dickinson et al., 1988; Steidtmann and Middleton, 1991) which reach a maximum elevation of ~4180 m in the Wind River Range. Uplift and erosion have resulted in the stripping of the sedimentary cover of the mountains and exposure of a pre-Cambrian metamorphic and intrusive basement at their core. At present, the Washakie and Great Divide basins are two structural troughs separated by the Wamsutter Arch, but in the early Maastrichtian these basins acted mainly as a single depocenter. Incipient arch growth probably influenced basin deposition, but not enough to partition the basin. Basins and uplifted areas are separated by a complex arrangement of faults, the main showing evidence of thrusting along 25-30^{o} planes (Blackstone, 1991; Steidtmann and Middleton, 1991). Maastrichtian thrusting is thought to have caused significant crustal loading and downwarping of the lithosphere (Hagen et al., 1985; Flemings et al., 1986; Shuster and Steidtmann, 1988) resulting in high rates of basin subsidence as compared with pre-Maastrichtian times. As developed in following sections, this loading-driven subsidence mechanism is interpreted to have caused intimate genetic relationships between uplift and basin development/infill, to the point that basin stratigraphy seems to reveal the history of uplift. This Maastrichtian mountain-building and basin-development event marks the onset of the Laramide Orogeny -a major deformation event, which continued through the Paleocene and Eocene (Dickison et al., 1988) and resulted on a series of basement core uplifts and highly subsiding depocenters across the Rocky Mountain region in North America.

In the early Maastrichtian, high eustatic sea level due to greenhouse conditions (Miller et al., 2004) and high rates of subsidence that far outpaced sediment input in the Washakie-Great Divide area, created a marine deepwater (bathyal) basin, as had never existed during the earlier Cretaceous history of the western United States (Figure 2.2, 2.3 and 2.4). The basin was gradually infilled by a well developed series of shelf-slope

clinoforms that have un-decompated amplitudes of more than 400 m. These clinoforms infilled the basin with very high progradation rates (>47 km/my) mainly toward the south, thus revealing a northern-sourced, relative high-volume sediment supply (Carvajal and Steel, 2006, see chapter 2). The recurrent imbalance between such supply and relative sea level in the basin produced high frequency events of shoreline transgression and regression (Figure 2.5). This, in turn, resulted in the frequent positioning of the fluvio-deltaic, sediment-delivery systems at the shelf edge of the basin, and repeated bypass of sand-rich turbidity currents to the deepwater slope and basin floor, even during sea-level highstand (Carvajal and Steel, 2006).

The fluvial-to-shelf-to-deep-marine depositional system along the migrating clinoforms is lithostratigraphically divided into the Lance Formation, the Fox Hills Sandstone and the Lewis Shale (Figures 2.2 and 2.3). The proximal topset segment of successive clinoforms is represented by the Lance Formation, a coal-bearing paralic to alluvial plain succession more than 200 m thick in the Rock Spring Uplift (Steidtmann, 1993). In the distal topset segment, the more sand-prone segments of the shorelines and shelf are represented by the Fox Hills Sandstone, up to 214 m thick in southern Wyoming (although maximum thickness estimates may vary significantly according to different authors, see Gill et al., 1970; Steidtmann, 1993). The Lewis Shale represents the muddy shelf, slope and basin floor segments, but also contains abundant deepwater sandstone (informally referred as the Dad Sandstone member) in successions up to 762 meters thick (Winn et al., 1985; 1987). Each of the three stratigraphic formations thus rise diachronously southwards as the Maastrichtian basin infilled (Figures 2.2 and 2.3).

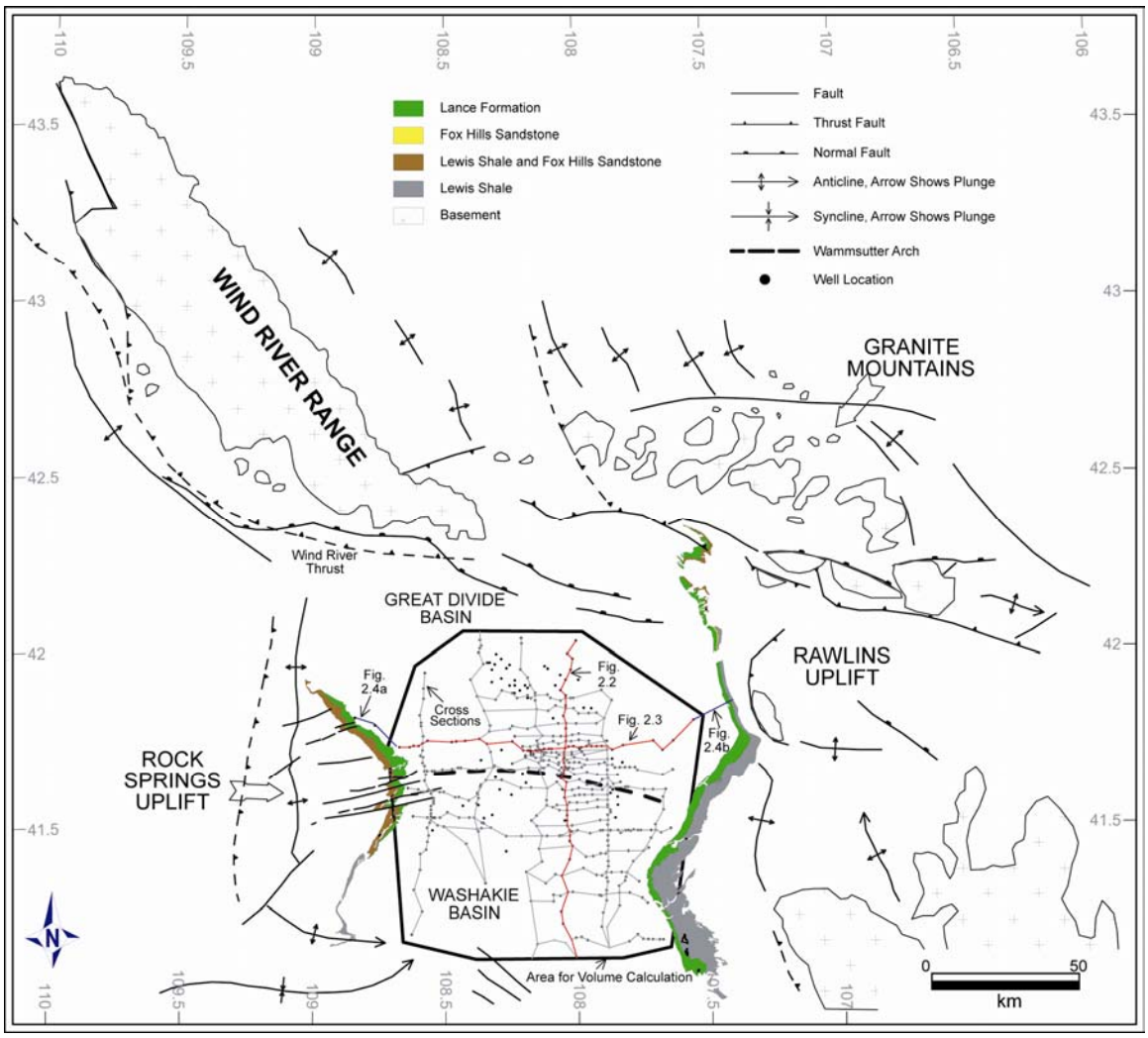

Figure 2.1: Geologic setting with map of basin and source outcrops, database, location of cross sections and Gill and Weimer outcrop logs (surface geology from Love and Christiansen, 1985; and Blackstone, 1991). Red lines mark locations of cross sections in Figures 2.2 and 2.3, and blue lines in Figure 2.4.

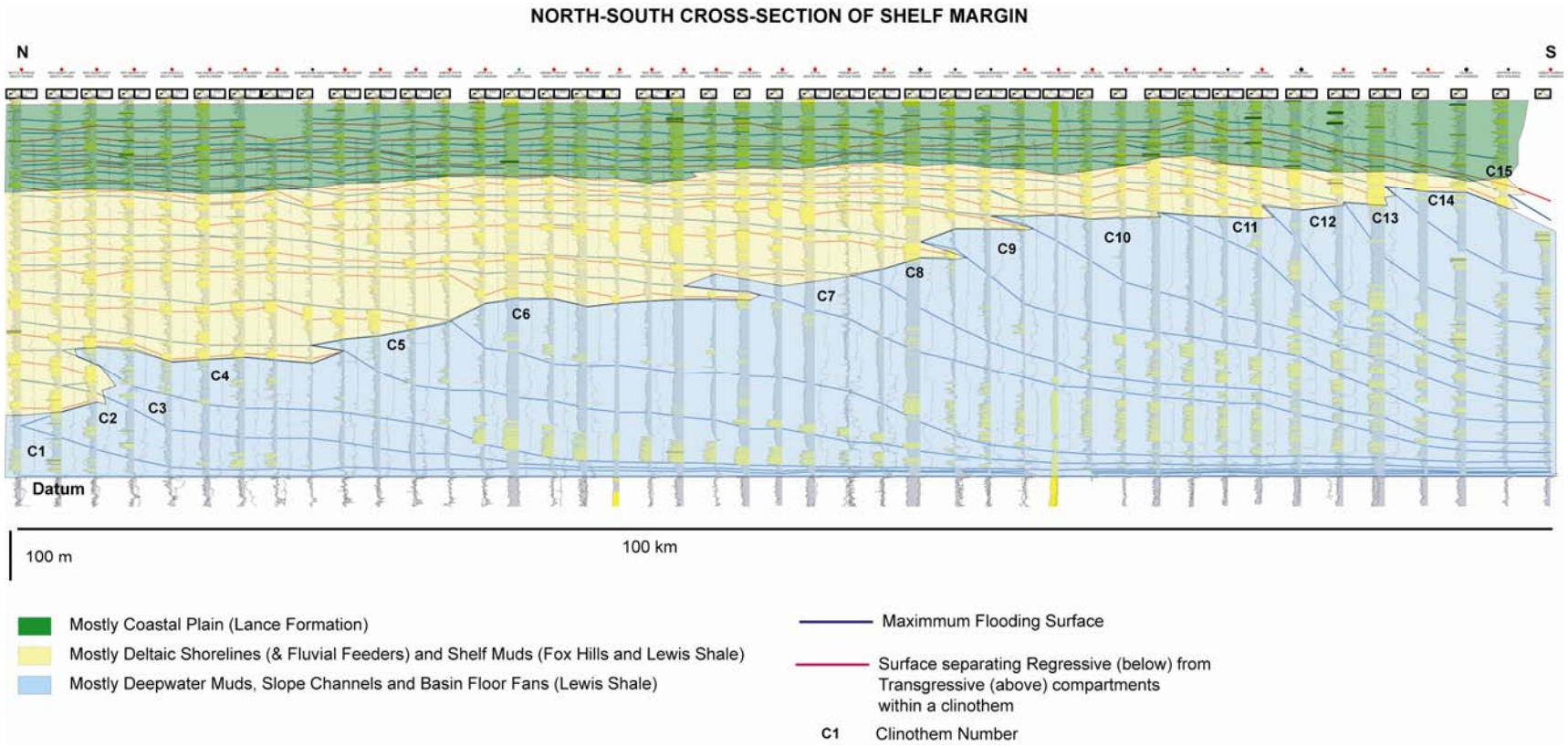

Figure 2.2: North-south cross section showing shelf margin progradation (see Figure 2.1 for location). Coloring in gamma-ray (most)/spontaneous potential logs (left track) of sandstone (yellow), shale (gray) and coal (black) is only approximate. Log in right track is conductivity (see cross section NS3 in appendix for labeling of the wells).

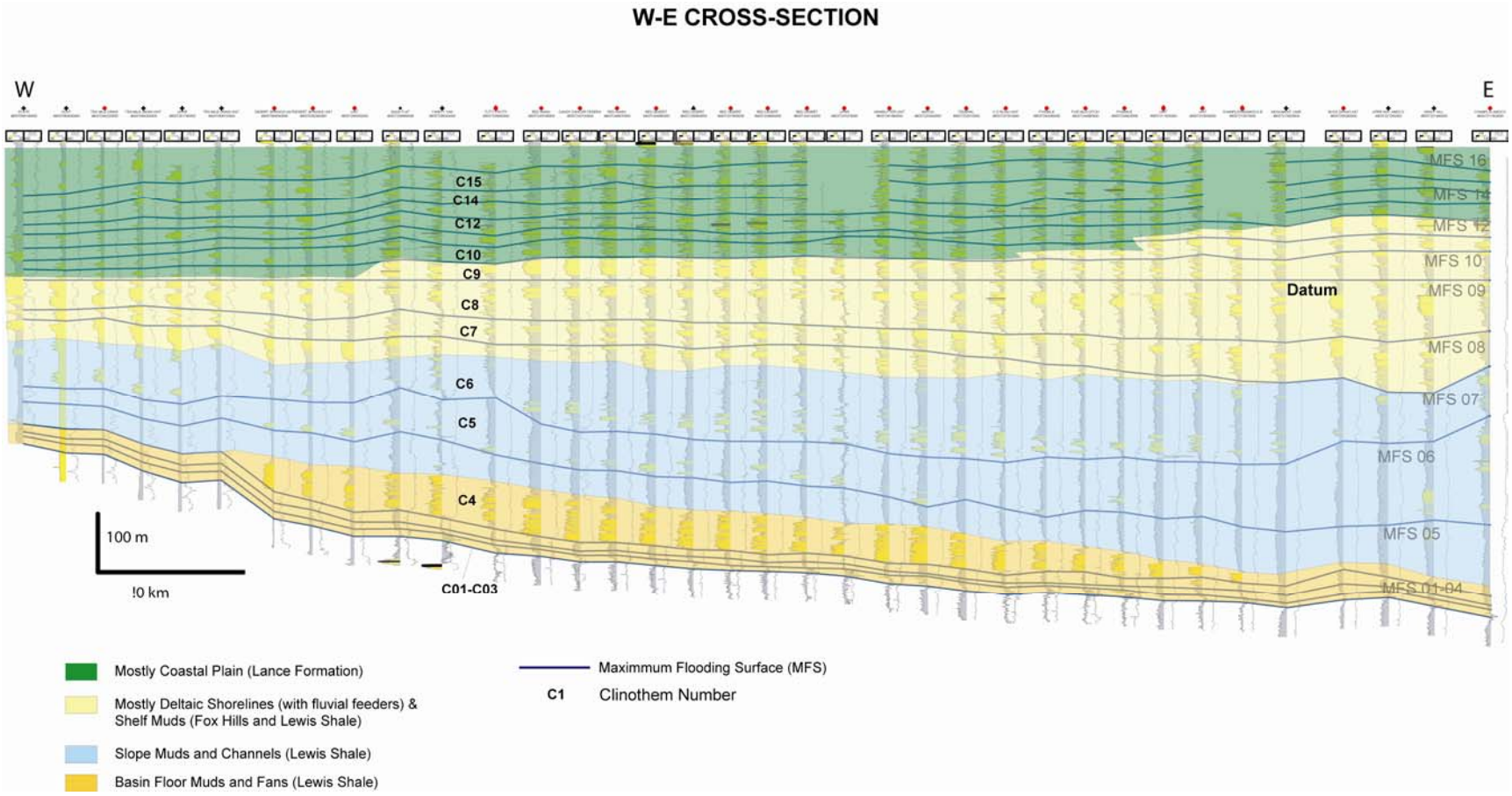

Figure 2.3: W-E cross section (see Figure 2.1 for location). This cross section is approximately perpendicular to southward direction of shelf-edge progradation. Eastward thickening reflects higher rates of subsidence in this direction (see cross section WE6 in Appendix for labeling of wells).

METHODOLOGY: DETERMINING CLINOTHEMS AND CALCULATING VOLUMES

The methodology involves three basic steps: 1) production of a reliable high-resolution stratigraphy, 2) delineation of sediment storage compartments and 3) calculation of rock and sediment volumes in compartments:

Producing a High Resolution Stratigraphy: Mapping of Clinothems

The basin-fill succession was subdivided into its component regressive-transgressive sequences because it was important to calculate compartment volumes at a high resolution. To do this I have used 16 marked intervals of shale formed during high-frequency maximum marine transgressions and so delineating maximum flooding surfaces. For the most part, the correlated surfaces and bounded lithosomes are the same as those in Carvajal and Steel (2006). These shales allowed me to correlate subsurface gamma-ray (most), conductivity and spontaneous potential (if gamma-ray is not present) curves from about ~520 wells. Correlation of the shales to the Western Interior Ammonite zones (Kauffman et al., 1993) present in outcrop sections in the basin margins (Weimer, 1961a; Gill et al., 1970) indicates that my succession encompasses approximately 1.8 my from the late stages of *B. Eliasi*, through *B. Baculus*, *B. Grandis* and *B. Clinolobatus* (Figure 2.4). In subsurface, I correlated surfaces between well logs using numerous cross sections (Figure 2.1 and see Appendix) oriented parallel (N-S) and perpendicular (W-E) to the direction of basin filling and most of them covering the entire study area. In this chapter, I present two of these cross-sections (Figures 2.2 and 2.3). Maximum flooding surface 8 (mfs 8) correlates with *B. Clinolobatus* at both basin margins, thus validating the across-basin correlation (Figure 2.4). Additional confirmation of the correlation is provided by the multiple correlation loops, close wells

spacing, and distinctive gamma-ray (low) and conductivity (high) log character of various shales. In areas of poorer well control and in the coastal plain reaches of the stratigraphy, however, correlation certainty decreases.

Within the study succession the basal shale (approximately the Asquith marker of Pyles and Slatt, 2000) is markedly radio active and clay rich (also with a high total organic carbon content (Pyles and Slatt, 2000) resulting in very high gamma-ray values. These characteristics make this shale a good stratigraphic datum for north-south cross-sections, the latter clearly showing the changing sand body characteristics along and between clinoform segments (Figures 2.2 and 2.5). *The coastal plain reaches* of any clinoform topset is defined by 'ratty', 'blocky' and 'bell-shaped' log motifs typical of a approximately flat-lying heterolithic and coaly floodplain dissected by sandy fluvial channels. *The more distal reaches of any clinoform topset* is characterized by upward-coarsening units, at times grading toward their tops to more blocky or bell-shaped log motifs, both signatures typical of prograding deltas (or strandplains) (Figure 2.5) that along feeder paths are truncated by their own fluvial distributaries. In our data set the deltas always reach the shelf-edge area of the clinoform, the staging area from which sands were fed to deepwater slope and basin floor (see Figures 2.2 and 2.5, north-south cross sections in appendix and chapter 4). *The slope reaches of clinoforms* are shale-prone, but also contain sands whose log motif is blocky to bell-shaped with occasional spikes. Discontinuous sandstones with changing thickness along both dip and strike directions of the slope suggest turbiditic sandstone deposits in slope channels (Figure 2.3). *Toward the base of slope and basin floor reaches of clinoforms*, blocky to serrate log motifs are continuous with thicknesses gradually thinning over several 10's of kms and forming broad lobes in map view (Figures 2.2 and 2.3 see also chapter 4 and

Appendix). This suggests turbidity currents whose expansion and loss of momentum causes sand and mud deposition on fans at the base of slope and on the basin floor.

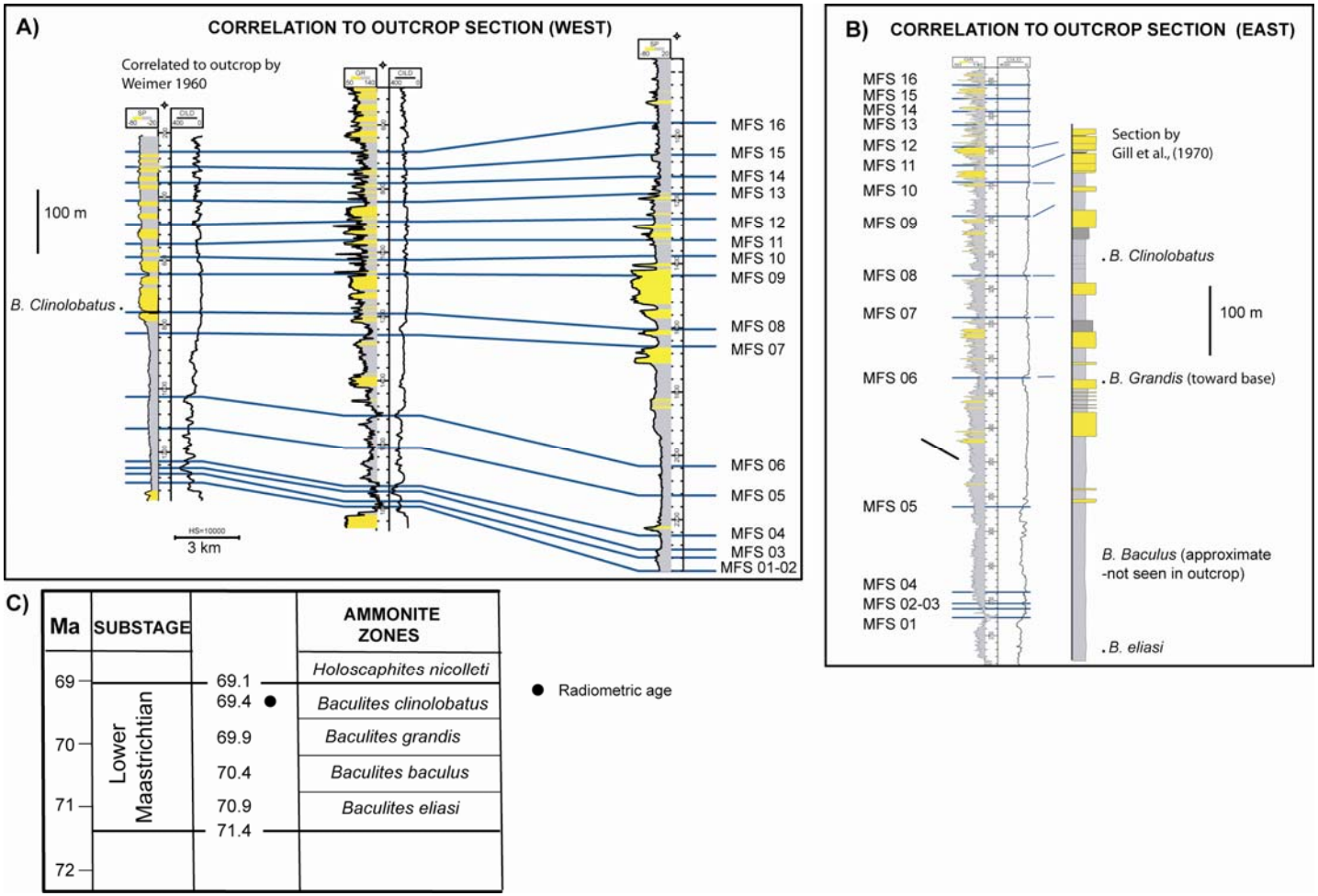

Figure 2.4: Correlation to outcrop cross sections in the west (A) and east (B) (see Figure 2.1 for location). C08 correlates in both basin margins with *B. clinolobatus*. (C) time scale with ammonite zones for Lower Maastrichtian (from Kauffman et al., 1993)

The above-outlined sandstone packages along the clinoform represent the result of deltaic shoreline regression across the pre-existing shelf platform. Upon reaching the shelf edge, the deltas fed bypassed sandy sediment to deepwater areas (Figures 2.2, 2.3 and 2.5). During the subsequent transgression sandy depocenters, commonly estuaries and barrier-lagoon systems, migrated landwards and eventually a layer of muddy shelf sediment blanketed the top of the marine clinoform. After maximum transgression, a new regressive succession developed during the ensuing shoreline progradation. These regressive-transgressive cycles, with their linked coastal plain and deepwater deposits, are the sandy lithosomes bound below and above by the thin transgressive shales; rock units I term clinothems (Rich, 1951), which also resemble the genetic sequences of Galloway (1989). As such these clinothems reflect basin-infill cycles or the main pulses of sandy sediment brought periodically into the basin and are the fundamental constructional element by which the shelf margin grows through time (Steel et al., in review) (Figures 2.2, 2.3 and 2.5).

The transgressive shales bounding the clinoform increments of sediment are ideal stratigraphic markers and an appropriate way of subdividing the stratigraphy to quantify the volume partitioning of the sediment budget. Less suitable here would be the alternative method of using surfaces generated by relative sea-level falls only (Vail et al., 1977; Vail et al., 1984; Posamentier et al., 1988; Posamentier and Vail, 1988; Van Wagoner et al., 1990; Posamentier and Allen, 1999). Carvajal and Steel (2006) and Steel et al. (in press) (see chapters 3, 4 and 5) demonstrated here that the very high sediment supply caused sand delivery to the basin floor without relative sea-level fall, in a significant number of the basin infill cycles. These cycles therefore have no through-going erosive sequence boundary. The clinothems provide a better basis for the

stratigraphic and volume partitioning analysis, because they result from the imbalance between both sediment supply and sea level, and not sea-level falls alone.

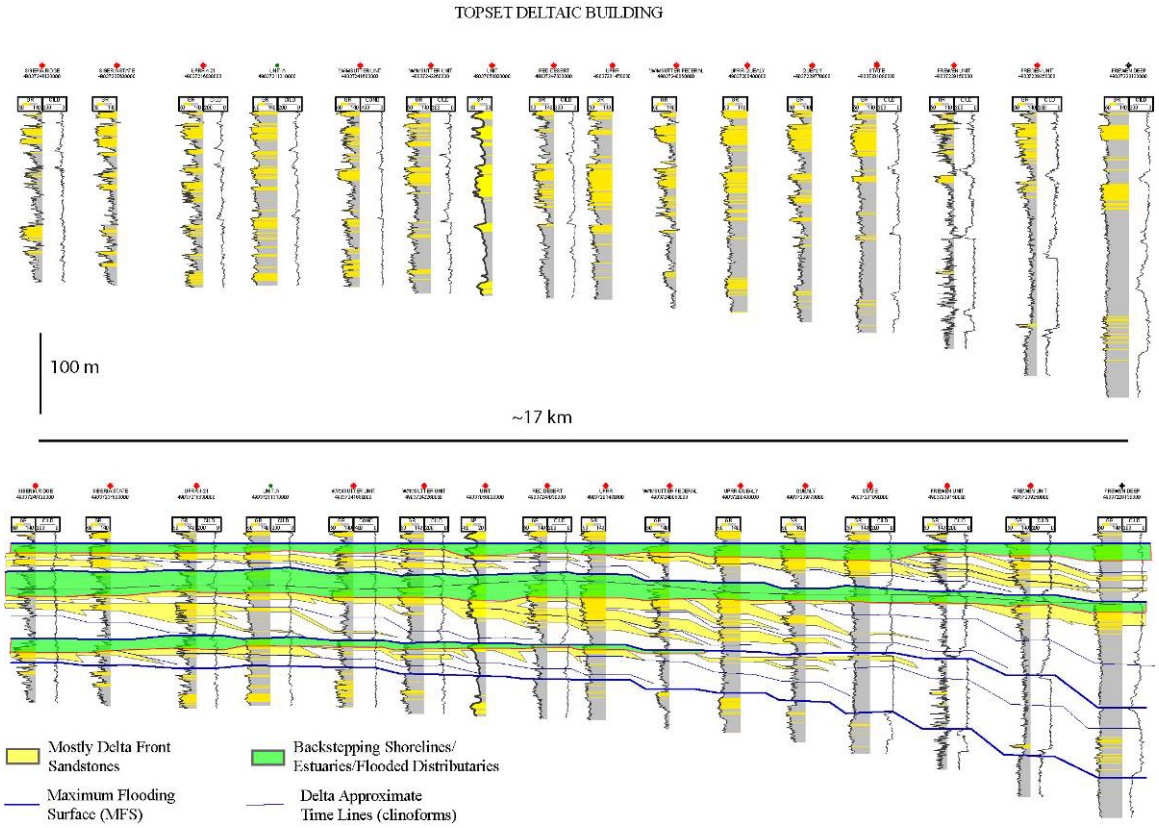

Figure 2.5: Deltaic building of the shelf. Un-interpreted (above) and interpreted (below).

Delineating Compartments

The main compartments to be delineated for sediment volume calculations are the topset, slope and basin floor segments of the clinoforms. The topsets were further divided into two additional sub-compartments. The lower topset compartment includes the lithosomes from the basal clinothem shale upward to the erosive surfaces formed during regressive shoreline transit by fluvial or distributary channels, in some instances during a relative sea-level fall (Figures 2.2 and 2.5). In areas off-axis from fluvial fairways this time surface may be reworked by tides (e.g. see chapter 4) or show minor signs of erosion (as inferred from well-log signatures). The second compartment includes the lithosomes between this erosive surface and the thin shale bounding the top of the clinothem. So defined, the lower sub-compartment includes mainly delta-front deposits, their landward equivalents and their distal-equivalent, basinward thinning prodelta and shelf muds. This topset sub-compartment is, thus mainly regressive and I term it 'regressive topset', a term without any implication for relative sea level, because a regression can occur under rising, stable or falling relative sea level. The upper sub-compartment includes the fluvial feeders of the deltas, flooded distributaries and backstepping estuaries and barrier lagoon systems. The last three systems tend to be mainly transgressive and in this sense I term this sub-compartment 'transgressive topset'. I realize, however, that included in the transgressive topset are fluvial lithosomes that may be purely regressive. This happens especially where there is shoreline progradation during rising sea level (normal regression), an scenario allowing significant fluvial and coastal-plain aggradation. Thus by the exclusion of these deposits I accept that regressive topset volume is a minimum estimate for true regressive volumes and transgressive topset volume is a maximum estimate for true transgressive volumes.

The boundary between the topset and slope compartments of clinothems was located by attempting to follow the shelf-edge trajectory (for a given clinothem), and separating sandstones of shelf-edge deltas from submarine channels/sheets below the shelf edge on the slope. The separation is not always perfect, because some delta-front sandstones may extend over the shelf edge down onto the upper slope. The error involved appears to be small, as it is restricted to the very upper slope and to a few cases. For the most part, the slope sandstone volumes represent channels throughout the slope and possibly some turbidite sheets on the upper slope. The boundary between the slope and the basin floor follows approximately the proximal pinch out of the fan and so represents the transition from slope channel to fan deposition. By doing so, we include lowermost slope aprons (proximal fan) in the basin-floor compartment of some clinothems, but I prefer this approach as the architecture, depositional processes and reservoir properties in the fans differ significantly from those in slope channels.

The boundaries between compartments for each clinothem were traced in the correlated cross sections and extended laterally with the aid of isopach maps of sandstone, shale and total thickness (see Appendix). So in map view each compartment is defined by the area of a polygon and in cross section by a thickness between the surfaces of interest.

Calculating Rock and Sediment Volumes

In each clinothem compartment, I calculated volumes for sandstone, shale and coal. Estimating these lithologies requires log normalization and cut off log values for each lithology. First, I normalized the curves according to a type gamma-ray curve (with 75 API for sandstone-shale cut off and 25 for sandstone-coal cut off) and a type spontaneous potential curve (with -10 mv for sandstone-shale cut off). Second I inspected individually each normalized curve to check that cut off values adequately separate

sandstone, shale and coal through the log, and correct these values in the necessary intervals. I identified the coals with very low gamma-ray values (<25 API), typically with a markedly spiky log response. The volume calculation is done with Petra software and involves 1) calculation of thickness for each lithology between surfaces of interest, 2) based on the log thickness, creation of a grid of thicknesses for the study area using the least square method and 3) calculation of the grid volume within the polygon of each compartment. To save computation time and polygon tracing the slope volumes were calculated by subtracting topset and basin floor volumes from total volume; and transgressive topset volumes by subtracting regressive volumes from total topset volumes.

Sandstone and shale volumes can be used to estimate original unconsolidated sediment volumes, which are useful to evaluate river load. I follow here, in a simplified version, the methodology of Liu and Galloway (1993; 1997) to estimate sediment volume through rock grain volume. This method is an alternative to decompacting stratigraphic thicknesses in each well log (which involves assumptions on original porosity of deposited sediments). The grain volume corresponds to the total rock volume minus the volumes of porosity and any externally derived cement (i.e. from outside the rock). Grain volume can be transformed to mass using a density of 2.65 g/cm^3. Our main simplification to Liu and Galloway's method is that we use average porosities for each lithology and cement. Porosity percentages provided by Hettinger and Roberts (2005) in approximately 20 sandstone reservoirs of the Lewis Shale fluctuate between 25% and 8% (most are <18%) with an average of 13.7%. Sandstones from the Lewis Shale described by Van Horn and Shannon (1989) contain cement percentages of about 23%. We do not have data on how much of this cement is externally derived and so a conservative approach, assuming that all of it is external, is taken. Regarding shales, documented

porosities vary between 3% and 18% with an average of 12.5 % (Almon et al., 2001, 2002). Average shale cement is ~6% (Bill Dawson pers. comm.) and most of it is believed to be internally derived, so we have ignored shale cements. Sediment volume estimates therefore represent averages and may underestimate sand volumes because some sandstone cement is likely to come from within the rock.

RESULTS: VOLUMES IN COMPARTMENTS AND THROUGH TIME TRENDS

Table 2.1 presents the calculated rock volumes (see also Figures 2.6 and 2.7). In the following I describe the results for relative sediment storage within the clinoform compartments, followed by a discussion of spatial and time trends of volumes during basin development.

Rock Volumes in Compartments

Sandstone Plus Shale Volume and its Relative Partitioning Ratio

The sandstone plus shale volumes range from 7 to 313 km^3 in the topset compartment of clinothems 02-15 (or C02-C15 abbreviated), 6 to 225 km^3 in the slope (C01-C15) and 72 to 240 km^3 in the basin floor (C01-C13) (Figure 2.6 B). Transformed to sediment mass, the ranges are 14-632, 13-511 and 167-508 x 10^9 ton (Table 2.1). In the regressive part of topsets, the volume range is 2-155 km^3 (C02-C15) and the transgressive topset range is 5-180 km^3 (C02-C15) with mass equivalents to 5-324 and 9-363 x 10^9 ton respectively. Coal volumes are very small (<1%) especially for C01-C09. In C10-C15, the coastal plain facies increase, as do coal volumes but they still remain very low. The main further focus is therefore on sandstone and shale volumes. One shortcoming with these ranges of values is that they are derived from clinothems with markedly different degrees of data coverage for their topsets and basin floors. In clinoforms C01-C04, significant areas of the topset (especially) and slope are not contained within the study

area, and so C01-C04 volumes are underestimated. In clinothems, C11-C15 much of the basin floor (especially) and slope areas is not present within the study area and their volumes are also underestimated (Table 2.1).

In C05-C10, which have overall more complete and comparable compartment areas (i.e. compartment area > ~1800 km^2 and area difference between compartments < 3300 km^2), sandstone plus shale volume ranges are 115-283 km^3 ($\bar{u}$ = 174 km^3, topset), 91-225 km^3 ($\bar{u}$ = 174 km^3, slope) and 99-229 km^3 ($\bar{u}$ = 162 km^3, basin floor), which are equivalent to masses of 241-577, 205-508 and 218-489 x 10^9 ton respectively. Therefore, in these clinothems, partitioning of the average rock volume ($\bar{u}$) in each compartment shows a ratio of 1.1:1.1:1.0. Consequently, it seems that provided topset, slope and basin floor are adequately represented by the well dataset, the compartments contain on average similar proportions of the total volume.

This ratio must be carefully considered, however, because it is an average ratio, and the following cases should be taken into account:

1. Clinothems with a topset area significantly larger than that of the basin floor (or vice verse) will have partitioned a greater volume or mass into the larger compartment (% < 45%, e.g. C05 and C08).
2. Some clinothems may have an architecture that departs significantly from the average. Clinothems with aggradational architectures (e.g. C07 and C08) tend to partition a larger fraction (< 45%) of the volume into the topset and a smaller fraction (e.g. 25%) to the basin floor. Clinothems with a markedly progradational style (e.g. C06) tend to partition a smaller fraction into the topset (e.g. 28%) and a larger fraction to the fan (< 36%).
3. Despite the similar volumes being partitioned, on average, into each main compartment, it is the slope that traps a larger volume per unit of area. The slope

area range is 1312-2804 km^2 (C03-C14), values usually smaller than the topset and basin floor areas, and yet the slope rock volume is comparable or larger than in the other compartments (e.g. C09-C10).

4. The ratios given here are representative of a high-supply margin (see chapters 3 and 5) that frequently partitions abundant sediment to the slope and basin floor. It remains to be seen if similar ratios occur in shelf margins with smaller supply or in those that do not develop extensive deepwater fans.

Regarding subdivision of the topsets, in C02-15 regressive volumes are < 155 km^3 ($\bar{u}$ = 77 km^3) and transgressive < 180 km^3 ($\bar{u}$ = 78 km^3). Although in any one clinothem, the two volumes tend to be different (by a variation < 60 km^3, but usually < 30 km^3) the ratio of their averages is 1.0:1.0.

Table 2.1: Clinothem (C) volumes for sandstone (ss), shale (sh) and coal (c). TOP = topset (regressive and transgressive), SL = slope and BF = basin floor.

C		A	Vss	Vss	Vsh	Vsh	Vc	Vc	TOT	TOT	Ss/Sh ratio	Ss Mass	Sh Mass	T Mass
		km^2	km^3	%	km^3	%	km^3	%	km^3	%		$x\ 10^9$ ton	$x\ 10^9$ ton	$x\ 10^9$ ton
01	**TOP**	0	0.0	0.0	0.0	0.0	0.0		0.0	0		0.0	0.0	0.0
	Top R		0.0	0.0	0.0	0.0	0.0		0.0			0.0	0.0	0.0
	Top T		0.0	0.0	0.0	0.0	0.0		0.0			0.0	0.0	0.0
	SL	71	1.3	23.7	4.8	5.0			6.1	6	0.28	2.2	11.0	13.3
	BF	8708	4.3	76.3	90.6	95.0			94.8	94	0.05	7.1	210.1	217.2
	TOT		5.6		95.4		0.0		100.9		0.06	9.4	221.1	230.5
02	**TOP**	159	2.2	8.9	4.4	3.8	0.0		6.7	5	0.50	3.7	10.3	14.0
	Top R		0.2	0.7	1.9	1.6	0.0		2.1		0.09	0.3	4.4	4.7
	Top T		2.1	8.3	2.5	2.2	0.0		4.6		0.81	3.5	5.9	9.4
	SL	403	12.1	48.4	27.5	23.5			39.7	28	0.44	20.4	63.9	84.2
	BF	8217	10.7	42.7	85.1	72.7			95.8	67	0.13	17.9	197.3	215.2
	TOT		25.0	100.0	117.1	100.0	0.0		142.1		0.21	42.1	271.4	313.5
03	**TOP**	234	5.6	33.2	5.1	3.4	0.0		10.8	6	1.10	9.4	11.9	21.3
	Top R		2.9	16.9	3.9	2.6	0.0		6.7		0.74	4.8	9.0	13.8
	Top T		2.8	16.3	1.2	0.8	0.0		4.0		2.22	4.6	2.9	7.5
	SL	1312	11.2	66.1	73.3	48.8			84.5	51	0.15	18.8	170.1	188.9
	BF	7308	0.1	0.7	71.8	47.8			71.9	43	0.00	0.2	166.4	166.6
	TOT		16.9	100.0	150.2	100.0	0.0		167.2		0.11	28.4	348.4	376.8
04	**TOP**	1688	24.8	24.7	33.2	9.6	0.4	100.0	58.4	13	0.75	41.6	77.0	118.6
	Top R		12.5	12.4	16.5	4.8	0.1	25.0	29.0		0.75	20.9	38.3	59.2
	Top T		12.3	12.3	16.7	4.8	0.3	75.0	29.3		0.74	20.7	38.8	59.5
	SL	1656	26.3	26.3	121.8	35.2			148.1	33	0.22	44.3	282.4	326.6
	BF	6888	49.1	49.0	191.2	55.2			240.3	54	0.26	82.5	443.4	525.9
	TOT		100.2	100.0	346.2	100.0	0.4	100.0	446.8		0.29	168.3	802.8	971.1
05	**TOP**	1916	39.4	54.9	75.4	20.5	0.1	100	114.8	26	0.52	66.2	174.7	240.9
	Top R		20.7	28.8	58.6	16.0	0.0	0	79.3		0.35	34.8	135.8	170.6
	Top T		18.7	26.1	16.8	4.6	0.1	100	35.6		1.11	31.4	38.9	70.4
	SL	1960	12.6	17.6	144.0	39.3			156.6	36	0.09	21.2	334.0	355.2
	BF	5131	19.7	27.5	147.4	40.2			167.2	38	0.13	33.2	341.8	375.0
	TOT		71.7	100.0	366.8	100.0	0.1	100	438.6		0.20	120.5	850.6	971.1
06	**TOP**	3008	68.0	43.7	111.7	23.4	0.2	100.0	180.0	28	0.61	114.3	259.0	373.3
	Top R		37.2	23.9	80.9	16.9	0.0	10.1	118.2		0.46	62.6	187.6	250.2
	Top T		30.8	19.8	30.8	6.4	0.2	80.5	61.7		1.00	51.7	71.4	123.1
	SL	2804	21.7	13.9	203.5	42.6			225.2	36	0.11	36.5	471.9	508.4
	BF	4059	65.9	42.3	163.0	34.1			228.9	36	0.40	110.7	378.0	488.7
	TOT		155.6	100.0	478.2	100.0	0.2	100.0	634.1		0.33	261.4	1108.9	1370.4
07	**TOP**	3394	55.6	65.6	98.4	37.9	0.3	100.0	154.3	45	0.57	93.5	228.2	321.7
	Top R		24.6	29.0	56.1	21.6	0.0	11.4	80.8		0.44	41.4	130.1	171.5
	Top T		31.0	36.5	42.3	16.3	0.3	87.9	73.6		0.73	52.1	98.1	150.2

C		A	Vss	Vss	Vsh	Vsh	Vc	Vc	TOT	TOT	Ss/Sh ratio	Ss Mass	Sh Mass	T Mass
		km^2	km^3	%	km^3	%	km^3	%	km^3	%		$x\ 10^9$ ton	$x\ 10^9$ ton	$x\ 10^9$ ton
	SL	2125	10.4	12.3	80.8	31.1			91.3	26	0.13	17.5	187.4	204.9
	BF	3645	18.8	22.2	80.5	31.0			99.3	29	0.23	31.6	186.8	218.3
	TOT		84.8	100.0	259.8	100.0	0.3	100.0	344.9		0.33	142.5	602.4	744.9
08	**TOP**	4170	116.0	64.6	164.9	36.8	2.3	100.0	283.3	45	0.70	195.0	382.5	577.4
	Top R		54.0	30.1	100.5	22.4	0.1	5.9	154.6		0.54	90.7	233.0	323.7
	Top T		62.1	34.5	64.5	14.4	2.1	92.4	128.7		0.96	104.3	149.5	253.8
	SL	2384	24.4	13.6	166.5	37.1			190.9	30	0.15	40.9	386.1	427.0
	BF	3000	39.3	21.9	117.0	26.1			156.2	25	0.34	66.0	271.2	337.2
	TOT		179.7	100.0	448.4	100.0	2.3	100.0	630.4		0.40	301.9	1039.8	1341.6
09	**TOP**	4538	61.4	46.6	92.4	23.2	1.5	100.0	155.4	29	0.66	103.2	214.3	317.6
	Top R		26.1	19.8	57.9	14.5	0.5	30.1	84.4		0.45	43.8	134.2	178.1
	Top T		35.3	26.8	34.5	8.7	1.0	67.3	70.9		1.02	59.4	80.1	139.5
	SL	2089	22.1	16.8	180.1	45.2			202.2	38	0.12	37.1	417.7	454.8
	BF	2519	48.2	36.6	126.1	31.6			174.3	33	0.38	81.0	292.4	373.3
	TOT		131.7	100.0	398.7	100.0	1.5	100.0	531.9		0.33	221.3	924.4	1145.7
10	**TOP**	5304	61.9	44.7	90.9	28.4	1.8	100.0	154.6	34	0.68	104.1	210.7	314.8
	Top R		21.0	15.1	47.7	14.9	0.1	7.1	68.8		0.44	35.2	110.6	145.8
	Top T		41.0	29.6	43.2	13.5	1.6	86.8	85.7		0.95	68.8	100.1	169.0
	SL	2246	24.0	17.3	134.1	41.9			158.0	34	0.18	40.3	310.9	351.2
	BF	1995	52.6	38.0	95.2	29.7			147.7	32	0.55	88.3	220.6	309.0
	TOT		138.5	100.0	320.1	100.0	1.8	100.0	460.4		0.43	232.7	742.2	974.9
11	**TOP**	5690	64.9	59.1	77.6	33.1	1.9	100.0	144.4	42	0.84	109.1	179.9	289.0
	Top R		23.9	21.8	39.0	16.6	0.3	18.4	63.3		0.61	40.1	90.5	130.6
	Top T		41.0	37.4	38.6	16.4	1.5	81.1	81.1		1.06	69.0	89.4	158.4
	SL	2143	29.0	26.4	119.8	51.1			148.8	43	0.24	48.8	277.7	326.5
	BF	1331	15.8	14.4	37.2	15.9			53.0	15	0.43	26.6	86.3	112.9
	TOT		109.8	100.0	234.6	100.0	1.9	100.0	346.3		0.47	184.5	543.9	728.4
12	**TOP**	6558	61.5	45.5	96.0	37.6	1.1	100.0	158.6	41	0.64	103.3	222.6	325.9
	Top R		19.1	14.1	43.2	16.9	0.1	5.9	62.3		0.44	32.0	100.2	132.2
	Top T		42.4	31.4	52.8	20.7	1.0	90.1	96.3		0.80	71.3	122.4	193.7
	SL	1959	28.4	21.0	96.6	37.9			125.0	32	0.29	47.7	223.9	271.6
	BF	1130	45.3	33.5	62.5	24.5			107.8	28	0.73	76.1	144.9	221.1
	TOT		135.2	100.0	255.1	100.0	1.1	100.0	391.4		0.53	227.2	591.4	818.6
13	**TOP**	7467	83.0	73.4	112.7	43.9	2.5	100.0	198.2	53	0.74	139.5	261.2	400.7
	Top R		38.3	33.8	61.7	24.0	0.3	24.0	100.3		0.62	64.3	143.1	207.4
	Top T		44.8	39.6	50.9	19.8	1.9	74.8	97.6		0.88	75.2	118.1	193.3
	SL	1821	23.0	20.3	120.6	47.0			143.6	39	0.19	38.7	279.6	318.3
	BF	399	7.1	6.3	23.5	9.2			30.7	8	0.30	12.0	54.5	66.5
	TOT		113.2	100.0	256.7	100.0	2.5	100.0	372.5		0.44	190.2	595.3	785.5
14	**TOP**	8177	100.9	91.3	131.3	58.1	2.9	100.0	235.1	69	0.77	169.5	304.5	474.0
	Top R		37.2	33.7	58.2	25.8	0.6	20.6	96.0		0.64	62.5	135.0	197.4
	Top T		63.7	57.7	73.1	32.4	2.3	78.6	139.1		0.87	107.0	169.6	276.6

C		A	Vss	Vss	Vsh	Vsh	Vc	Vc	TOT	TOT	Ss/Sh ratio	Ss Mass	Sh Mass	T Mass
		km^2	km^3	%	km^3	%	km^3	%	km^3	%		$x\ 10^9$ ton	$x\ 10^9$ ton	$x\ 10^9$ ton
	SL	1312	9.6	8.7	94.7	41.9			104.2	31	0.10	16.1	219.5	235.6
	BF	0	0.0	0.0	0.0	0.0			0.0	0		0.0	0.0	0.0
	TOT		110.4	100.0	226.0	100.0	2.9	100.0	339.3		0.49	185.5	524.0	709.6
15	**TOP**	8779	128.4	100.0	179.5	100.0	5.3	100.0	313.3	100	0.72	215.8	416.2	632.0
	Top R		45.0	35.0	83.2	46.4	2.1	39.3	129.2		0.54	75.5	193.0	268.6
	Top T		83.5	65.0	96.3	53.6	3.2	59.7	182.9		0.87	140.2	223.2	363.4
	SL	601	0.0	0.0	0.0	0.0			0.0	0	1.86	0.0	0.0	0.0
	BF	0	0.0	0.0	0.0	0.0			0.0	0		0.0	0.0	0.0
	TOT		128.4	100.0	179.5	100.0	5.3	100.0	313.3		0.72	215.8	416.2	632.0

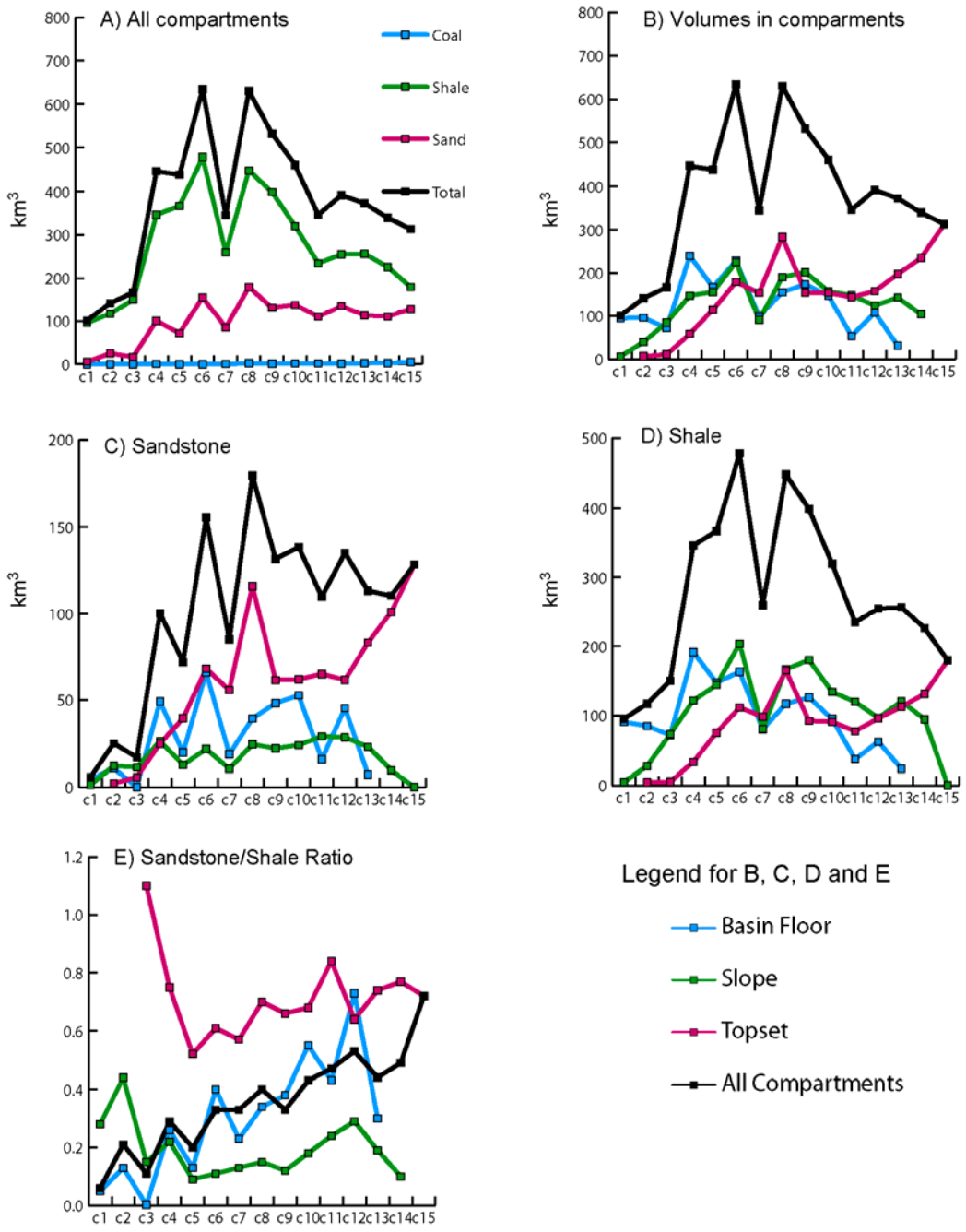

Figure 2.6: Rock Volumes in Clinothems.

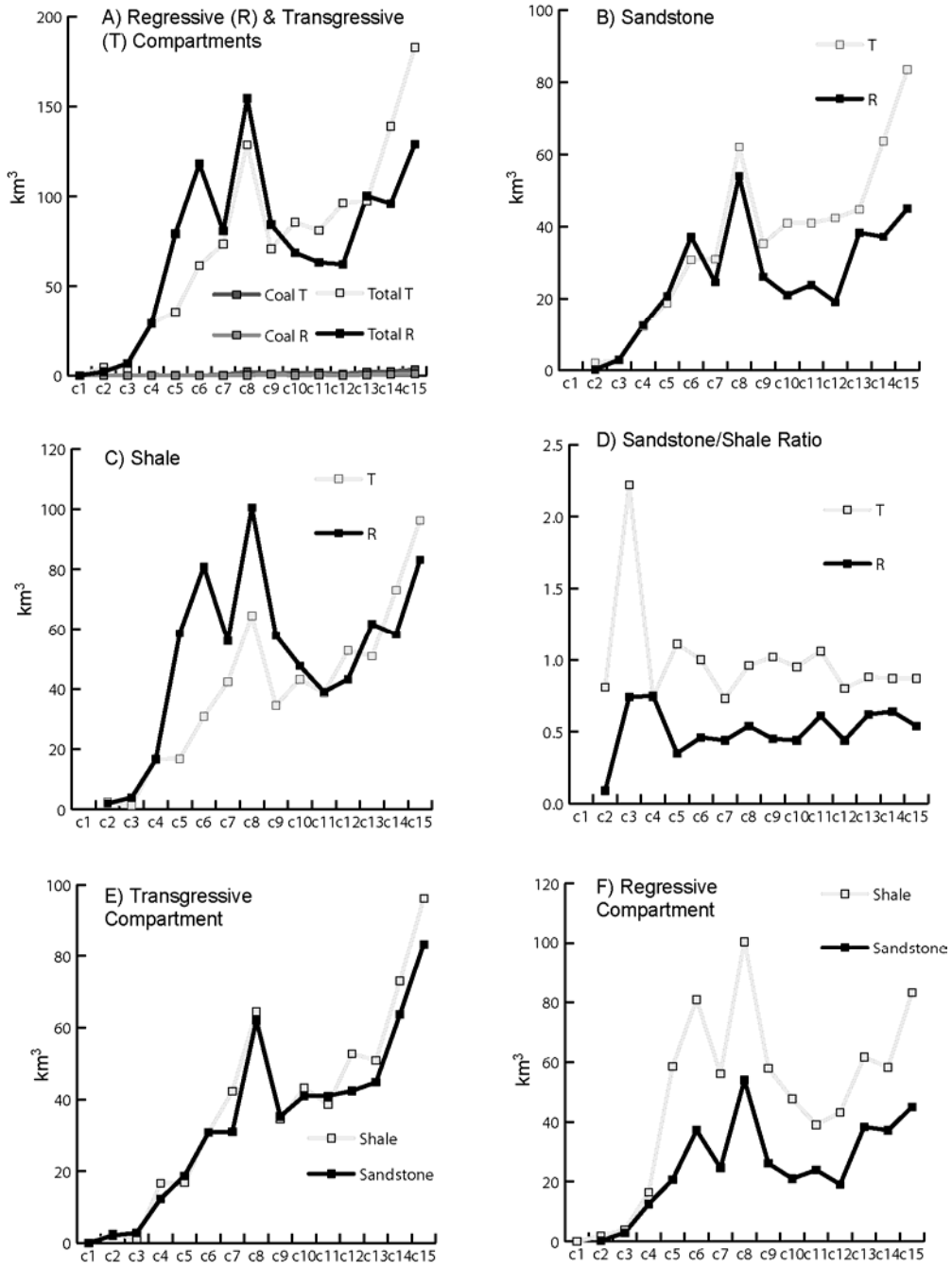

Figure 2.7: Rock volumes in topset.

Individual Sandstone and Shale Volumes and Their Relative Partitioning Ratio

Sandstone and shale volumes stored in the main compartments show significant departures from the trends on total volume partitioning (Figure 2.6 B, C & D). Sandstone volume ranges are 39-128 km^3 ($\bar{u}$ = 77, C05-C15 topsets), 10-26 km^3 ($\bar{u}$ = 20, C03-C14 slopes) and 19-66 km^3 ($\bar{u}$ = 39, C04-C12 basin floors). The reported volumes for basin floor sandstones support the contention of Carvajal and Steel (2006) that clinothems with greater maximum progradation and greater progradation/aggradational ratios tend to have larger fans (Table 2.1). The volumes above are equivalent to mass ranges of 66-216 ($\bar{u}$ = 128), 18-44 ($\bar{u}$ = 34) and 32-111 ($\bar{u}$ = 66) x 10^9 ton. The corresponding ranges of sandstone/shale ratio are 0.52-0.71 ($\bar{u}$ = 0.63), 0.09-0.32 ($\bar{u}$ = 0.19) and 0.13-0.73 ($\bar{u}$ = 0.38).

In clinothems C05-C10 (i.e. with good data coverage for all compartments), the average sandstone partitioning ratio is 3.5:1.0:2.1, and shale ratio is 1.0:1.4:1.2. These and the above data show clearly that the topset is the sandiest compartment (Figure 2.6 C), followed by the basin floor and then by the slope (as averages, these ratios must also be evaluated according to the considerations for total volume ratios). The reverse trend is true for shale (Figure 2.6 D). Evidently the greater partitioning of sand into the topsets reflects the importance of shoreline and fluvial system transits on the shelf, whereas on the basin floor it reflects sand deposition in fans. Although the slope traps the smallest fraction of sand, there are cases where these volumes are comparable to the volumes in small fans (e.g. compare C08 slopes with C07 fans).

Regarding subdivision of the C02-C15 topsets, in most clinothems, volumes of regressive sandstone (max. = 54 km^3) are smaller than those transgressive (max. = 84 km^3) and the ratio of their averages is 1.0:1.4 respectively. In contrast, in any one clinothem, volumes of regressive shale (max = 101 km^3) are greater than or similar to

those of transgressive shale (max = 96 km^3) and the ratio of their averages is 1.3:1.0. Transgressive coal volumes (< 3.5 km^3) are larger than regressive coal volumes (< 1.0 km^3).

Time Trends in Sediment Volume Storage

Increasing-decreasing trend in clinothem total volume

The total rock volume per clinothem ranges from 100 to 635 km^3 (Figure 2.6 A) but there is a marked overall increase up to C08 (630 km^3) and from there it decreases to C15 (312 km^3). This increase-to-decrease in clinothem volume trend does not seem to be simply an artifact of the poor representation of topsets in the oldest clinothems and of basin-floor fans in the youngest. Addition of a topset volume of ~150 km^3 (typical of wide topsets) to the oldest clinothems would increase their volumes to 300-370 km^3 i.e. still low relative to peak values. So the lower volumes in older clinothems (i.e. C01-C04) are a reflection of real smaller volumes and not clinothem preservation. The continued decline in volumes in C11-C15 is clearly influenced by the reduced basin-floor fan data, so their volumes ought to be higher. However, after adding a 240 km^3 basin floor volume (the largest) to C15 its volume will become ~540 km^3, still smaller than peak values. Therefore the observed trend of increase-to-decrease in total clinothem volume through time holds true.

Sandstone/shale ratio increase through time

The trend in total volume correlates well with the trend in shale volume which also rises and falls, but it only shows a minor correlation with sandstone volumes (Figure 2.6 A). Sandstone volumes do show a sustained increase up to C08, albeit not so steep as shale volume increases. However, in C08-C15 sandstone volumes tend to remain somewhat constant at around 110 km^3: this suggests that clinothems are becoming

sandier through time. This is clearly shown by the sandstone to shale ratio that systematically increases from 0.1 to 0.7 (Figure 2.6 E). The increase in this ratio also is clear in topset, slope and basin floor compartments indicating the rise is not an artifact of clinoform compartment area preservation. This systematic rise in sandstone to shale ratio must represent therefore a change in the sand to mud ratio supplied to the basin through time.

Topset volumes increase irregularly through time

Total topset volumes exhibit a marked increase up to C08 (274 km^3), after which they fall in C09 (151 km^3) to rise again up to C15 (251 km^3) (Figure 2.7 B). This trend represents the combined effects of topset width increase in relatively thick clinothems up to C08, and then continued topset widening but with relatively small thickness up to C15. Such thinning is especially clear from C10 and onwards (Figures 2.2 and 2.3). A somewhat similar trend is also observed in total, sandstone and shale regressive and transgressive volumes (Figure 2.7 A, B, C), and is related to the same reasons. Total coal volumes increase through time (without a decline), probably simply a reflection of the increased width of the coastal plain and entire shelf platform through time.

As regards lithological trends within topset compartments, transgressive coal volume is slightly larger than regressive, but both are <1% of total volume (Figure 2.7 A). Sandstone volumes are smaller than shales in both regressive and transgressive compartments and especially in the former (Figure 2.7 E & F). This results in a systematically higher sandstone/shale ratio in the transgressive compartment (Figure 2.7 D).

When regressive and transgressive volumes are compared there seems to be an interesting break at C09. Total and shale regressive volumes tend to be slightly greater than transgressive volumes up to C09 (Figure 2.7 A & C), but thereafter they are similar

or slightly smaller. Opposing this trend, sandstone regressive volumes are slightly smaller or similar than transgressive volumes up to C09, and thereafter they became much smaller up to C15.

Through time, therefore, increased shelf widths produce increasing topset volumes, up to C08, followed by a decline at C09 and continued rise thereafter. In addition, at C10 the partitioning between regressive and transgressive topsets also changes, and total clinothem volumes decline. Therefore the time interval at C09 or slightly after marks a significant change in basin infilling conditions, as discussed further below.

Decreasing fan volumes through time

The deepwater compartments show totally different trends of volume change. Slope total volume tends to remain relatively constant at about 180 km^3, probably indicating that once the slope attains a certain area, it tends to trap relatively similar amounts of sediment. Basin floor volumes show an overall gentle decline from C04 (240 km^3) to C13 (31 km^3). The lower volumes in C11-C13 are clearly related to the smaller data coverage of the fan in these cycles. In C04-C10 the decline (240 km^3 to 148 km^3) is produced by a clear fall in shale volumes probably reflecting larger shale trapping on thick topsets that widen through time.

DISCUSSION: VOLUMES, SHELF MARGIN GROWTH, AND TECTONIC AND SOURCE TO SINK MODEL

The sediment-volume partitioning and the time trends of these volumes will provide an improved understanding of the tectonic and basin-fill history of this Laramide Basin. As argued below, active uplift of the source terranes can explain the sand/shale ratios in the basin, and the shelf margin architecture and volumes suggest two stages of basin infill and development. McMillen and Winn (1991), Ross et al. (1995) and Pyles and Slatt (2000) have produced cross sections in which some elements of these phases are clear. However there has been no previous attempt to use sediment volumes and the dynamics of stratigraphic analysis to improve our model of Laramide Basins, specifically to understand the relationships between developing tectonics, sediment supply and sea level.

Implications of Sediment Partitioning into Compartments

Slope Volumes, Growth and Processes

The fact that the slope tends to trap relatively larger volumes per unit of area than the topset and basin floor (Table 1) reflects the aggradational growth style of these latter compartments compared to the progradational style of the slope. An analogous large trapping potential is observed in the slopes of the West Siberia (Neocomian) and Spitsbergen (Eocence) shelf margins (Johannessen and Steel, 2005; Pinous et al., 2001).

The general muddiness of shelf-margin slopes compared to basin floors along the sandier sediment fairways, such as shown here in the Lewis system is also well known from other systems (Erskine and Vail, 1988; McMillen and Winn, 1991; Brink et al., 1993; Johannessen and Steel, 2005). This suggests that some slope transport processes tend to sort the shelf-edge delta-derived, mud-rich sediment that eventually reaches the basin floor as sand-rich flows. Most slope accretion results from sediment gravity flows,

and turbidity currents are the most efficient at sorting sediment. In turbidity currents, velocities are larger near the base of the flow, and decrease upwards (Kneller and Buckee, 2000). Lower segments of the flow tend to be denser and carry the sandier sediments, whereas muddier sediments are transported higher in the current. On the slope, turbidity currents will typically flow confined within slope channels and unconfined as they spill over the channel across levee and overbank areas. Such spilling of the flow is likely to be significant, because the current and ambient marine fluid have a small density difference which favors spreading of the current beyond the channel. In addition, channel geometry may accentuate spilling if channels are shallow, have local highs at their base or sharp bends, where the flow centripetal component will tend to make the current strip away from the channel. Spilling has a double significance: on one hand, it removes the muddier and most diluted upper segment of the flow, which settles on levee and overbank areas of the slope; on the other, the removal of the muddy, diluted flow causes an increase in density and velocity of the channelized flow which, along with confinement provided by the channel, allows the current to maintain its momentum and reach the basin floor. Upon reaching the basin floor the current becomes unconfined, and deposits the sandier sediments forming a fan. Thus, whereas overall sediment loads to deepwater areas may be mud-prone, turbidity currents can sort this sediment promoting mud accretion on the slope and sand on the fans.

Topset and Slope Volumes: A Proxy for Total Volume

Despite the abundance of basin-floor turbidites in the Lewis-Fox Hills basin, the average volume partitioning results indicate that more than two thirds of the supply budget is stored in the slope and topset compartments. Clearly this figure is a minimum value because it is derived from clinothem maps that omit some of the topset area, but contain the complete or nearly complete area of the fans on the basin floor. Areas beyond

the fans are sediment starved and so their incorporation increases the basin-floor volume by insignificant amounts. In contrast, incorporating larger topset areas will result in a significant volumes increase for the topsets. The implication is that the topset plus slope fraction of the total volume may reach 80% or more. Because topset plus slope volume correlates significantly with total volume, the former can therefore function as a reasonable proxy for total volume (albeit underestimating it).

The above results suggest that shelf-edge accretion rate (i.e. progradation and aggradation rates) may also provide a reasonable measure of discrimination between low-supply and high-supply shelf margins, provided margins of broadly similar water depth (clinoform height) are compared. This is because shelf-edge accretion is essentially a result of topset aggradation and slope progradation, and it is therefore an indirect measure of the volumes contained in the topset and slope. This technique would work less well for destructional shelf margins or margins with very narrow topsets, where much bypass to deepwater may occur without topset or slope building. The use of shelf-edge accretion rates and their impact on supply and depositional systems has been used by Carvajal and Steel (2006) and is further explored in Chapters 2 and 5.

Changing Sandstone to Shale Ratio: Indication of Maastrichtian Tectonic Uplift

Uplift in source-area hinterlands and concomitant unroofing of the sedimentary cover seems to provide the best explanation for the observed changing sand to shale ratio. Many workers have documented that uplift and basin subsidence were already underway during the Maastrichtian or earlier in the Rocky Mountains region. Evidence for such uplift in the Wind River Range, Granite Mountains and Rawlins Uplift area includes (Figure 2.8): 1) the subsidence pattern in the Washakie and Great Divide basins is unrelated to flexural subsidence and loading from the western thrust belt because it was quiescent at this time (DeCelles, 1994) and because the Maastrichtian strata thicken

toward the northern and eastern uplifts listed above and not toward the western thrust belt (see also Figure 2.3); 2) the Lance Formation clearly thins over structural highs in the Pacific Creek area just south of the Wind River Range in the northern Great Divide Basin (MacLeod, 1981); 3) there is erosional truncation of the Lewis Shale in the Lost Soldier area just south of the Granite Mountains (Reynolds, 1976); 4) paleocurrent directions in the fluvial channels of the Lance Formation diverge from the Granite Mountains indicating a paleo-high in this area resulting in drainage away from it; such paleocurrents are to the N-NE on the eastern side of the Granite Mountains (Connor, 1992) and to the S and SW in the eastern Washakie and Great Divide basins (Pyles and Slatt, 2002); 5) immature fluvial sandstones of the Lance Formation have potassium feldspar more abundant than plagioclase, suggesting a source in the Granite Mountains and exposure of the intrusive basement (Connor, 1992); these are the same sandstones that contain eastward directed paleocurrents (Connor, 1992); and 6) this study demonstrates prominent southward shelf margin progradation that originates just south of the Wind River Range and Granite Mountains (Carvajal and Steel, 2006). This Maastrichtian uplift is therefore consistent with observations by Steidtmann and Middleton (1991) and Steidtmann and others (1991) documenting K-feldespar granules in early Paleocene alluvial fans just west and south of the Wind River Range indicating basement exposure already at this time and previous uplift in the Maastrichtian. Resulting from compression, uplift takes place through 25^{o}-30^{o} thrust faults and may involve folding as well (Berg, 1962; Brown, 1988; Blackstone, 1991; Willis and Brown, 1993). These faults bound the south and west sides of the Wind River Range, Granite Mountains and Rawlins Uplift.

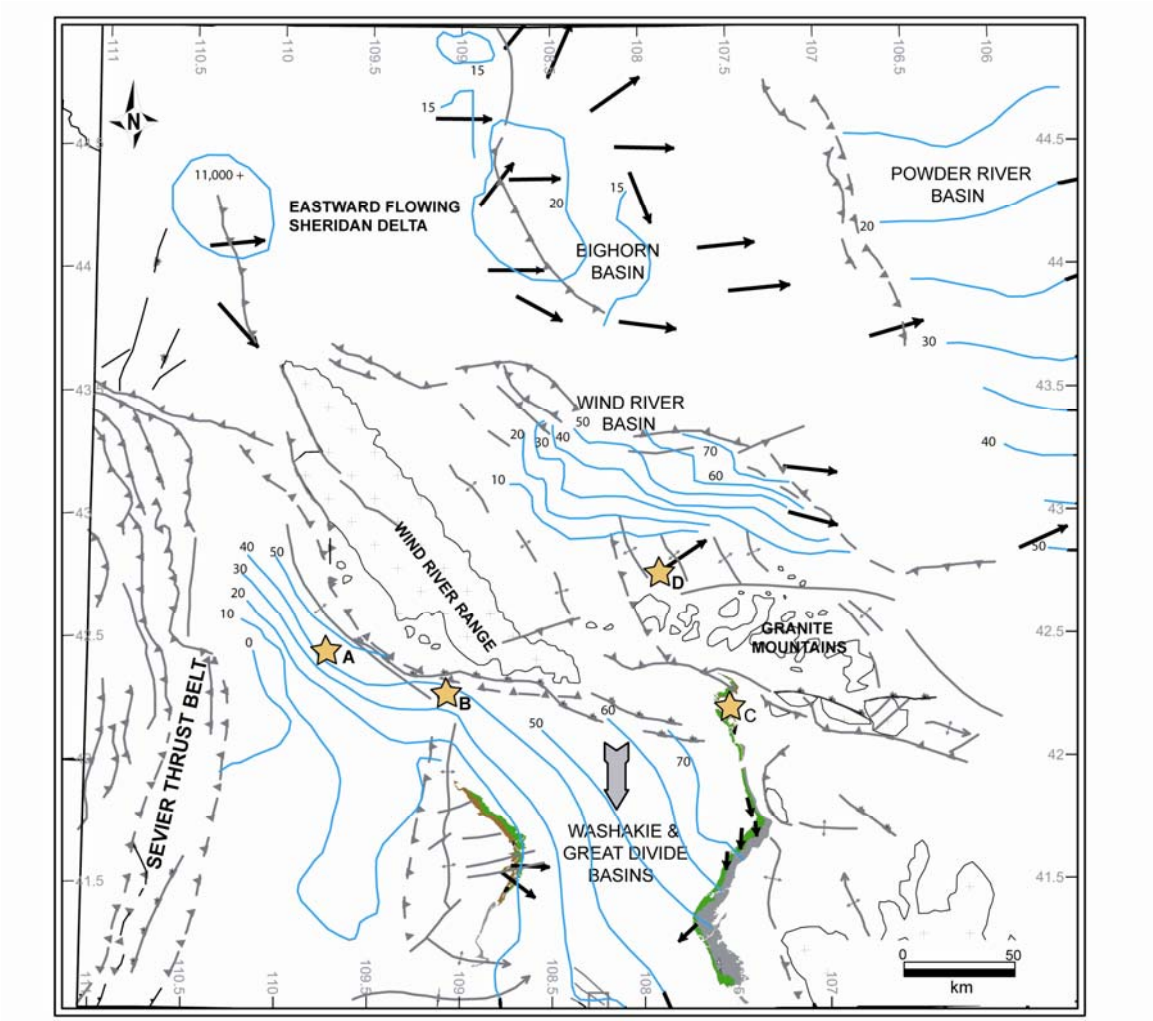

Figure 2.8: Summary of evidence for Maastrichtian uplift (legend for strata in Figure 2.1). Blue lines are contour lines for Maastrichtian strata thickness (in hundreds of feet). Notice clear thickening toward the uplifts. Stars: (A) south-west and east dipping foresets (from MicroImager logs (FMI), (B) thinning of the Lance Formation over structural highs at the Pacific Anticline area, (C) erosional truncation of the Lewis Shale due to uplift in the Lost Soldier area and (D) NE directed paleocurrents and immature sandstones in Lance Formation (with plagioclase and K-feldspar) suggesting source in Granite Mountains. Gray thick arrow represents main direction of shelf margin progradation. Thin arrows are paleocurrents data in the Lance Formation (compiled from my data and from Reynolds, 1976; MacLeod, 1981; Connor, 1992; Pyles and Slatt, 2002; Hanson et al., 2004; Johnson et al., 2004).

As Maastrichtian uplift took place along the above faults successively older strata would have been eroded (eventually basement as seen today) to provide sediments for the basin. Blackstone (1991) provided data on the Paleozoic-Mesozoic sedimentary cover along the northern margin of the Great Divide Basin just south of the Wind River Range and Granite Mountains, suggesting that the unroofing succession would have been some 3350 m thick in the west and 3200 m in the east. From oldest to youngest the succession becomes finer grained (Figure 2.9), from a systematic decrease in sandstone and corresponding increase in shale through time. Uplift of such a column would have initially exposed some sandstones and then thick shale-rich units to follow later with sandier lithologies. The resulting basinal deposits should exhibit the opposite trend, i.e. their sandstone to shale ratio should increase through time as is now observed in the Lewis-Fox Hills basin infill. It is not clear whether the metamorphic-intrusive basement was exposed during the time interval of this study (early Maastrichtian). The petrography supports Maastrichtian exposure, but it could have taken place in the late Maastrichtian. However, at least the sand-prone Jurassic and Triassic rocks were already likely exposed in the early Maastrichtian, and the erosion of these would have increased the sandstone to shale ratio in the basin. The agreement between sand and mud compositions between source rocks and sediments in the basin is additional evidence of the intimate linkage of the Wind River Range, Granite Mountains and Rawlins Uplift with the development and infill of Washakie and Great Divide basins.

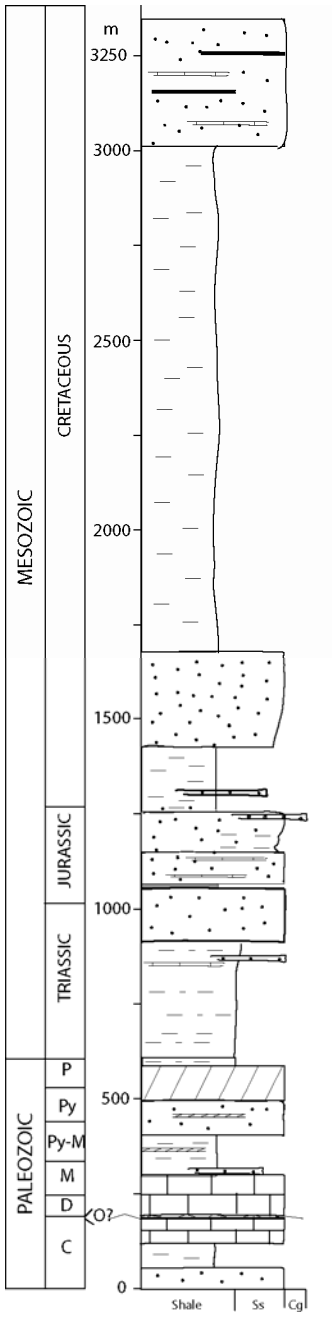

Figure 2.9: Mesozoic and Paleozoic sedimentary section in the northern area of the Great Divide basin (from Blackstone, 1991).

A Tectono-Stratigraphic Model for the Maastrichtian Laramide Basin

Stage 1

Showing a distinctly more aggradational architecture compared to stage 2 clinothems (Figure 2.2), stage 1 corresponds to C01 through C09 and was formed from late *B. eliasi* to early *B. Clinolobatus* (Figures 2.4 and 2.10) This represents a time interval of ~1 my (Figure 2.4) and total rock volume of ~3440 km^3 or a sediment mass of 7470 x 10^9 ton. Therefore average rock volume per clinothem is 380 km^3, and average rock volume per time is 350 km^3/100ky and sediment supply rate 747 x 10^9 ton/100ky. The aggradational character to this early succession is indicated by the relatively thick clinothem topsets. Coupled with this architecture, clinoform amplitude steadily increases; for instance in Figure 2.2 the increase is from ~200m at mfs 4 to about 360 meters at mfs 9. Further east toward areas of higher subsidence (Figure 2.3) the increase is greater.

The topsets of these clinothems contain marine shale tongues that penetrate relatively far landwards, creating moderately wide shelves at these times of maximum transgression. The ensuing regressions consequently contain well-developed shoreline systems (Figure 2.5) that transit long cross-shelf distances. Consequently, total and shale volumes in the regressive topset are larger than in the transgressive compartment. Furthermore, during regression, the coastal plain tends to be represented by the paralic tails of the prograding shoreline, tails that form basinward tongues that reach the shelf-edge only as their linked-shorelines do (see Figure 3.1 in Chapter 3).

Stage 2

Exhibiting a more progradational architecture, stage 2 of basin infill encompasses C10-C15 and is completely within *B. Clinolobatus* (< 0.55 my) (Figures 2.2, 2.4). Stage 2 clinothems have an average duration of less than 100ky, a total rock volume of ca. 2200

km^3 or total sediment mass of 4650 x 10^9 ton. The average rock volume per clinothem is some 370 km^3, per unit of time is >400 km^3/100ky or an average sediment supply rate greater than 845 x 10^9 ton/100ky. Stage 2 therefore has a smaller average clinothem volume, but slightly greater average supply rate as compared with Stage 1.

Clinothems in stage 2 tend to be more progradational, resulting in thinner clinothem topsets. In these clinothems, clinoform amplitude tends to remain fairly constant or to increase slightly (Figure 2.2). Marine shale tongues penetrate landwards for shorter distances during transgression forming narrower marine shelves through time (e.g. see north-south cross-sections in appendix). Therefore following transgression, deltas have to cross shorter distances (as compared to stage 1) to reach the shelf edge under lower accommodation. Consequently, total and shale volumes in the regressive topset tend to be smaller than in the transgressive compartment. So the coastal plain tends to permanently occupy a longer segment of the topset and through time get much closer to the shelf edge (Figure 2.2).

Basin Infill Stages, Subsidence and Tectonics

In stage 1, the aggradational architecture, more marine topset and increasing clinoform amplitude, all indicate increasing basinal water depth through a strongly rising relative sea level regime. In the study case, water deepening and sea-level rise are mainly the result of rapid basin subsidence and not eustasy. During the early Maastrichtian, although Greenhouse conditions produced generally high eustatic sea level, it is likely that the amplitude of sea level change were a few tens of meters at most (Miller et al., 1999; Miller et al., 2004; Miller et al., 2005). Eustatic rise of this magnitude would have been insufficient either to create individual clinoforms with topset thicknesses of more than 100 m or to provide the accommodation to accumulate hundreds meters of marine

aggradation recorded in stage 1. Continuously rising relative sea level and gradual basin deepening are therefore largely the result of high basin subsidence rates, and slightly increasing through time. In contrast, the progradational architectures, wider and thinner terrestrial topsets and fairly stable clinoform amplitudes in stage 2 indicate an overall lower and decreasing rate of relative sea level rise, i.e., lower and decreasing rates of tectonic subsidence.

It is thought that, in general, foreland basins subside as a result of downwarping of an elastic lithosphere due to thrust loads emplaced on the crust (Beaumont, 1981; Jordan, 1981; Heller et al., 1988) and it has been postulated and modeled that this subsidence mechanism operates in Laramide Basins as well (Hagen et al., 1985; Flemings et al., 1986; Shuster and Steidtmann, 1988). At any given time and for a given lithospheric flexural rigidity, the basin subsides trying to attain a mechanical equilibrium with the mountain belt load and basin sediment weight. Subsidence and basin stratigraphy thus largely represent the history of thrusting and uplift. Therefore, stage 1 high and increasing subsidence rates (and higher relative sea levels) occurred during increased thrust loading and uplift. Increasing uplift would have produced greater sediment volumes through time and the increased rising of relative sea level would have resulted in thicker clinothem topsets and consequently greater total clinothem volumes. During stage 2, lower and decreasing rates of thrusting and reduced loading would have produced decreased subsidence rates and a diminishing rate of rise of sea level (and possibly sea level falls too, through isostatic rebounding, see below). Lower rates of sea level rise tended to produce thinner clinothem topsets, and smaller total clinothem volumes (Figure 2.10).

Increased Sediment Supply During Stage 2

Interestingly, the data suggest that on average, sediment supply rate increased in stage 2. This is a somewhat counter-intuitive result, because decreasing uplift rates should tend to result in smaller sediment supply rates. For instance, present world denudation rates tend to be higher in drainage basins with recently uplifted orogens than in drainage basins where the orogenic phase is old (Pinet and Souriau, 1988). It is worth noticing, however, that the orogeny in the latter case occurred more than 250 millions years ago. In the study basin, in contrast, the higher sediment supply rates of stage 2 came shortly after the highest uplift/subsidence rates. At this time, an erosional regime greater than during thrust driven uplift appears to have persisted despite decreasing uplift rates. This is probably because termination of thrusting does not necessarily implies tectonic quiescence; it is thought that isostatic rebound should follow main uplift (Heller et al., 1988). After thrusting, continued mountain erosion reduces the mass of mountain belts and so reduces the load on the lithosphere imposed by previously thrust-emplaced loads. The lithosphere then responds by rising or rebounding to balance the smaller load, causing continued uplift. It is possible that this continued uplift kept erosion rates high in stage 2.

Moreover, stage 2 rebound may not only have greatly reduced subsidence rates but even could have produced periods of basin uplift. In a marine basin this could have triggered falls of relative sea level at these times. This is consistent with Carvajal and Steel's (2006) interpretation, based on clinoform architecture, that there were frequent relative sea level falls during stage 2, and one of these falls has been supported by outcrop evidence (see Chapter 5). Therefore, whereas the shorter duration of high-frequency regressive-transgressive cycles and overall lower rates of subsidence in stage 2

produced thinner clinothems with smaller volumes, continued source areas uplift by isostatic rebound kept average sediment-supply rates high (Figure 2.10).

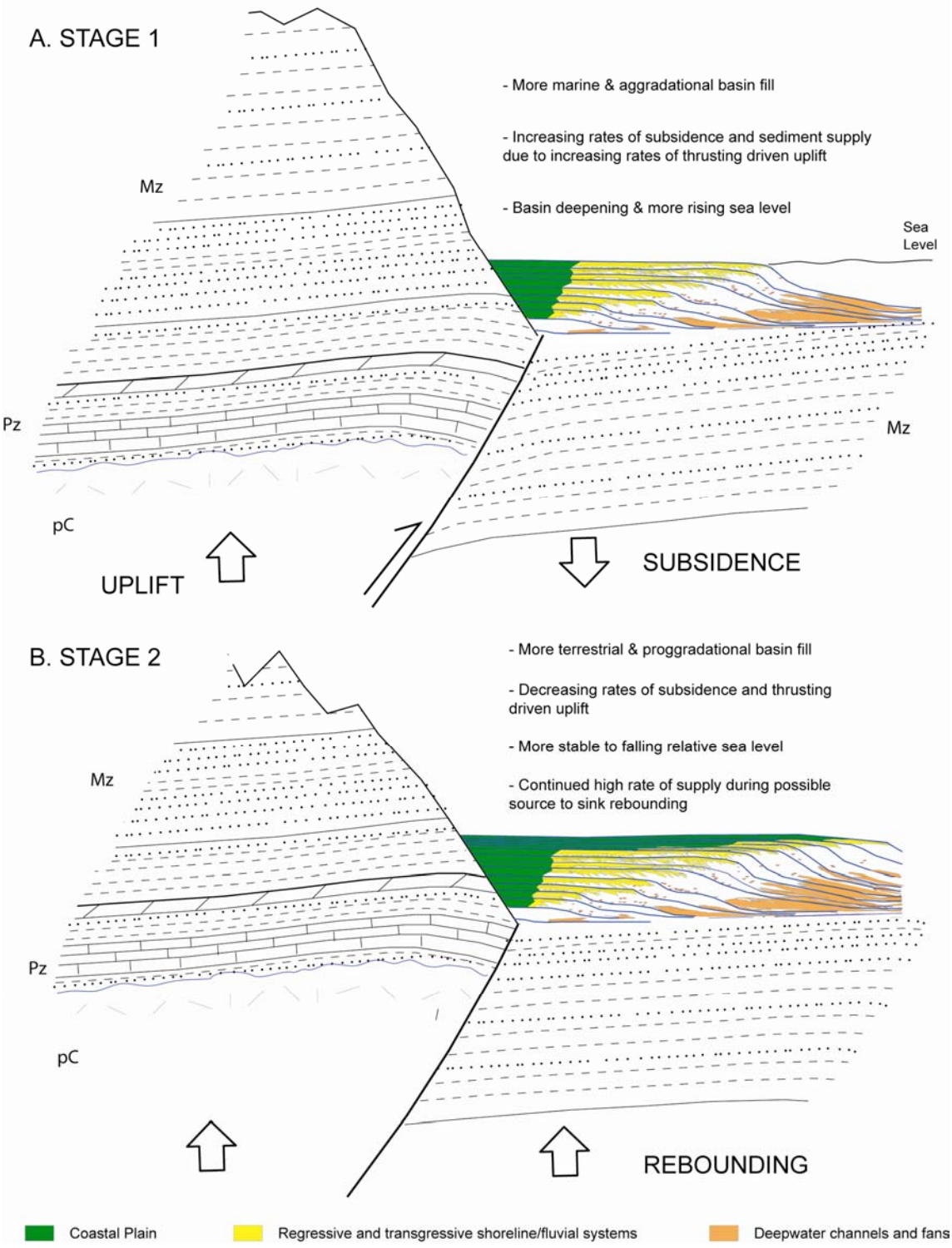

Figure 2.10: Two stages model for basin infill.

Uplifts and Basin as a Complete Source-to-Sink System

The analysis developed in previous sections clearly indicates that the Wind River Range, Granite Mountains and Rawlins Uplift area and the adjacent Washakie-Great Divide basin constituted a nearly complete, self-contained source-to-sink system. This opens an interesting opportunity to apply some of the findings derived from modern source-to-sink systems (Milliman and Meade, 1983; Pinet and Souriau, 1988; Milliman and Syvitski, 1992; Mulder and Syvitski, 1996; Hovius, 1998; Mulder et al., 2003; Syvitski et al., 2003; Syvitski et al., 2004), which may allow characterization of Laramide mountain relief, river discharge, uplift and denudation rates. Prior to this, however, it is necessary to 1) investigate the possibility of externally derived drainage (that is not from the principal uplifts), 2) reasonably estimate river load reaching the marine basin and 3) reasonably constrain the catchment area.

Sediment Provenance

Following the pioneer work of Gill and Cobban (1973), some authors have speculated that the supply to the basin was provided by the southern distributaries of a mainly eastward flowing delta of regional extent located in northern Wyoming and southern Montana, and reaching into areas of North and South Dakota (Winn et al., 1987; Perman, 1990; McMillen and Winn, 1991); the so called Sheridan Delta (Gill and Cobban, 1973) (Figure 2.8). It seems possible that Gill and Cobban's (1973) Maastrichtian interpretations were influenced by their knowledge of the well-known depositional patterns typical of the pre-Maastrichtian foreland basin in which relatively continuous packages of strata accumulated over wide areas of western North America (DeCelles, 2004). However, researchers agree today that the break-up of the main

foreland basin and its separation into isolated depocenters had already started during Maastrichtian times (Figure 2.8).

As regards the Sheridan Delta, paleocurrent data support its existence as a strong eastward and northward prograding deltaic shoreline in northern Wyoming and southern Montana (Figure 2.8). Nonetheless, in the lower Maastrichtian, there are no data that support a southern directed distributary from this system over the Wind River Range and Granite Mountains area; on the contrary, the data largely disprove such an interpretation, because as outlined in previous sections, much data support active uplift and provenance from the Wind River Range, Granite Mountains and Rawlins Uplift directly into the Washakie-Great Divide basin (Figure 2.8).

This does not mean that all sediment came necessarily from these mountains. Outcrops of minor east-flowing fluvial rivers exist in the southern Rock Springs Uplift suggesting a western to northwestern source (see Chapter 5). Albeit these rivers could have drained the western flank of the Wind River Range, they could have also drained other areas. In any case, these rivers were quite minor suppliers of sediment because their outcrops are scarce and shelf-edge progradation, delta transits across the shelf, basin-floor sourcing, and orientation of major drainages on the coastal plain, etc., all indicate a clear northern provenance (Figure 2.2, see also Appendix). Nonetheless to account for this potentially external source I will reduce volumes by a 20%.

River Load to the Marine Basin

The marine slope and basin floor sediment volumes are the most obvious components of the sediment load delivered to the marine basin. Topset transgressive volumes tend to be terrestrial, and so I exclude them. Regressive topset volumes tend to be predominantly marine in the aggradational clinoform set of stage 1, but in the

progradational clinoform set (stage 2) they include larger portions of the coastal plain. However I include the regressive volumes, and note that the addition of the coastal-plain deposits somewhat compensates for the exclusion of the marine portion in the transgressive volumes. Thus, the regressive topset, slope and basin floor deposits equal 1000 km^3 of sandstone and 3660 km^3 of shale, equivalent to grain volumes of 663 and 3121 km^3 respectively, with a total of 3834 km^3. This is the grain volume preserved within the study area (8778 km^2), which proportionally extrapolated to nearly the entire Washakie and Great Divide basins area (Figure 2.11) (17700 km^2) is equivalent to 7730 km^3 and reduced by 20% (outside provenance) becomes ~6200 km^3. The extrapolation is acceptable because, covering about half of the basin, the study area adequately represents the thickness patterns within the basin, as least as seen in isopach maps for the Maastrichtian (Figure 2.8). In terms of mass, the reduced volume (6200 km^3) is equivalent to ~16 x 10^{12} ton of sediment. Although this mass estimate would change if porosities or cementation percentages are refined or outside provenance was different, it is very unlikely that the order of magnitude of this estimate (i.e. low tens x10^{12} ton) would not change, and in this sense it is a robust result. This sediment mass was deposited during a period of approximately 1.8 my, so *average* sediment load to the marine basin is 9 x 10^9 kg/y (= 9 x 10^6 ton/y or 290 kg/s).

Catchment Area

As defined by their basement outcrops and bounding faults, the present area of the Wind River Range, Granite Mountains and Rawlins Uplift is ~ 15700 km^2 (Figure 2.8) This represents an upper estimate of the mountainous catchment area, because some rivers would have flowed away from the Washakie and Great Divide basins especially in the northern areas of the Wind River Range (Figure 2.8). The catchment in the alluvial

and coastal plains is more difficult to estimate, because as a shelf margin progrades its topset width increases inducing changes and possibly enlargement in the drainage basin. Even during a single regressive-transgressive cycle the terrestrial topset length changes and so should the catchment as the shoreline delivery system transits the shelf. In a compilation of the geomorphology of 279 modern catchments, Mulder and Syvitsky (1996) documented that the majority of these rivers have elongated catchments (length perpendicular to the coast longer than length parallel to it) with a significant proportion of their area in the coastal plain. All these considerations have led me to use an average catchment with the geometry portrayed in Figure 2.11 and area of 23200 km^2. Notice that whereas this catchment's geometry may certainly vary, its area seems well constrained because uplift (15700 km^2) and basin (17700 km^2) areas combined total 33400 km^2, but as discussed catchment area should be smaller than this. This value for the catchment combined with load delivered to the ocean (16 x 10^{12} ton) suggests an average yield of ~400 ton/km^2/y.

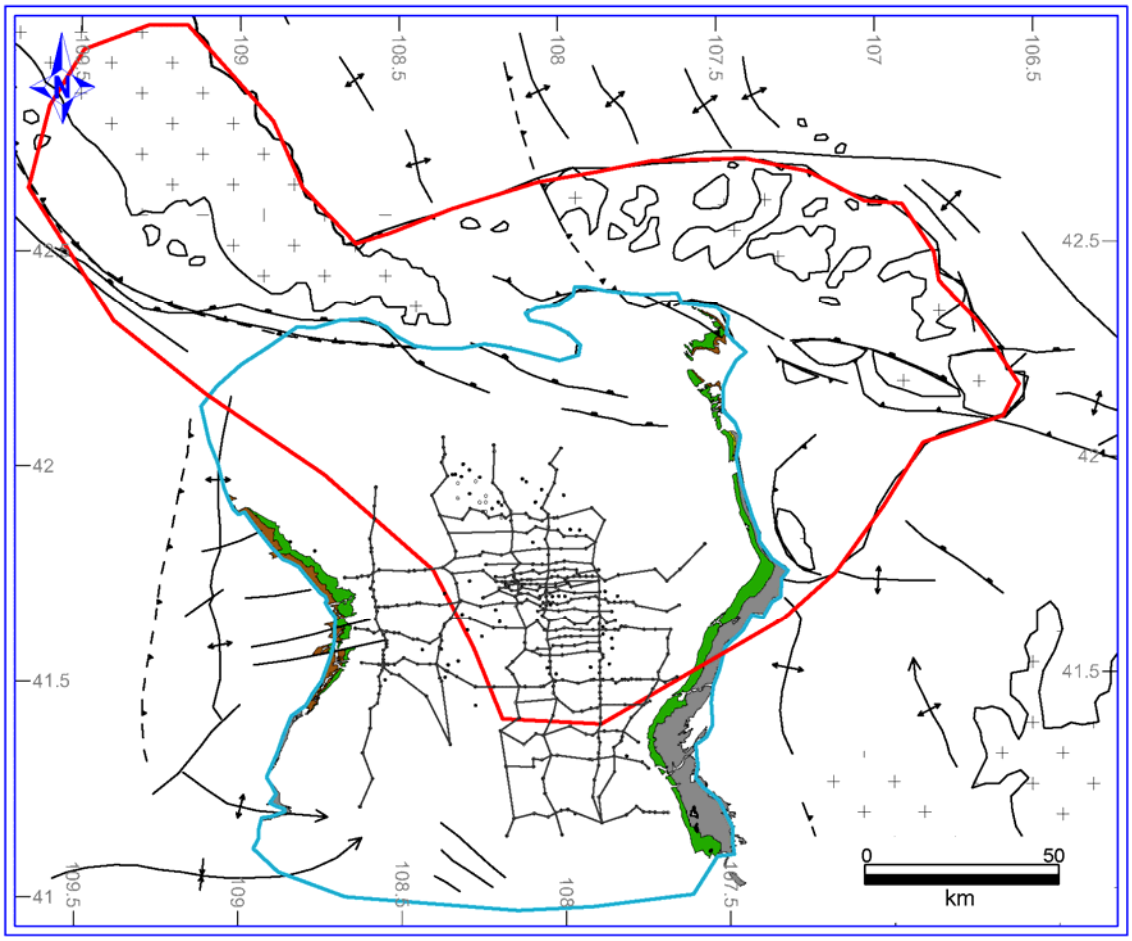

Figure 2.11: Areas used for volume extrapolation in Washakie and Great Divide basins (blue) and average catchment area (red) (see Figure 2.1 for legend).

Character of the Lewis-Fox Hills Sourc- to-Sink System

Sediment load estimates for the Lance rivers (9 x 10^6 ton/y) are much smaller than the load in rivers like the Mississippi, Bramaputhra, Orinoco or Amazon that carry 100's of millions ton/y. Obviously these loads are much larger because of the extremely large catchment of these rivers (millions of km^2). On the other hand, the Lance catchment yield (400 ton/km^2/y) is larger than the yield of the Mississippi, Orinoco and Amazon rivers (120, 150 and 190 ton/km^2/y respectively), and comparable to the Ganges River yield

(520) and smaller than the Bramaputra River yield (890). Therefore Lance catchment was more productive than the catchments of the Orinoco, Amazon and Missippippi rivers which probably reflects that these latter catchments are large and trap much sediment in the coastal plain, whereas the smaller coastal plain of Lance rivers allowed a proportionally larger bypass to the ocean basin. It may also be due to the generally more tectonically active relief in the Lance catchment. When compared with East Asian rivers, which at present provide the largest volumes of sediment to the ocean, Lance yields tend to be an order of magnitude smaller. This probably reflects that these rivers still have catchments larger than in the Lance, but more importantly some of them drain mountains of high elevation (e.g. ~3000 m in the island of Java). The estimates for load and area in the Lance rivers place them as 'mountainous' in Milliman and Syvitsky's (1992) classification, i.e., rivers that drain areas of a maximum relief between 1000 and 3000 m; and place the catchment within the contractional tectonic setting of Hovious (1998), quite consistent with the Laramide setting. Further estimates for the catchment maximum relief of Lance rivers maybe obtained through the equation (Syvitski et al., 2003; Syvitski et al., 2004):

$$Qs = \alpha_3 * A^{\alpha 4} * R^{\alpha 5} * e^{kT}$$

Where Qs = sediment load (kg/s), A = basin area (km^2), R = basin maximum relief (m) and T = temperature (^oC); α_3, α_4, α_5 and k are regression coefficients for different latitudinal belts (northern and southern tropical, template and polar zones). I have estimates for area and load. Regarding temperature, paleobotany suggests that lowland climate during Maastrichtian in southern Wyoming was warm, equable, subhumid with abundant broad leave evergreen forests and small proportion of leaves

with drip tips indicating precipitation smaller than in rain forests (Wolfe and Upchurch, 1987; Upchurch and Wolfe, 1993). The boundary between megathermal and mesothermal vegetation (mean annual temperature = 20°C) was between 40°-50° of paleolatitude and the Washakie and Great Divide basins were between 46°-48° paleolatitude. Therefore I have selected a mean long-term temperature of 20°C and the correlation coefficients for the northern template latitudinal zone ($\alpha_3 = 6.1 \times 10^{-5}$, $\alpha_4 = 0.55$, $\alpha_5 = 1.12$ and $k = 0.07$), although the area could have been intermittently tropical. Solving the above equation, *average maximum* relief would have been ~1800 m in the hinterlands of the Wind River-Granite Mountains-Rawlins Uplift source area.

A check for this relief estimate is given by using Pinet and Souriau's equation: Ds [m/ky]=419*10^{-6}*H [m] - 0.245, where Ds = denudation rate and H = *mean* basin relief. Denudation rate corresponds to marine basin sediment volume (6200 km^3) divided by catchment area (23200 km^2) and by time (1.8 my). So Ds = 0.15 m/ky resulting in a mean basin relief of 918 m or 975 m applying a correction for dissolved loads. These are mean reliefs and so are consistent with a ~1800 m average for maximum relief.

An additional indirect check for these relief estimates is provided by the thickness of the strata undergoing uplift and erosion. As suggested in previous sections, uplift was most likely able to expose rocks at least down to the base of the Triassic (Figure 2.9) (possibly deeper). From this base to the base of the Maastrichtian, the stratigraphic thickness is ~2800 m, which was raised during a 1.8 my implying an uplift rate of ~ 1.5 mm/y. This is an uplift rate that has the potential to create a maximum relief value such as the one obtained above.

Overall Implications for Supply, Tectonics and Deepwater Deposits

Because of the methodology used, my estimates for load, yield and relief represent average values. Note that, during early stages of uplift and basin development,

load and relief would have tended to be smaller and during the climax of uplift probably at the end of stage 1, they would have been greater. This means that at times load and yield could have reached much larger values, so at these times the Lance system could rightly have been classed as a high-supply system even by present world standards (comparable to Asian rivers). This lends validity to the analysis of Carvajal and Steel (2006) (see Chapters 3 and 5) that suggests that shelf margins with large accretion rates, such as the Fox Hills-Lewis margin, are symptomatic of a large sediment supply, at least as large as to easily fill their depocenters.

The calculated 1800 m average maximum relief is a result worth emphasizing as well. As an *average maximum relief*, it indicates that at times relief was even greater possibly reaching 2000-3000 m. This is in agreement with independent results by other authors who have postulated, on the basis of isotopic compositions of freshwater mollusks, that uplift was prominent in the Maastrichtian creating a relief of 2500-3000 m (Dettman and Lohmann, 2000). This is important because although researchers have recognized that the Laramide Orogeny was causing uplift and deforming the Rocky Mountain region already during Maastrichtian, they have tended to see this deformation as relatively minor or they have overlooked it, thus hampering the development of Laramide models for uplift, basin development and sediment delivery.

CONCLUSIONS

Shelf Margin Accretion: Volumes show that when topsets, slopes and basin floors are adequately represented within the study area, partitioning of their average total rock volumes follows a 1.1:1.1:1.0 ratio. The slope, however, traps the largest volumes of sediment per unit of area due to its progradational character. Regarding sandstone and shale partitioning, ratios for their averages are 3.5:1.0:2.1 and 1.0:1.4:1.2 respectively.

Departures from all these average ratios occur 1) when compartment areas differ greatly; compartments of larger area naturally tend to trap more sediment and 2) when clinothem architecture is markedly aggradational or progradational; the former trapping more sediment in the topset and the latter in the basin floor. The ratios show that in the compartments sand content decreases from the topset, to the basin floor and to the slope. The reverse trend is true for shale. Whereas topset higher sand proportion reflects deposition in fluvio-deltaic systems, basin floor sandiness results through fan formation by turbidity currents. Slope muddiness also results from accretion through turbidity currents. On average, topset and slope volumes combined represent more than two thirds of total volume, a proportion bound to significantly increase were the full topset considered. This indicates that as a measure of topset aggradation and slope progradation, and so as a measure of their respective volumes, progradation and aggradation rates of the shelf edge may serve as proxy for sediment supply.

Two-Stage Tectono-Stratigraphic Model: Basin development and fill evolved in two stages mainly driven by source tectonics through its influence on sediment supply and basin subsidence. During stage 1, source uplift occurred through increasing thrusting along low-angle faults in the Wind River Range, Granite Mountains and Rawlins Uplift. This thrust-driven uplift resulted in increasing sediment supply rate and through crustal loading of the lithosphere, increased basin subsidence leading to rise of relative sea level and increasing basinal water depths. The basin responded through aggradational clinothems of increasing volume and with thicker and more marine topsets. In stage 2, decrease or cessation of thrusting would have reduced mountain loads and so reduced basin subsidence leading to smaller rates of sea level rise and stable to slightly increasing basinal water depths. The basin responded through more progradational clinothems with decreased volumes and with thinner and more terrestrial topsets. Isostatic rebounding in

stage 2 would have followed main thrusting and would have caused continued source uplift keeping sediment supply rates high. This rebounding would have also caused periods of basin uplift and relative sea level falls. Through stages 1 and 2, the continued uplift of source terranes exposed successively sandier rocks producing a systematic increase in the sandstone to shale ratio in the basin fill. These terranes and coastal plain formed a catchment (~23200 km^2) that supplied river loads to the ocean estimated to be on average ~9 x 10^9 kg/y suggesting a yield of ~400 ton/km^2/y and denudation rate of 0.15 mm/y. Catchment and river load estimates imply therefore that through stages 1 and 2 average maximum relief in hinterland areas was about ~1800 m, indicating that at the peak uplift probably achieved toward the end stage 1, source area maximum relief was in the range of 2000-3000 m. Thus this two-stage model shows the intimate relationships between tectonics and sedimentation in this Laramide source-to-sink system.

CHAPTER 3: THICK TURBIDITE SUCCESSIONS FROM SUPPLY-DOMINATED SHELVES DURING SEA-LEVEL HIGHSTAND

ABSTRACT

Emphasis on the association between relative sea-level lowstand and the formation of sandy deepwater fans has tended to downplay the significance of high sediment supply and its potential to create deep-water fans, even during sea-level highstands. The Lance–Fox Hills–Lewis shelf margin in southern Wyoming suggests that high supply was critical in causing the accretion of this moderately wide Maastrichtian shelf margin, at a minimum rate of 47.8 km/my, and the generation of large, sand-rich fans during every shoreline regression across the shelf. It is surprising that fans developed from shelf-margin clinoforms that show systematically rising shelf-edge trajectories (proxy for rising relative sea level) as well as from those that show flat trajectories (stable to falling relative sea level). However, the latter, producing more sediment bypass, resulted in bigger and thicker fans, whereas the former produced somewhat smaller and thinner fans. I term the former highstand fans and suggest caution in using the lowstand model for high-supply systems.

INTRODUCTION

The growth of submarine fans, both modern (Flood and Piper, 1997) and ancient (Mutti, 1985; Posamentier et al., 1988), has been widely accepted as being preferentially associated with relative sea-level lowstand. In this model, fall of relative sea level below the shelf edge causes rivers both to reach the outer shelf and to entrench at the shelf edge (Johannessen and Steel, 2005), thus focusing the delivery of sand to deep-water areas. Conversely, this model postulates that during times of relative sea-level highstand much of the sand budget is stored on the shelf and coastal plain, and that deep-water fans

become draped by muds (e.g. see Damuth et al., 1988). This model has been challenged using examples from narrow shelf settings (e.g., fans in the California Borderland, Gulf of Corinth, and Mediterranean Sea; see Ito and Masuda, 1988; Piper and Normark, 2001) or extremely high supply systems (e.g., Bengal Fan; Weber et al., 1997). In these cases slope canyons extending to almost the shoreline may receive sand from littoral drift or shelf currents during rising sea level. In addition, deltas may easily cross narrow shelves and provide sand for deep-water deposits under normal supply conditions during relative sea-level highstand. It has also been postulated that in moderately wide (tens of kilometers) to wide (hundreds of kilometers) shelf settings, significant volumes of sand can be bypassed to deep-water areas at highstand through shelf-edge deltas (Burgess and Hovius, 1998; Porębski and Steel, 2006). Nonetheless, documenting such delivery either in the modern or ancient has been difficult (except for suggestions from studies at the third-order time scale, e.g., McMillen and Winn, 1991), biasing researchers to interpret ancient deep-water deposits preferentially following the lowstand model. Thus, focus on this lowstand model has tended to cause us to overlook (1) the dominant role that sediment supply may play in deep-water sediment delivery, and (2) how such supply-dominated shelf margins can generate deep-water fans even during periods of rising relative sea level.

I provide here an example of how Maastrichtian deep-water fans of the Lewis Shale in southern Wyoming formed from shelf-edge deltas that I can document crossed moderately wide shelves in a high-supply setting. The submarine fans were generated by every one of at least 15 deltaic regressive shelf transits (Figures. 3.1 and 3.2), during a total time interval of less than 1.8 my, and there is evidence that many of these shelf transits happened while relative sea level was rising. Note that “rising” cannot be

interpreted as late lowstand rising (Posamentier and Vail, 1988), but is highstand rising because it links back to a major shelf regression of the deltas.

GEOLOGIC SETTING AND DATA SET

My data are from the Lance–Fox Hills–Lewis depositional system in southern Wyoming. This Maastrichtian succession is the final third-order shoreline regression of the Cretaceous Western Interior Seaway (Winn et al., 1987). The onset of the Laramide orogeny and associated tectonic subsidence resulted in rapid and significant southward shelf-margin progradation into the deep-water (as much as 430 m from undecompacted clinoform amplitudes) Washakie and Great Divide basins (Figures. 3.1 and 3.2). These basins formed a single asymmetric trough at that time, with higher rates of subsidence in the east. Correlation of ~500 well logs (with gamma ray, spontaneous potential, and conductivity curves) in this basin allows a three-dimensional tracking of individual fourth-order cycles through the linked fluvial to shelf to deep-marine depositional system of the Lance Formation, Fox Hills Sandstone, and Lewis Shale (Figures. 3.1 and 3.2).

In this system, the rivers of the Lance Formation (paralic and coal bearing, >200 m thick) and deltas of the Fox Hills Sandstone (mainly sandy river-wave deltas, >214 m thick) fed large volumes of sediment to deep-water areas of the Lewis Shale (>762 m). The high-supply character of the Fox Hills deltas allowed them easily to cross a moderately wide shelf (tens of kilometers), delivering large volumes of sand as slope and basin-floor turbidites.

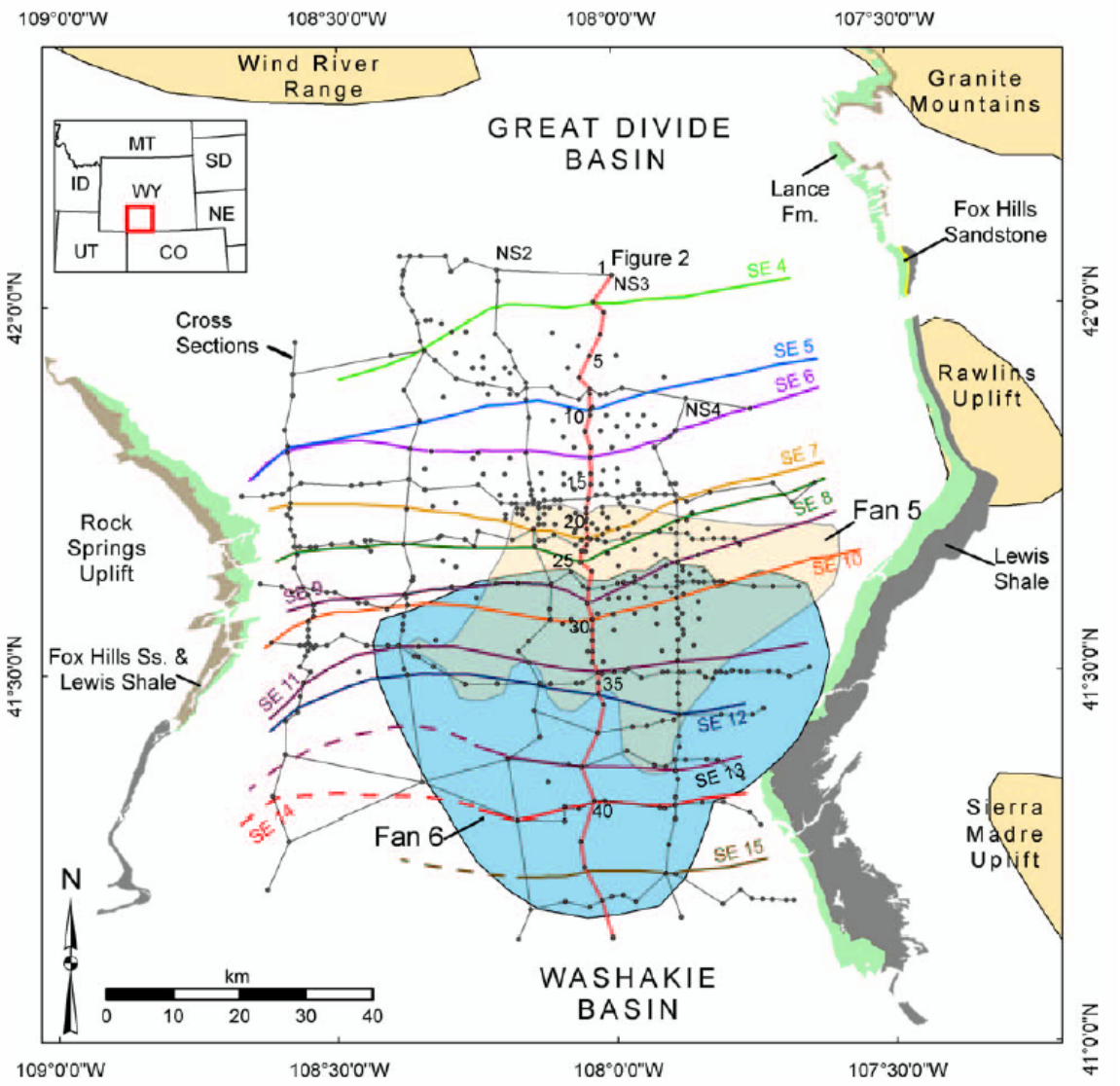

Figure 3.1: Location of study area (inset map), local geology (from Love and Christiansen, 1985), well database, shelf-edge positions (at the time of maximum flooding during the beginning of each cycle), and two basin-floor fans. Fan 5 was deposited during rising shelf-edge trajectory, whereas the larger fan 6 was generated during flatter shelf-edge trajectory.

DETERMINING CLINOTHEMS—UNITS OF SHELF-MARGIN ACCRETION

The term clinoform was introduced by Rich (1951) for the sloping segment of a shelf-margin profile. Here I use it for the entire surface connecting shoreline-shelf areas

via deep-water slopes to basin-floor areas. Clinothems are the sand-prone lithosomes bounded by easily identifiable shale intervals (representing transgressions and maximum flooding surfaces; see Figure 3.2) that in the Lewis–Fox Hills clinoforms penetrate landward up to 40-50 km. This distance, therefore, documents that the shelf was moderately wide. This is also the distance that the deltas/strandplains had to cross to reach the shelf-edge during the subsequent regression. Clinothems (commonly with amplitudes of as much as 430 m) thus consist of (1) a regressive lower component produced by deltas and/or strandplains crossing the shelf, and in my data set always reaching the shelf edge, (2) a more steeply dipping basinward component created by sediment gravity flows on a long slope below the shelf edge, reflecting an increment of shelf-margin growth, and (3) a transgressive upper component produced by landward-migrating coastal plain, estuary, and barrier lagoon systems.

Clinothems in my data set are easily visualized by using a marked shale of basin-floor origin as stratigraphic datum (Figure 3.2). This shale is of nearly basin-wide aerial extent, has high organic content and gamma-ray values (Pyles and Slatt, 2000), and helps to tie well logs regionally. The shales bounding the clinothems have been correlated before (e.g., Asquith, 1970; Winn et al., 1987; McMillen and Winn, 1991; Ross et al., 1995; Pyles and Slatt, 2000), resulting in correlation schemes somewhat similar to mine and so increasing the confidence of the correctness of the correlation and quantification of key elements of the shelf-edge to deep-water system.

Such elements include the shelf-edge trajectory, fan thickness and area (where enough of the fan area is present), and the character and/or geometry of the sand accumulated on the slope. The shelf-edge trajectory (Steel and Olsen, 2002) represents the pathway of the shelf edge during the development of a given clinothem or group of clinothems (Figure 3.2). I have quantified this trajectory by calculating the ratio between

the average progradation and average aggradation of the shelf edge (Figure 3.1) along cross-sections NS2, NS3, and NS4 (Figure 3.1), which cross most of the deep-water depocenters. My measures are undecompacted, but my trajectory trends and relationship to deep-water fans seem to be similar to those that can be inferred from a decompacted published section in the area (Ross et al., 1995).

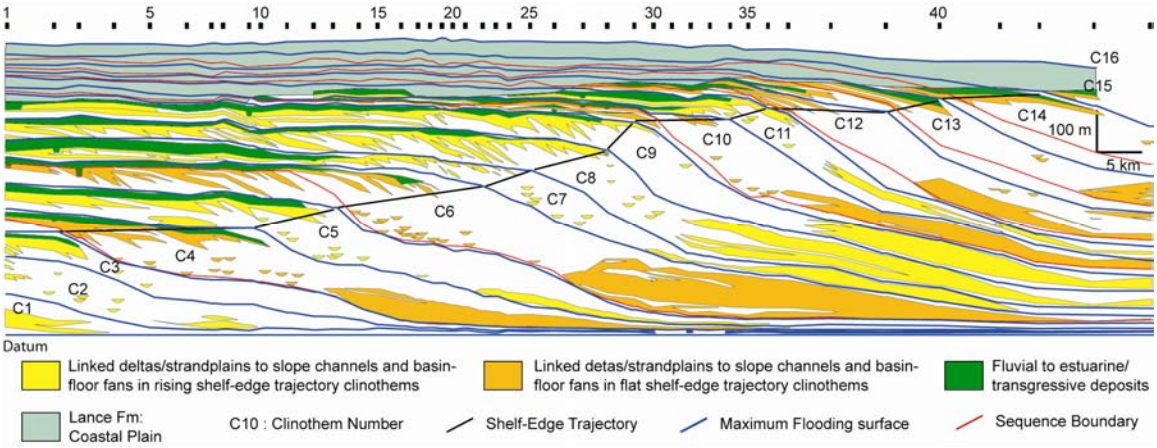

Figure 3.2: NS3 cross-section. Notice that fan maximum thickness does not necessarily coincide with this cross section because fan depocenters shifted through time. Trajectory quantification was done using NS2, NS3 and NS4.

FOX HILLS–LEWIS MARGIN AS A HIGH SEDIMENT-SUPPLY SYSTEM

Shelf-margin progradation and aggradation rates have been calculated for the Fox Hills–Lewis system and for a number of ancient shelf margins in which clinoform amplitudes are <1000 m (Table 3.1). The average progradation and aggradation rates for the Lewis shelf margin were 47.8 km/my and 267 m/my, respectively. These are conservative estimates, as they do not consider the progradation and aggradation of the shelf margin prior to shelf-edge 4 (Figure 3.1; Table 3.1) because I do not have data on the early shelf-edge positions. Despite this, the Lewis margin aggradation and

progradation rates are high compared to other margins, indicating that it was supply dominated.

Table 3.1: Aggradation and progradation rates in margins of similar clinoform height that in the Lewis.

Shelf Margin	*Age*	*Aggradation (m)*	*Progradation Distance (km)*	*Time (my)*	*Aggradation Rate (m/my)*	*Progradation Rate (km/my)*	*Reference*
Lewis-Fox Hills, Wyoming	Late Cretaceous	480<	86<	1.8	267	47.8	This work
West Siberia	Early Cretaceous	~1000	550	9.0	111	61.1	Pinous et al., 2001
Spitsbergen, Norway	Early Eocene	1125	34	6.0	188	5.7	Johannessen & Steel, 2005
Porcupine Basin, Offshore Ireland	Early Eocene	400	33	4.0-5.0	80-100	6.6-8.3	Johannessen & Steel, 2005
North Slope, Alaska	Early to Late Cretaceous	~1000	155	10.0	100	15.5	McMillen, 1991
Exmouth Plateau, Offshore Australia	Early Cretaceous	610	57<	6.0	102	9.5	Erskine & Vail, 1988
Pletmos Basin, Offshore S. Africa	Early Cretaceous	594	54	3.6	165	15.0	Brink et al., 1993
New Jersey	Middle Miocene	A few meters	31	1.8	Small	17.2	Steckler et al., 1999

***Progradation distance and aggradation measured in undecompacted cross-sections (except for New Jersey). Errors may arise from cross-sections orientations, lack of depth-converted seismic data and limited aerial coverage (e.g. in the North Slope). Dating is reasonably good for all margins except for the North Slope whose time interval is poorly constrained. In the Lewis-Fox Hills margin, progradation distance is from shelf-edges 4-15 (Fig. 1) and time estimate is given by the Western Interior Seaway ammonites zones from *B. eliasi* (ca. 70.9) to the top of *B. clinolobatus* (ca. 69.1) (Winn et al., 1987; Kauffman et al., 1993).**

LEWIS DEEP-WATER FANS

A main result of my analysis is that all the Lewis clinothems (for which I have enough basin floor and slope data) contain thick and aerially extensive deep-water fans. I have focused my analysis on clinothems 4 through 12 because in these cases I have access to nearly complete clinothems and can therefore measure most of the necessary variables. Fans in these clinothems are on the basin floor and toe of slope, although turbidite sandstones are also present on the upper slope. The fans (Figures 3.1 and 3.2)

form a southward- and eastward-migrating series of broad, lobe-like bodies. These sand-prone bodies have largely blocky to slightly serrate gamma-ray signatures, have maximum thicknesses between 52 and 121 m, and areas between 1387 and 2580 km^2. On the basin floor, they are rarely interbedded with shales (<3 m), but shale layers increase in number and thickness toward the toe-of-slope and fan-fringe areas (e.g., ~10 m).

SLOPE SANDSTONES

Slope sandstones, in contrast to basin-floor fans, are typically <12 m thick and may occur vertically stacked with intervening shale layers. Their log patterns tend to be blocky to serrate and spiky, and some have an upward-fining cap. Commonly these sandstones are laterally discontinuous or show drastic lateral thickness changes. I interpret the slope sandstone bodies as channel fills and inner levee deposits, in some cases forming multistory and multilateral channel belts. These channels acted as conduits through which sand was transported to the basin floor.

FAN DIMENSIONS AND SHELF-EDGE TRAJECTORY

In my data set, clinothems with either rising or with flattish shelf-edge trajectories partitioned significant volumes of sandstone into deep-water areas (Figures 3.2 and 3.3). However, fan dimensions tend to be greater in those clinothems with flat to falling or very low angle trajectory, compared to the fans linked to rising shelf-edge trajectories. I define flat to falling or slightly rising shelf-edge growth trajectory by a progradation versus aggradation (P/A) average ratio of 0.22×10^3–1.27×10^3, or negative values, and a maximum shelf-edge progradation distance of 10–15 km (clinothems 4, 6, 10, and 12). These clinothems contain fans with a maximum thickness from 102 to 121 m (average = 110 m) and an area from 2212 to 2580 km^2 (average 2359 km^2). In contrast, more steeply rising shelf-margin growth has a P/A ratio between 0.07×10^3 and 0.25×10^3 and

maximum progradation distance of 5–8 km (clinothems 5, 7, 8, 9, and 11). In these clinothems, fan maximum thickness ranges from 52 to 91 m (average = 68 m) and fan area ranges from 1387 to 2234 km^2 (average = 1830 km^2). Thus, both flattish and rising shelf-margin growth produces fans, but there is a clear tendency for steeper shelf-margin accretion (and accompanying greater storage of the sediment budget on the shelf) to be associated with smaller volumes of sand delivery into the deep-water slope and basin floor.

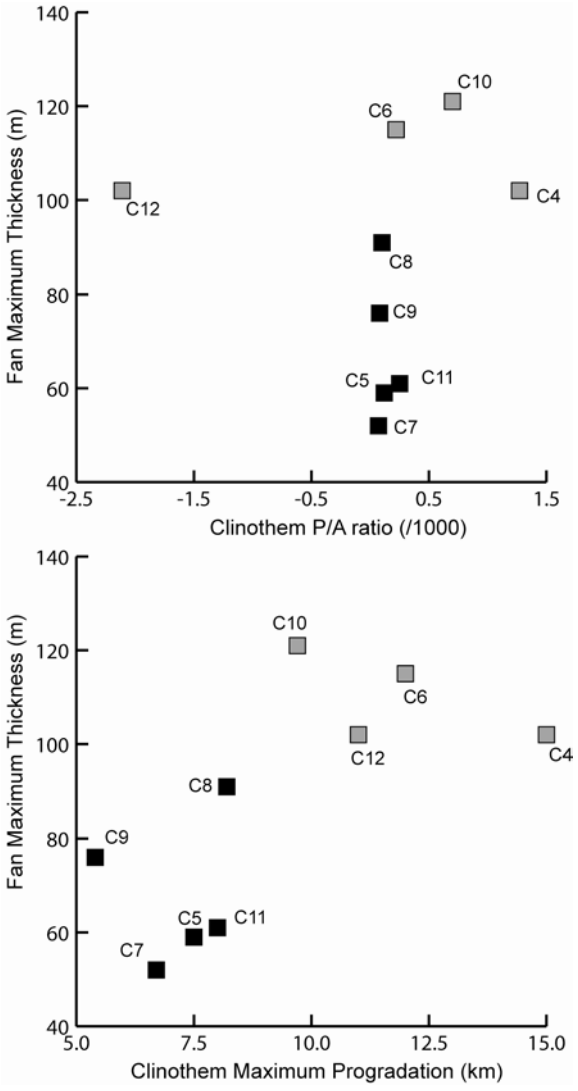

Figure 3.3: Maximum progradation and progradation/aggradation ratios versus fan maximum thickness.

DISCUSSION: FANS DURING RISING SEA LEVEL AND THEIR LINKAGE TO SHELF-EDGE DELTAS

The shelf-edge trajectory, whether rising, flat, or falling, reflects the degree of aggradation or degradation at the shelf edge. This trajectory is largely controlled by the imbalance between the rate of relative sea-level change and the rate of sediment supply; a flat, highly prograding shelf-edge trajectory reflects stillstand to slightly falling relative sea level and implies that much of the sediment budget reaching the shoreline bypassed the shelf edge and was delivered into deep water. This scenario favors the generation of a sequence boundary and the deposition of thicker and more extensive deep-water fans, as happens in the Lewis clinothems (Figures 3.3 and 3.5). Low accommodation therefore drives the progradation of the shelf margin and delivery of sand to deepwater areas.

However, fans are also present in all cases of rising shelf-edge trajectory (contrast with Johannessen and Steel, 2005), implying that they were generated when deltas arrived at the shelf edge even under conditions of rising relative sea level (and so without the generation of a sequence boundary), and even after significant sediment storage on the aggrading shelf (Figure 3.4). These fans, albeit smaller, still reflect significant delivery of sand into the deep-water areas. Such delivery supports the hypothesis by Burgess and Hovius (1998) (i.e., highstand fan generation); however, I stress that this scenario in moderately wide shelves is largely controlled by a high sediment supply, as suggested by Porębski and Steel (2006). The key role of a high sediment supply is that it is able to force the progradation of deltas and/or strandplains to the preexisting shelf edge despite rising relative sea level, and this is more easily achieved where shelf gradients are low and shelf currents do not rework much sediment along strike. Once deltas are at the shelf edge, then slumping, hyperpycnal flows, and other processes may cause turbidity currents and allow bypass of sand to deep-water areas (Piper and Normark, 2001). In this

scenario, therefore, high supply drives the progradation of the shelf margin and delivery of sand to the slope and basin floor (Figure 3.4).

Thus, it is likely that in cases of documented high sediment supply, the shelf-edge trajectory, rather than predicting the presence or absence of deep-water fans (Johannessen and Steel, 2005), would instead predict how voluminous these fans are. Flattish trajectories are linked to thicker and more extensive fans, whereas rising trajectories are linked to smaller fans (Figure 3.5).

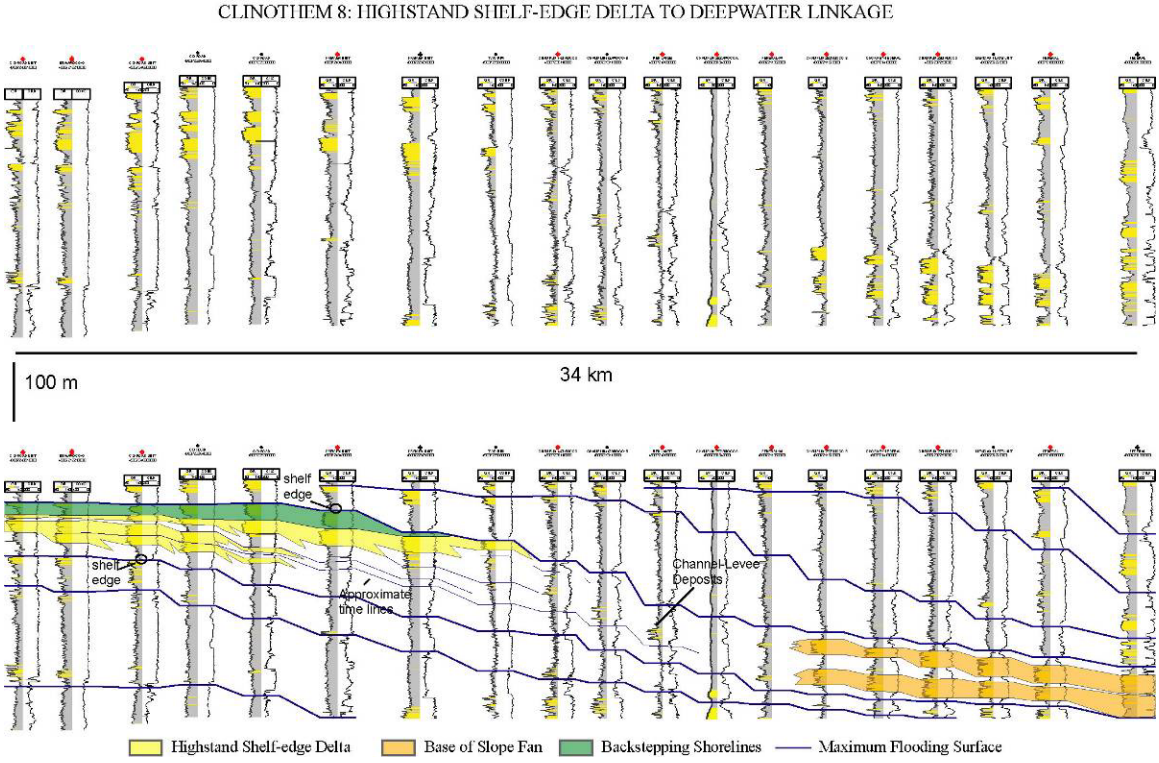

Figure 3.4: Linkage of highstand shelf-edge deltas to the slope and proximal areas of deepwater fans.

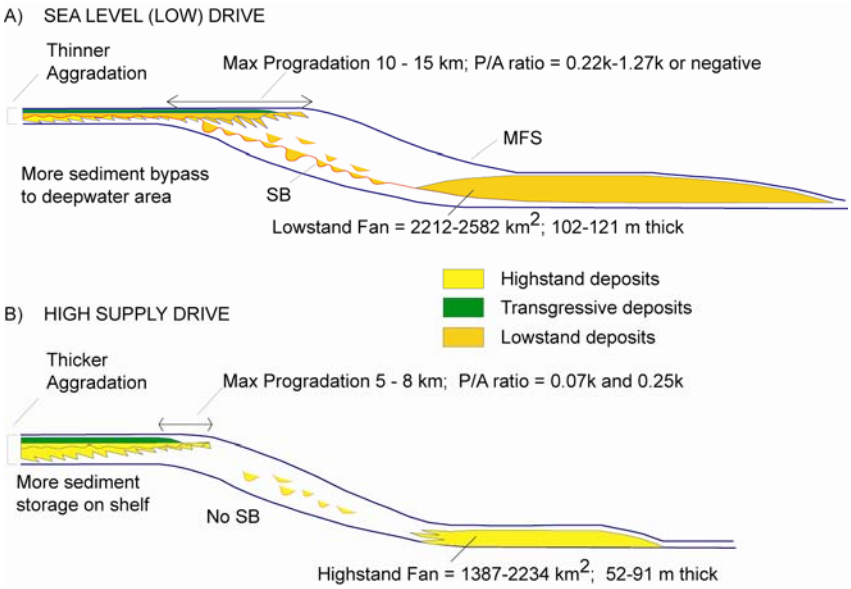

Figure 3.5: Sea level (Low) and supply drive on deepwater sand bypass.

CONCLUSIONS

Thick and aerially extensive deep-water fans were formed in the Lewis Shale basin of southern Wyoming, regardless of whether the updip-linked Fox Hills shelf-edge trajectory shows a rising or falling tendency for any particular or group of delivery cycles. This indicates that submarine fans can develop either during sea-level lowstands (as conventionally predicted) or highstands. For the success of this scenario, the shelf delivery system needs to qualify as high supply, with typically high rates of shelf-edge accretion. In such high-supply shelf-margin systems, the deep-water fan volumes may be large even during highstand delivery, but fan volumes will become greater with the lowering of the shelf-edge trajectory and increase of the progradation distance, reflecting times of bypass of larger volumes of sediment to the basin floor.

CHAPTER 4: RIVER WAVE AND TIDE INFLUENCE ON SHELF-EDGE DELTAS: SIGNIFICANCE OF SAND BYPASS AT HIGHSTAND AND LOWSTAND OF SEA LEVEL

ABSTRACT

The interaction of river, tide and wave influence in deltas is complex; and variability of sea level, sediment supply and coastal morphology further complicates how sediment is dispersed and stored on the shelf as a result of these interactions. For shelf-edge deltas, understanding this interaction is critical, because it will control shelf margin accretion rate/style as well as the absolute amount of sediment delivered to deepwater areas beyond the shelf edge. I address this problem in the Washakie and Great Divide basins of southern Wyoming (Maastrichtian) by using outcrop and subsurface data to interpret facies, architecture and paleogeography. For two shelf-edge delta complexes, I analyze processes and their evident impact in coastal morphology, as well as on deepwater sediment delivery at sea-level lowstand and highstand.

At sea-level highstand, river and wave influence on the deltas resulted in significant coastal progradation, aggradation and sand bypass to the basin floor. Rivers evidently supplied large volumes of sediment for delivery onto the shelf-edge area and beyond, most likely through hyperpycnal flows and mouth bar failure. Also by regular channeling, rivers generated shelf-edge conduits that turbidity currents most likely used to access the deepwater slope. In contrast, there is little evidence that wave processes themselves resulted in significant bypass of sandy sediment. However waves induced strong alongshore drift that vigorously built the coast and when this drift intersected canyon heads extending to the shelf edge, it would have been able to supply sand for bypass. In addition, drift strength was high enough compared with riverine outflow to create an asymmetric coastal distribution of sand with sandier areas up-drift respect to

river mouths. Furthermore, the alongshore currents seem to have been strong enough to deflect mouth bars, and so influence the direction of slope channels and, in turn, the orientation of fan lobes. The fact that there was mappable coastal and shelf-edge accretion as well as significant sand bypass to the basin floor during intervals of sea-level highstand undoubtedly reflects a high sediment supply to the Laramide basin.

At sea-level lowstand, river and tidal processes coexisted in the deltas. Smaller sand volumes were trapped and stored along the outer-shelf and shelf-edge coastlines, and measurably greater volumes of sand were funneled to the deepwater areas. As at highstand, rivers generated channels at the shelf edge, but these channels seem to have been more prominent. Also mouth-bar failure and hyperpycnal flows probably created underflows and ignited turbidity currents to transport sand to deepwater. Incisions and possibly birdfoot-delta geometries apparently created a more irregular, indented coast, where tidal currents were amplified and left strong tidal signatures in the deltas. It is also possible, because of tidal current circulation in the basin, that tidal currents brought distantly sourced sand that became available for bypass. Also tidal influence is known to be strong in some present slope canyons and may be able to transport sand to deepwater. In our case, dominance of flood tides in the shelf-edge area likely precluded much down-canyon tidal transport. However, even where tides transported sand to canyons, the sand would be incorporated into subsequent turbidity currents, losing their tidal signature.

INTRODUCTION

River, tidal and wave influences are the main process components in deltas, to the point that we classify deltas according to the relative prevalence of these processes (Galloway, 1975; Galloway and Hobday, 1996 p. 102). Emphasis on the dominance of one process through time has produced reasonably good models to predict delta geometry, internal architecture and overall coastal building. However although not intended by Galloway (1975), emphasis on end members

has tended to narrow our view of deltas by downplaying the potentially complex interaction among these processes within the same delta complex (Giosan and Bhattacharya, 2005). Further narrowing this view, in the present world our natural database contains mainly examples of deltas during highstand of sea level and icehouse conditions, and sited at the inner to mid shelf locations. Moreover, recent research has call attention to the possible process evolution that may take place in deltas as they make cross-shelf transits to the shelf edge (Yoshida et al., 2007); an evolution additionally complicated by whether such transit happens during rising or falling relative sea level (Porębski and Steel, 2006).

When deltas are sited at the shelf edge, process interaction and evolution are not only important to predict overall deltaic and coastal architecture, but they are also important to predict shelf-margin accretion and sand bypass to deepwater areas (Porębski and Steel, 2003) . For such prediction, fluvial domination has been emphasized because many modern and ancient deepwater fans are clearly linked to rivers (Kolla and Perlmutter, 1993; Flood and Piper, 1997; Posamentier and Allen, 1999; Plink-Björklund and Steel, 2004; Johannessen and Steel, 2005; Petter and Steel, 2006). However, waves and tides also influence shelf-edge deltas, and complexly interact with and at times provide an energy fence to the river processes; this interaction in turn will be further molded by sea-level position and sediment supply. As a result, sand bypass may not only result from strong river drive, despite its obvious importance, but waves and tides may also contribute to such bypass resulting in distinctive coastal-to-deepwater sandstone architectures.

I use an outcrop and extensive well-log database from the southerly migrating clinoforms of an accreting Maastrichtian shelf margin in the Washakie and Great Divide basins of southern Wyoming (Figure 4.1). Through outcrop facies analysis on the clinoform ‘topsets’, I characterize strongly contrasting processes in two shelf-edge delta complexes (and associated coastal-plain deposits) that are located along eastern and western reaches of the south-migrating shelf margin. Through subsurface correlation, I then calibrate the outcrops to the topset, slope and basin-floor

segments of individual shelf-margin clinoforms. This type of shelf-edge delta to deepwater linkage has been demonstrated previously in excellent two-dimensional exposures from Spitsbergen (Plink-Björklund et al., 2001; Mellere et al., 2002; Plink-Björklund and Steel, 2002, 2004; Petter and Steel, 2006). Here I build on this work, adding data on along-strike shelf-edge variability and its influence on coastal morphology, deepwater sandstones and sea level. Although I conclude that coastal river processes are critical for the bypass of large volumes of sand, waves and tides may also contribute to such bypass.

GEOLOGIC SETTING

A well developed shelf margin existed in the Washakie and Great Divide basins of southern Wyoming during the Maastrichtian (Asquith, 1970; Winn et al., 1985; Winn et al., 1987; McMillen and Winn, 1991; Pyles and Slatt, 2000; Carvajal and Steel, 2006). Although these basins presently form two structural troughs separated by the Wamsutter Arch, in the Maastrichtian they constituted a large, single deepwater depocenter. Presence of neritic to bathyal (~400 m undecompacted) water depths in this depocenter marks a sharp contrast to the Late Cretaceous history of the western interior United States that was dominated by a shallow-water foreland basin (DeCelles, 2004). In the Maastrichtian, however, the Wind River Range, Granite Mountains and Rawlins Uplift area underwent significant thick-skinned uplift, causing great tectonic subsidence of the adjacent basin (Reynolds, 1976; MacLeod, 1981; Steidtmann and Middleton, 1991; Connor, 1992) (see chapter 2). Subsidence was asymmetric, much greater toward the east in areas adjacent to the rising uplifts. Localized rapid uplift and subsidence represented the early, but prominent stages of the Laramide Orogeny, a mountain building and basin development episode that over time affected the complete Rocky Mountain Region, breaking up the former wide foreland basin (Dickinson et al., 1988; Steidtmann and Middleton, 1991; Steidtmann, 1993).

Maastrichtian infilling of the study basin was initially outpaced by subsidence, resulting in development of deepwater (>600 m at times) and an accreting shelf margin with a clear topset, slope and basin-floor morphology. With inclinations <1-2 degrees, the slope height is ~430 m (un-decompacted), providing a minimum estimate for basinal water depth from shelf edge to basin floor. Water depth was not the same across the deepwater areas; subsidence was greater toward the eastern margins of the basin and so clinoform amplitudes and water depths increased from west to east.

The integrated fluvial-to-shelf-to-deep-marine depositional system in the margin is grouped in the Lance Formation, the Fox Hills Sandstone and the Lewis Shale. It encompasses 1.8 my duration in the Lower Maastrichtian and contains the *Baculites Eliasi*, *B. Baculus*, *B. Grandis* and *B. Clinolobatus* ammonite zones (Winn et al., 1987; Kauffman et al., 1993). The Lewis Shale contains deep-water shale and siltstone with abundant deepwater sandstone (informally referred as the Dad Sandstone) in successions up to 762 meters thick (Winn et al., 1985; 1987). The Fox Hills Formation represents the sand-prone shoreline to shelf succession and is up to 214 meters thick in southern Wyoming (although maximum thickness estimates may vary significantly according to different authors, see Gill et al., 1970; Steidtmann, 1993), whereas the Lance Formation, also exceeding 200 meters in the Rock Spring Uplift, is a coal-bearing paralic to alluvial plain succession. The vertical succession of these three units mirrors a partial, lateral time equivalence. The upstream Lance fluvial system fed sediment out into the Fox Hills deltas and shorefaces, and the latter, in turn, fed sediment down into the deeper water Lewis system (Weimer, 1961b; Land, 1972; Winn et al., 1985; Winn et al., 1987). High sediment supply, mainly sourced from the north, caused vigorous southern progradation of this integrated system (Gill et al., 1970; Winn et al., 1985; Winn et al., 1987; Perman, 1990; McMillen and Winn, 1991; Carvajal and Steel, 2006).

METHODOLOGY

The methodology integrates outcrop facies analysis with subsurface well-log correlation. I describe two main outcrops, one in the Rock Springs Uplift (west), the other near the Rawlins Uplift (east) (Figure 4.1) and both known from mapping to be at the shelf-edge area. The exposures correlate with the lower segments of the *B. Clinolobatus* ammonite zone (Weimer, 1961b; Gill and Cobban, 1973; Kauffman et al., 1993) placing them in the upper, Lower Maastrichtian. However the outcrop in the west is slightly older than that in the east and subsurface correlation shows that they belong to two consecutive cycles; clinothem 9 (west) and 10 (east) (Carvajal and Steel, 2006). The outcrops and their subsurface equivalents exhibit sharp contrasts in their processes, architecture and sandstone distributions making them suitable for investigating contrasting shelf-edge processes, relative sea-level behavior, and the impact that these deltas had on deepwater sand accumulation.

In the outcrops, using standard sedimentological methods, I have characterized and correlated facies associations to infer process and stratigraphic architecture. Although most of the exposures are good, the upper third of the eastern outcrop is covered and I obtained data from excavated trenches. My sections are closely spaced and I can walk many beds and surfaces along exposures facilitating correlation. In addition, to improve outcrop correlation and to calibrate well-log trends to possible processes, I collected gamma-ray logs for each stratigraphic section. These logs are also very useful for correlating the outcrops with subsurface well-log cross sections, which I have extended to near the exposures to improve confidence in the subsurface-outcrop tie.

The subsurface correlation is based on ~520 wells, most with gamma-ray (or spontaneous potential) and conductivity curves. Correlation is based on the determination of genetic sequences (Galloway, 1989) or clinothems (Rich, 1951), which emphasize transgressive shales to subdivide stratigraphy. Correlation of the outcrops to the subsurface well logs allows a basin-

scale tracing of individual cycles and therefore the mapping of their strike variability along the shelf-edge, slope and basin floor.

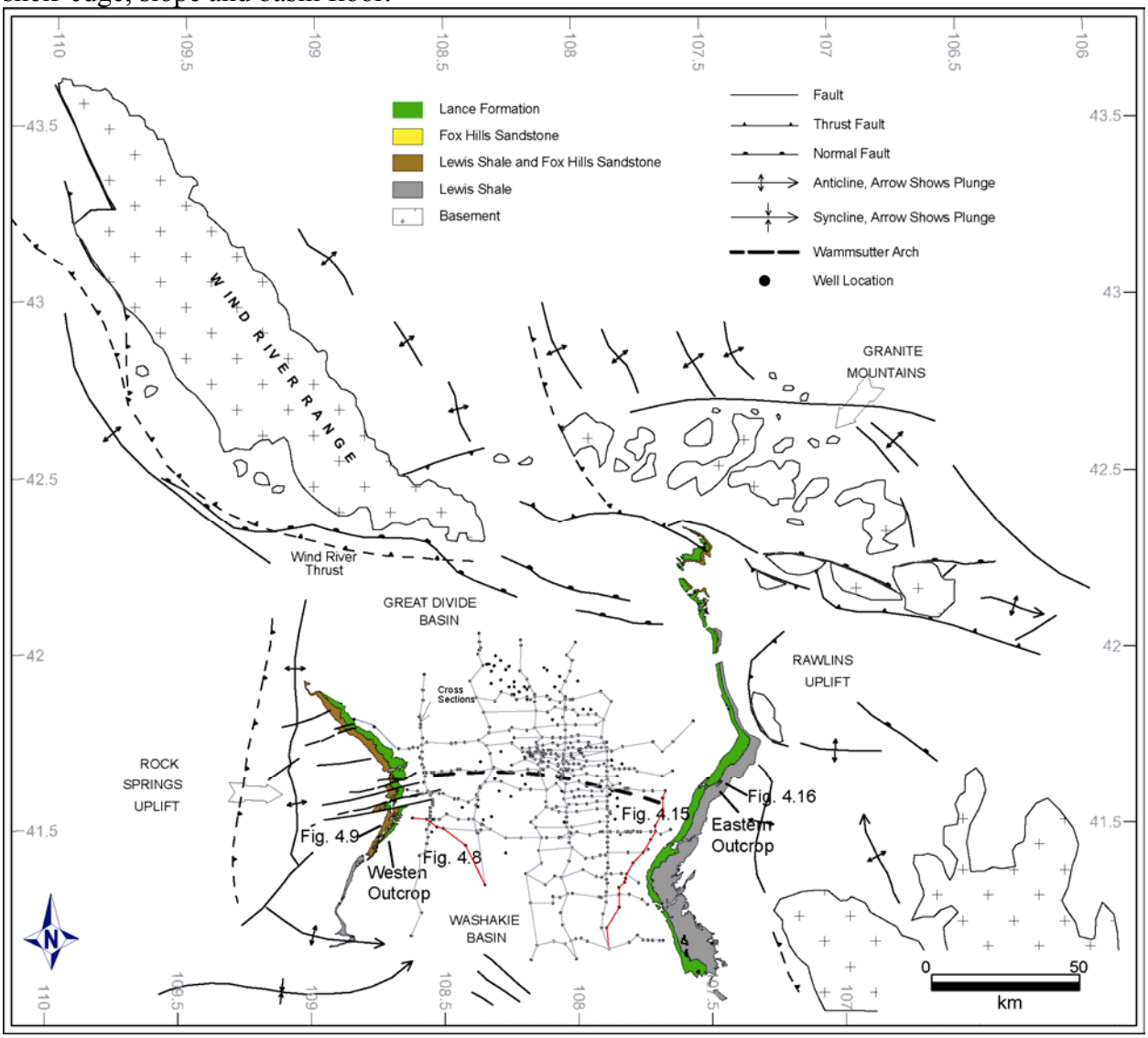

Figure 4.1: Location of study area with wells and cross-sections referred to in the text. Western and eastern outcrops are also shown.

COASTAL REGIME AND LINKED DEEPWATER SETTING ON THE WESTERN BASIN MARGIN

The study outcrops along the western reaches of the basin margin occupy the clinothem 9 topsets, and contain delta, estuary and coal swamp deposits (Land, 1972). Toward the lower half of this succession, prominent progradational to aggradational packages of deltaic sandstones contain clear evidence for strong wave influence. These deposits occupy the western margin of a sand-prone, shelf-edge succession that passes eastward along strike into co-eval strata with major fluvial channels, demonstrating the overall deltaic origin of this association. The wave-dominated deltaic deposits are overlain by tidally influenced sandy estuarine deposits, a change interpreted in terms of the onset of transgression across clinothem 9 (Figure 4.2). Continued aggradation of clinothem 9 topsets gave way to swamps with peat. Thin mudstones mark the climax of transgression across this clinothem, after which there was renewed progradation of clinothem 10 wave-dominated deltas. Fluvial feeder channels are scarce along the study outcrop, suggesting that the area was not along main distributary-channel fairway; this lay farther east in coeval deposits.

Depositional Environments

Wave-Dominated Shelf-Edge Deltas

High-Energy, Storm-Wave Dominated Upper Delta-Front Facies Association

Description: This facies consists of very thickly bedded sandstone dominated by swaley and hummocky cross-stratification, as well as low-angle laminations (Figures 4.2 and 4.3). The sandstones are very fine to fine grained and occur in packages < 17 m thick that exhibit a slight upward-coarsening occasionally accentuated by a basal shale. Upward coarsening in the outcrop packages is shown clearly in funnel-shaped gamma-ray log patterns. In some locations, individual sets of hummocky, swaley and low-angle laminae are some 30 cm thick; otherwise amalgamation makes it difficult to distinguish individual sets. Rarely present are sets with convolute laminae and pockets (<15 cm wide) of sandstone pebbles (<3 cm). Although

uncommon, gutter casts mark the bottom of sharp-based sandstone units. The casts are relatively wide and shallow and filled by sandstones with hummocky laminae. Bioturbation is low and largely restricted to *Ophiomorpha* traces with well developed pelleted walls, lengths < 10's cm and occasional structures of barely interconnected burrows.

Interpretation: Hummocky, swaley and low-angle laminations suggest deposition from strong oscillatory flows formed by storm waves during frequent storm events at the shoreline (Harms et al., 1982; Dumas and Arnott, 2006) (Figures 4.2 and 4.3). Upward coarsening of sandstone units indicates upward shallowing and basin infilling through pulses of shoreline progradation (Van Wagoner et al., 1990, p. 8). The sandiness of the shoreline suggests that between storms the coast remained of relatively high energy, so as to keep mud in suspension; or alternatively successive storms were strong enough to erode the mud deposited during fair weather intervals. Storms were also strong enough as to scour the muddy sea floor of distal shoreline areas and transport sand to these places forming sharp based sandstones with bottom gutter casts filled with hummocks (Einsele and Seilacher, 1991; Seilacher and Aigner, 1991). The overall regime during coastal construction was therefore one dominated by high-energy storm waves. This was a highly stressed environment for organisms to inhabit, a stress further enhanced by possible brackish water incursions from nearby riverine outflows. These conditions would have prevented thorough bioturbation of the marine substrate and erosion from successive storms would have removed bioturbated beds (MacEachern et al., 2005). In addition, eastwards in the subsurface along strike on the shelf-edge, these sandstones are linked to major fluvial feeder channels (Figures 4.5 and 4.6) demonstrating that this shoreline system was a delta influenced by strong waves rather than a strand plain (Bhattacharya and Giosan, 2003).

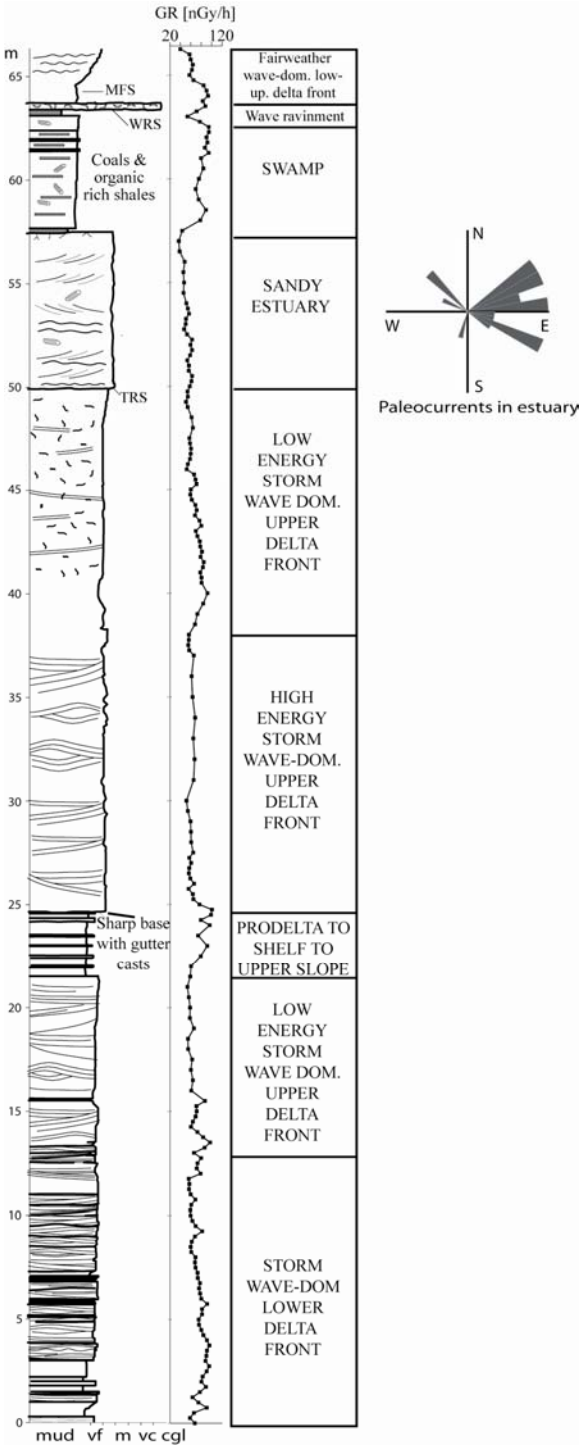

Figure 4.2: Outcrop log through the shelf-edge area at the western outcrop.

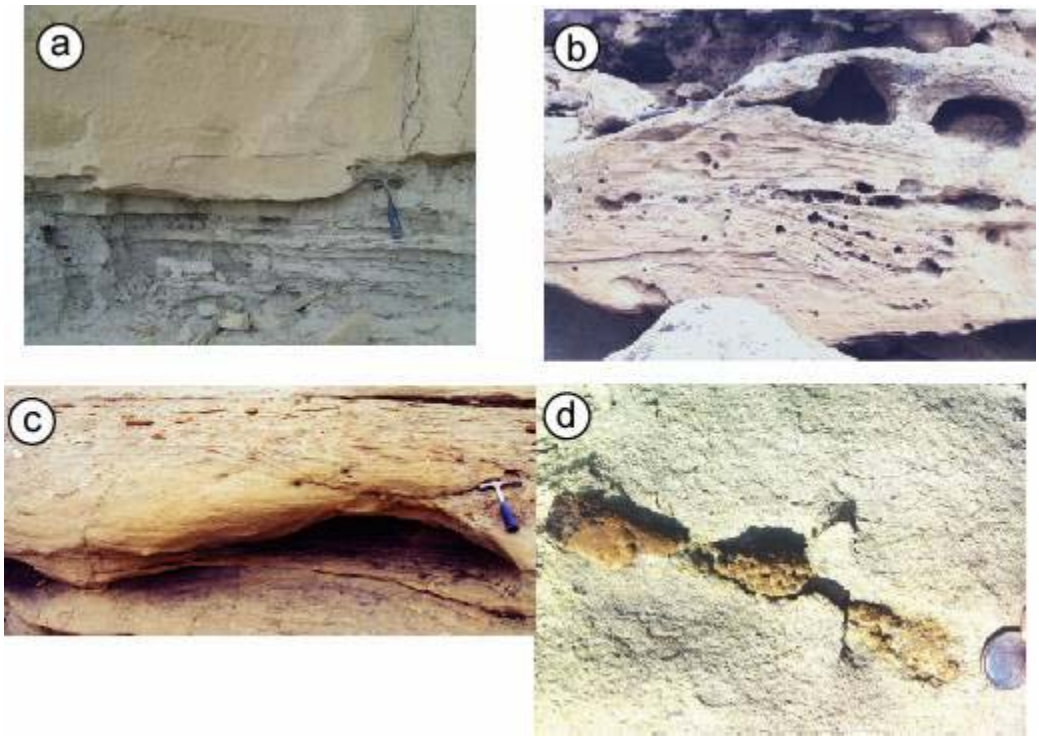

Figure 4.3: Structures and bioturbation in wave dominated shelf-edge deltas of the western outcrop. Gutter casts at the base of hummocky bedded sandstone (a), hummocky and swaley cross stratification (b, c) and *Ophiomorpha* burrow (d).

Low Energy Storm-Wave Dominated Upper Delta-Front Facies Association

Description: This facies is also characterized by units of thick, very fine to fine-grained sandstones with upward-coarsening motifs. However in many locations these sandstones are thoroughly bioturbated as clearly shown by networks of abundant burrows. In other areas, burrows are barely distinguishable and the sandstone appears more structureless. The trace fossil assemblage is largely monospecific, composed by *Ophiomorpha.* Only in few places are well-developed, low- angle laminations discernable.

Interpretation: These sandstones have many features in common with the previous facies suggesting a similar origin in deltaic shorelines. These features include their vertical and laterally conformable juxtaposition, their similar thickness, upward-coarsening motifs and connection to fluvial feeders farther to the east. However, the environment here was much less stressed so that sands could be abundantly burrowed and preserved. Fresh water river outflows could still have reached the area because of the observed connection to eastwards rivers (Figures 4.5 and 4.6). This possible freshening may explain the apparently reduced diversity in the trace fossils assemblage which otherwise should be high under purely marine conditions (MacEachern et al., 2005). I attribute the reduced stress to a decrease in energy due to a diminished storm impact in the area. Such a decrease would not only have allowed increased bioturbation but, more importantly, increased preservation by reducing the rate at which recently bioturbated sediments were removed by successive storm events. Decreasing storminess may be achieved through a change either in climate, in the impact angle of coast-approaching swales or in the coast morphology by creating more protected shoreline segments. Without ruling out the former, based on the immediate position of this facies below tidally influenced sandstones interpreted as transgressive, I suggest that a change in coastline morphology was likely already underway during this facies deposition.

Storm-Wave Dominated Lower Delta Front Facies Association

Description: This facies consists mainly of interbedded sandstone and shale in packages usually < 10 m thick (Figure 4.2). In most cases, it lies conformably below the low energy deltas previously described. The sandstone beds in packages tend to thicken and become coarser-grained (low-upper very fine) upwards from basal shales and very fine-grained sandstones. Within each package, smaller scale, but similar motifs may be

present. Sandstone-shale contacts are occasionally gradational, but are commonly sharp and erosive. Sandstones are generally hummocky cross-stratified and trace fossils include *Ophiomorpha*. Shales are light gray, generally flaggy to fissile, calcareous and carbonaceous (small dark organic particles <3%).

Interpretation: The conformable contact with upper delta-front deposits, stratal organization into upward coarsening packages and hummocky cross strata indicate that this facies is simply a distal equivalent of the wave-dominated, upper delta-front deposits (Harms et al., 1982; Walker, 1984; Bhattacharya and Giosan, 2003). Preservation of intervening mudstone layers suggests much of the lower delta front was below fair-weather wave base, but above storm wave base, as indicated by the hummocks. As a result, sand leaden storm flows were able to scour the muddy sea floor and so generate sharp and erosive contacts.

Fair-weather Wave-Dominated Lower to Upper Delta Front Facies Association

Description: This facies is at the top of the outcrop study section and consists of sandstones, shales and shell conglomerates with a total thickness < ~8 m (Figure 4.2). Vertically, stratification is well organized into a basal shell conglomerate below a shale and sandstone succession ordered in an upward thickening and coarsening trend. The basal conglomerate has a highly variable thickness (< 70 cm) and is supported by the shells, typically broken. It marks a sharp transition from the coaly and muddy deposits of the swamp facies (described below) upwards to this facies, thereby representing a drastic change in lithology, bed stacking pattern and as discussed depositional environment. Overlying sandstones in the middle of the succession are cross-stratified and toward the top present thick (<2 m) ripple cross laminated intervals. Bioturbation is low.

Interpretation: The upward thickening and coarsening trend in the siliciclastic succession mimics the trends observed in the underlying deltaic succession. However in this case we did not observe hummocks or swales, but wave rippled intervals and therefore we interpret the succession as formed in wave-dominated deltas under a fair-weather wave regime. The succession thus records upward shallowing from distal delta front shales and therefore a shoreline transgression over the area previously occupied by the swamp. In this sense, the basal shell conglomerate represents a nearshore environment in which waves accumulated shells as the shoreline transgressed over the area. The basal conglomerate surface is therefore a wave ravinement surface (WRS).

Prodelta to Shelf to Upper Slope Facies Association

Description: This facies consists of mudstones with thin sandstones, and conformably underlies the sand-prone delta-front deposits (Figure 4.2). It forms thick (10's m) outcrop slopes. It also interfingers with the delta-front deposits as thinner (<10 m) mudstone tongues. Weathering has created a thin cover on the mudstone that when removed reveals a carbonaceous, dark gray, calcareous mudstone, commonly with some few thin sets of very fine-grained and hummocky cross-stratified sandstone, and containing burrows of *Arenicolites* and *Rhizocorallium (*Land*,* 1972*)*. Organism trails also occur on sandstone bedding planes.

Interpretation: The conformable contact and interfingering with deltaic facies and its mudstone rich composition indicates that it represents prodelta to shelf areas, opening onto the upper slope where the muddy units become thicker. The area was below fairweather wave base, but based on the hummocky sandstones, the area could still receive sand from episodic strong storm events (Frey and Pemberton, 1984; MacEachern et al., 2005).

Estuary and Swamp

Sandy Estuary Facies Association

Description: This facies consists of fine-grained sandstone units up to 12 m thick, dominated by sets of planar and trough-cross strata (Figures 4.2 and 4.4). Everywhere across the study area, and within the same clinothem, this facies overlies the wave-dominated shelf-edge deltas and usually lies directly on the highly bioturbated sandstones. The contact between these two lithosomes is an irregular, low relief (< 1-2 m) erosion surface across which grain size increases slightly. At a few places there are vertebrate bones and red (brick-like) coloration above the sharp surface. Cross-strata sets thin upwards from ~70 cm at the base to < 10-15 cm toward the top. Thick sets tend to taper laterally forming wedge geometries with ripple cross laminations in their bottom sets; thin sets appear to be more tabular. Some sets are laterally separated by inclined planar surfaces across which there can be slight dip changes. These surfaces may also be more irregular suggesting some erosion. Thick sets show coaly laminations draping foresets and bottomsets, at times bundling thicker and thinner sandy foreset laninae. Coaly laminations drape ripples and erosive surfaces. Bi-directional cross strata are present at some locations in herringbone cross-bedding (Figure 4.4). Foreset paleocurrents are bidirectional trending north-east, south-east and north-west. Abundant small wood fragments (<10 cm) occur on some bedding planes, at times in association with bivalves. Bioturbation is relatively low; we have observed traces of *Planolites* and some fossil wood contains *Teredolites*. The upper contact of this facies is sharp and relatively flat, marked by an abrupt transition from sandstone to a coal bed (<30 cm, although it is unclear whether the coal bed is the same across the area). From this contact, a horizon of root traces penetrate downwards into the sandstone to very shallow depths (<

~2-4 cm); the roots have a tight spacing (few cm to few m), a branched structure and are present everywhere across the area.

Interpretation: Wood fragments, vertebrate bone fossils, root traces, lack of a marine fauna and low bioturbation generally indicate a brackish to non-marine, sub-aqueous environment for this facies. To judge from its vertical position immediately above regressive shoreline deposits, its close proximity to the shelf-edge and the presence of *Teredolites*, the environment was marginal marine with brackish salinity. A lagoon or estuary are possible environments, but I favor an estuary from the presence of relatively high-energy 2-D and 3-D dunes, and from the subsurface presence of linked fluvial channels (albeit connected at some distance to the east). Organic drapes, sometimes in bundles, herringbone cross strata and bidirectional currents demonstrate that ebb- and flood-tidal currents were the main flows transporting and depositing sediment in the estuary (Nio and Yang, 1991). These currents would have transported the coarser sand either from areas close to river outflows or from the estuary mouth in the seaward end of the estuary. Also these tidal currents would have scoured the estuary bottom producing its lower erosive contact -a tidal ravinement surface (TRS). Bedform erosion by flood and ebb tides during estuary filling would have produced truncation and discontinuities within cross sets and compound dunes. The upward-decreasing thickness of these sets suggests that bedform formative flows were of lesser depth through time, indicating that the estuary was being infilled. Shallowing and estuary filling is further supported by the roots at the upper facies contact. Their presence throughout the area, position immediately below a coal bed, downward extension and branching demonstrate that these roots are in situ and belong to the plants that grew in salt marshes and supratidal areas of the system. In these settings, the estuary infill brought a shutting down of clastic detrital supply and allowed widespread supratidal plant growth and accumulation of

autochthonous and possibly allochthonous organic matter, clean enough to form (after burial) the overlying coal beds. This facies, thus, marks a drastic change from the preceding stages of wave-dominated delta deposition; the environment became a tidal-dominated estuary that through time became infilled and eventually evolved to salt marshes and mires.

Swamp Facies Association

Description: This facies is up to 10-15 thick and consists of coal beds and shales. Across the entire area it lies on top of the sandy estuarine facies with a sharp and root-marked contact on which usually lies a coal bed (Figure 4.4). Usually less than 50 cm thick, the coal horizons are tabular and vertically occur in uneven numbers in different sections suggesting that they maybe of local extent, but persistent through the area. Shales tend to be dark, organic rich, some of them with abundant plant fragments. Sandstone beds exist, but are sporadic. At some localities, the upper contact of this facies is marked by an oyster conglomerate occasionally quite thick (<70 cm).

Interpretation: The presence of coal and plant-rich shales in this facies evidently demonstrates a terrestrial, but sub-aqueous highly vegetated environment, possibly a swamp. The setting was still marginal marine however because of its close proximity to the ocean. However the organic rich composition of the facies and scattered presence of sandstone beds indicates that neither ocean tides nor rivers were able to bring coarse detrital sediments to the setting. Surface connection to river outflows or to the ocean was therefore likely ephemeral or non-existent. Through time, these conditions allowed the repetitive formation of mires, from which coal would eventually formed after burial. In addition, water level in the mire had to be delicately maintained; too high or too low and the mire is submerged or exposed and does not develop (Bohacs and Sutter, 1999). At

these times and also during accumulation of shales the environment was below the water table as to remain sub-aqueous. This indicates that through time the water table level had to rise to accumulate the ~12 m (more if decompated) thickness of this facies.

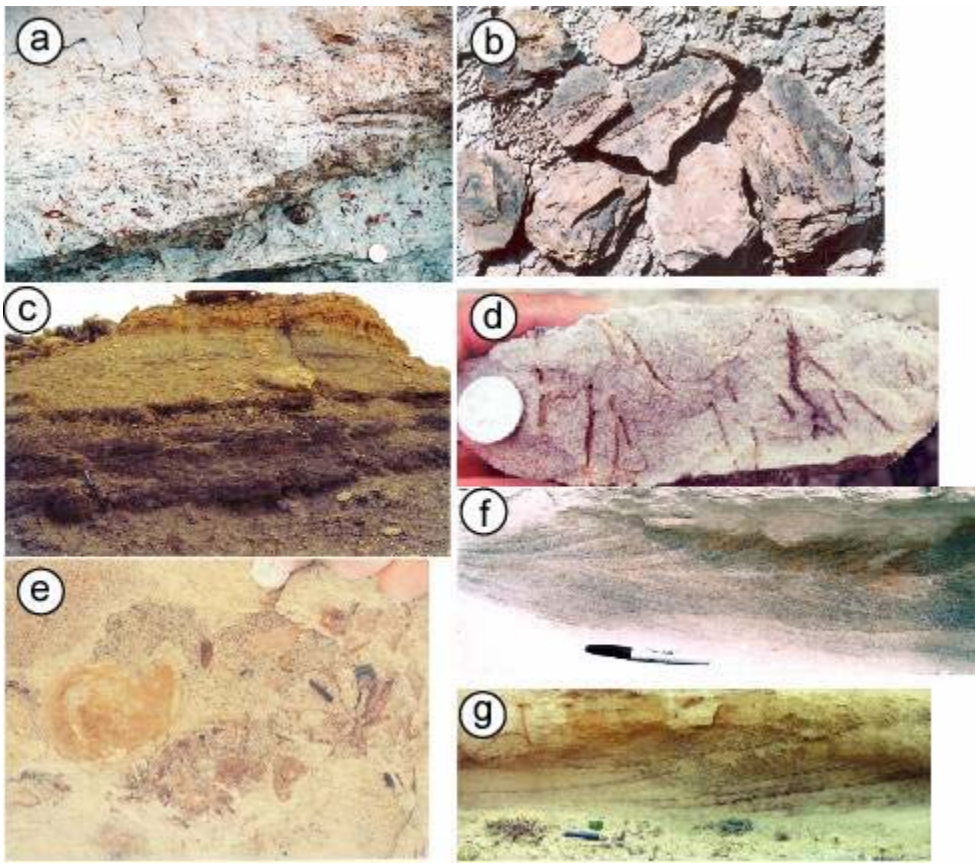

Figure 4.4: Estuary and swamp deposits. Shell conglomerate (a), plant imprints in organic-rich shales (b) and coals and shales overlain by shoreline deposits. (c). In estuary deposits, roots at their top (d), bivalve casts, (e) herringbone cross bedding (f) and planar cross sets with organic rich drapes.

Fluvial Channel Facies Association

Description: This facies is restricted to a single exposure, present toward the outcrop top. Contained within the swamp facies, its outcrop is laterally discontinuous fading out over a short distance laterally. It is composed of sandstones and conglomerates reaching a composite maximum thickness < 7 m. Marking the base of the succession, the main conglomerate is ~ 2m thick, with sub-angular mudstone clasts (< 5-10 cm) barely supported by a medium-grained sand matrix. With the same characteristics, a few thin (10 cm) conglomerate lenses are within the 1.5 m section on the basal conglomerate. Sandstones are medium-grained and trough-cross stratified with eastward (basinward) oriented foresets.

Interpretation: The coarse texture of this facies with basal conglomerates and medium grained sand along with the laterally lenticular outcrop architecture clearly indicates strong currents and probable channelized river flow in an otherwise muddy and organic rich coastal plain. This facies represents the only outcrop of fluvial channels I have observed within the length of the outcrop (~15 miles) and as such it does prove that at least at this time, eastward flowing rivers did exist in the area, but that they were ephemeral.

Paleogeography, Coastal Processes and Deepwater Setting

Figure 4.5 and 4.6 show a sandstone isopach map and its interpretation to reconstruct the coastal paleogeography and deepwater environments (see also Figures 4.7 and Figure 4.8). During Fox Hills delta progradation, the main fluvial feeders along the basin axis provided abundant sediment. However, the outcropping fluvial channel indicates that smaller rivers were also present in the western reaches. The morphology of the sand belt along coast shows an elongated, shelf-edge-parallel geometry. This

morphology and the wave processes evidenced in the western outcrop indicate that the complete shelf-edge coastline experience significant wave energy resulting in vigorous shoreline/shelf-margin accretion and aggradation. This wave-driven transport, sediment accumulation, and coastal accretion resulted in an asymmetric sand distribution, with respect to the main river-mouth sites along the basin axis; the thickest sands accumulated in the west indicating a possible eastward littoral drift. In modern wave-influenced deltas, asymmetry of sand distribution is well documented (Bhattacharya and Giosan, 2003). For instance, it occurs in the Danube (Black Sea), Brazos (Gulf of Mexico), Guadiana (Spain and Portugal), Nile (Mediterranean Sea) and other deltas. Such asymmetry reflects the interplay between wave-driven alongshore currents and strength of direct fluvial discharge. Despite wave influence on the delta, the strong river discharge acts as a 'fence', tending to accumulate the largest sand volume on its up-drift side by accretion storage. During times of decreased discharge the river mouth bar becomes deflected in a down-drift direction, with an extreme deflection when river discharge is very weak relative to the alongshore drift. The suggested eastward drift along the coast would have caused N-S channels to swing into NW-SE orientations, perhaps contributing to the observed NW-SE orientation of the long axes of both slope channels and deepwater fans. The presence of these fans and the abundant sand at the shelf edge indicates that the main basin-axis rivers and the smaller rivers in the west provided large volumes of sediment to sustain accretion and deepwater bypass.

The coastal processes and paleogeographic configuration clearly changed during shelf transgression and the accumulation of the estuary and swamp deposits. During this stage much sand was trapped in embayments with significant tidal currents, whereas areas away from detrital input accumulated abundant organic matter to form coal and organic rich shales.

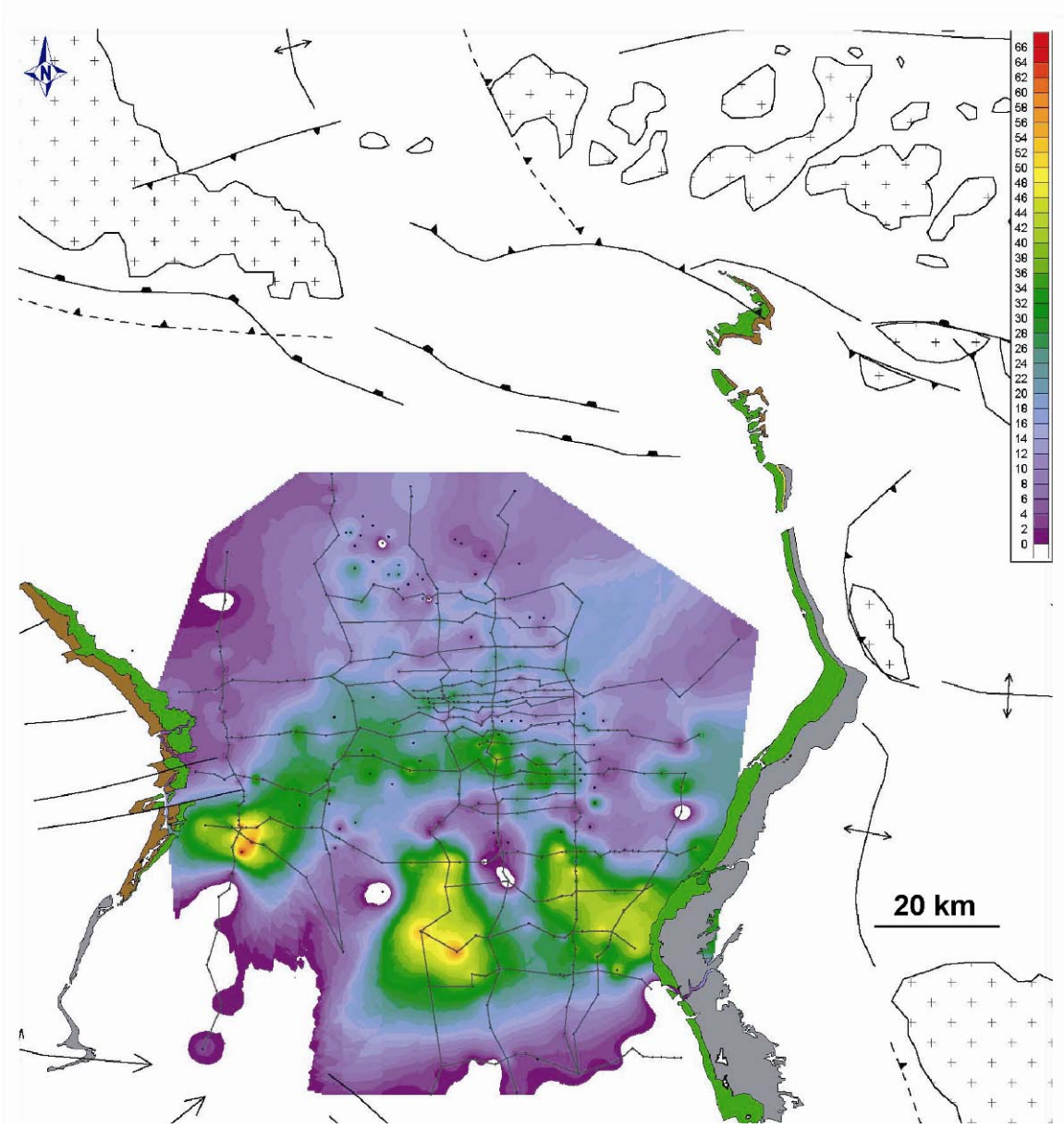

Figure 4.5: Sandstone isopach map (in meters) for clinothem 09 across the study area.

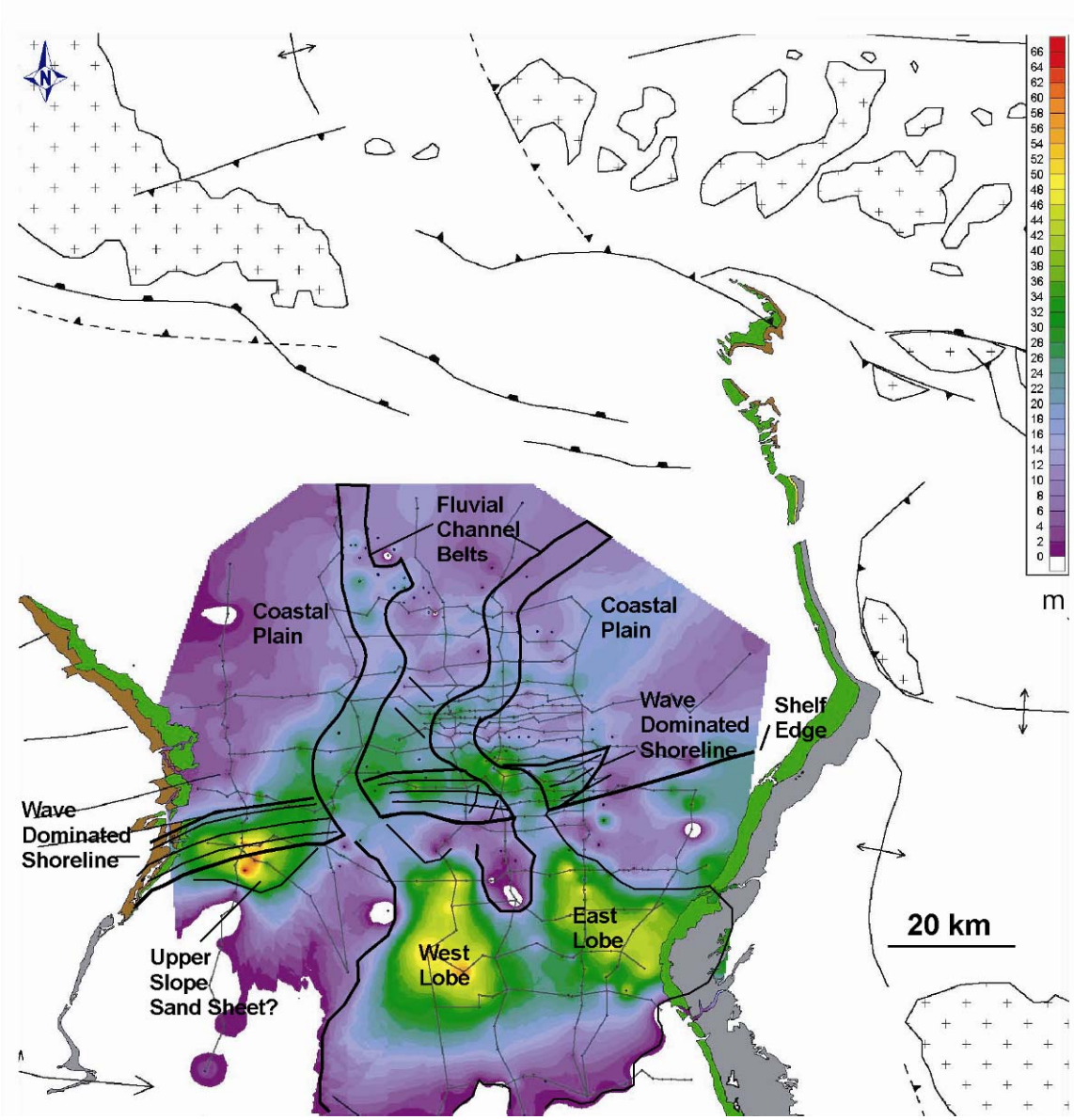

Figure 4.6: Interpreted sandstone isopach map for C09. Notice interpreted wave domination on sandstone belt at the shelf edge as deduced from outcrop evidence. Shelf-edge position at the end of the cycle.

Sea Level

The aggradational stacking pattern of the western deltas (Figures 4.7 and 4.8) clearly indicates that relative sea level was rising. Such aggradation took place while deltas prograded and by definition, therefore, the delta stacking represents a highstand systems tract. Under these conditions, strong wave influence is somewhat predictable, because the high sea level, shoreline positioning at the shelf edge and rapid basin deepening in the the slope beyond the shoreline would have caused large open-ocean waves to break directly against this coastline. Regarding the development of the estuary and associated swamp environments, a rising relative sea level is implied by the rising water table (Bohacs and Suter, 1997). The presence of a marine shale and wave ravinement surface covering the succession is consistent with this rise. Therefore, the entire clinothem succession records an evolution from highstand to transgressive systems tract. The outcrops do not provide any evidence for a sea-level fall; on the contrary, the thick aggradation points to sustained rise of sea level. This rise is consistent with subsurface stratigraphic architecture, because the outcrop is part of a shelf margin section which shows systematic rising of the shelf-edge trajectory, a proxy for sustained rise in sea level (see clinothem 09 in chapters 2 and 3 and Carvajal and Steel, 2006).

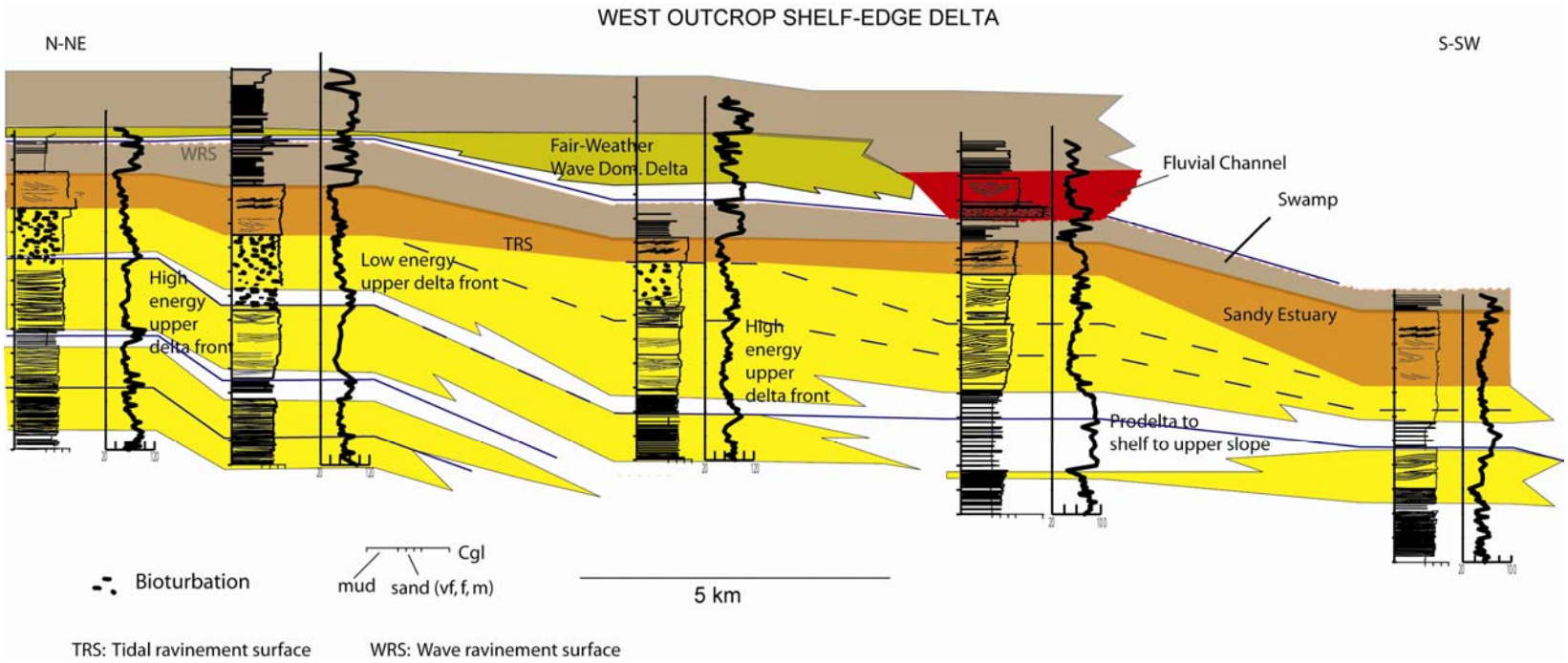

Figure 4.7: Outcrop based cross section up through the wave-dominated shelf-edge delta to estuary and swamp/salt marsh succession in the western outcrop (see Figure 4.1 for location).

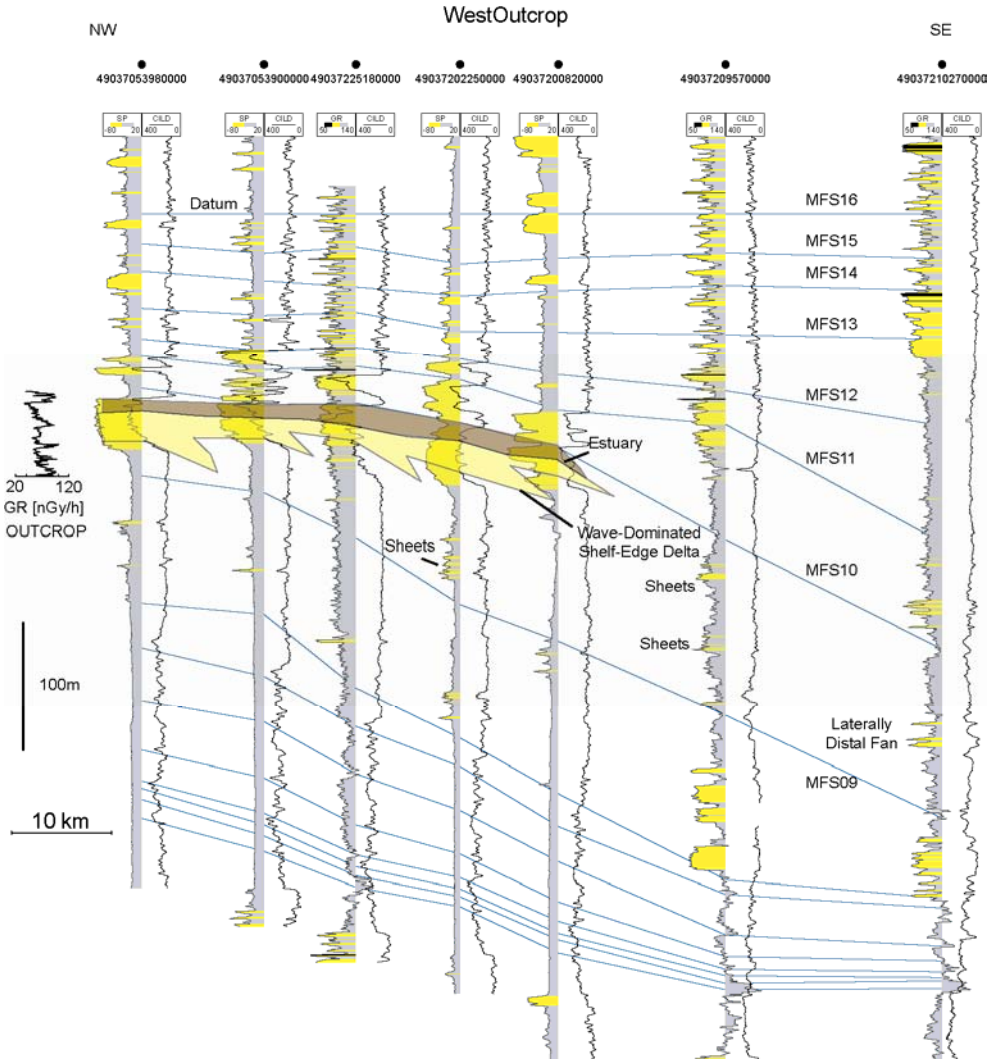

Figure 4.8: Shelf edge to deepwater correlation and log patterns in a cross-section in the western area. Notice the muddy slope in interpreted clinoform. Outcrop log for linkage to subsurface is on the left (see Figure 4.1 for location).

COASTAL REGIME AND LINKED DEEPWATER SETTING ON THE EASTERN BASIN MARGIN

Along the eastern reaches of the basin margin, the shoreline and shelf-edge setting were clearly different from those described in the west. Here, there is no evidence for strong waves, but tidal currents are well recorded both in the deltas and estuaries. However, the primary distinction between west and east is the presence of prominent fluvial channels in the east that incised deeply into the shelf-edge. These fluvial feeders and their shelf-edge deltas connected directly to deepwater slope channels leading to a basin floor fan with very large sandstone volumes. Here in the east there is also evidence to indicate that sea level was not continuously rising, but was stable or falling at times.

Depositional Environments

Shelf-Edge Delta with Mixed Fluvial-Tidal Energy

The tidal- and fluvial-dominated shelf-edge delta facies association includes a main distributary channel that sharply incises foreset strata. The latter are strongly tide- and river-influenced. The two process regimes clearly co-existed in the same regressive package. Volumetrically, the tidal influence on the delta complex is less prominent or preserved than the fluvial influence.

Distributary Channel Facies Association

Description: This facies consists of fine to medium-grained sandstone with prominent 3-D dune sets that form a 6-12 m thick unit traceable in outcrop for nearly 2 km (Figures 4.9 and 4.10). Cross strata sets (<30-40 cm thick) are lenticular and exhibit mostly westward-directed foreset paleocurrents with a subordinate eastward component. Convolute bedding is present in the basinward half of the outcrop and typically restricted

to its lower few meters. Here, deformation of the trough-cross strata progresses from small patchy areas to larger (few-meter scale) deformed intervals. At some locations, it is possible to observe how undeformed sets gradually transition to highly convoluted sets. Rarely present at the base are ripple cross-stratified very thin sandstones, draped by laminations (or slightly thicker layers) of mudstone.

Along the outcrop length, the sandstone unit has basal contact that sharply truncates and incises into underlying foreset strata (Figure 4.9). In proximal outcrop reaches, the truncation has lower relief and sandstone thickness is about 6 m. Basinward, the erosion surface has more relief and the sandstone thickens to ~12 m. At the distal outcrop end, the surface rises, only to cut down again (~1-2 m over ~10-30 m) and continue into the subsurface toward the paleo-slope. Typically sand grain size increases across the basal surface from lower fine-grained below to upper fine- or medium-grained above. At some places, the surface supports thin (< ~20 cm) and discontinuous conglomerate beds, matrix supported and with mudstone clasts (< 5 cm) as well as occasional isolated trunk casts (< 1 m) and big mudstone rip-up clasts (< 20 cm). *Teredolites* is pervasively present in fossil wood. In the sub-surface, this basal erosion surface extends laterally for several km toward the west.

Interpretation: The erosively-based, cross-stratified unit is interpreted as a fluvial channel (Porębski and Steel, 2003) with its basal incision surface resulting from multiple river cuts produced from channel migration. Trough cross strata with mostly basinward paleocurrents, basal conglomerates and tree trunks all indicate strong, river flows that received land-derived material. Very subordinate mud drapes and landward-oriented foresets suggest possible influence by tides and *Teredolites* indicates brackish water and closeness to the ocean. Convolute bedding suggests deformation from fast deposition,

dewatering and increased gradients toward the shelf-edge and slope. However, sand remobilization was very local.

River Mouth-Bar Facies Association

Description: Along the northern edge of the outcrop, a spectacular set of large-scale inclined strata characterizes the river mouth-bar facies (Figure 4.9 and 4.16). The strata consistently dip basinward at steep angles (< 10^{o}) and the river-channel erosion surface truncates them. This facies is mainly fine-grained sandstone beds (typically <70 cm thick) separated by very thin beds or laminae of mudstone. Sandstones beds are continuous over the outcrop length and relatively tabular with only very gentle and quite minor lateral thicknesses variations. They are organized into packages defined by both bed-thickening and thinning upward trends. Individual beds typically show a sharp lower contact with very shallow scours. Upward from this basal contact, beds are usually flat-laminated and toward the top they can show ripple cross-lamination. Some beds are normally graded, with only rare cases of reverse to normal grading. A thin layer of mudstone drapes each bed. Bioturbation in the sandstone beds is rare, but I have observed subvertical to slightly inclined burrows, possibly *Skolithos*.

Interpretation: The inclined stratal architecture, their truncation by a fluvial channel, and their outer-shelf location suggest that these are deltaic foresets at the shelf-edge area. Trends of bed sets thickening and thinning may represent autocyclic shifts of the delta progradation or channel avulsion. The relatively steep foreset inclination is probably due to: 1) deepening of water toward the shelf-edge (Pirmez et al., 1998; Plink-Björklund and Steel, 2005) and 2) small mud percentage in the river effluent. Another possible explanation is that the delta was prograding into a large-scale incision or collapse scar, not an uncommon possibility at the shelf-edge (Cummings et al., 2006).

The sharp and shallowly scoured beds of the delta foresets are dominated by flat-lamination or, in few cases, current-ripple lamination. This indicates tractive deposition in upper-flow regime conditions. Flat laminated intervals up to several tens of cm thick indicate these conditions were sustained for relatively long periods. Normal grading on some beds, ripple lamination towards the top in others and the thin mud cappings in all record waning-flow deposition. The tabular bed geometries suggest that (at the outcrop scale) the flows were unconfined and spread as sheets on the delta front. They may represent fluvial discharge that upon debouching at the river mouth expand sub-aqueously and radially on the delta front as sheets, maintained by their inherited inertia enhanced by gravity. However the overlying fluvial incision surface may indicate that these facies are laterally linked to an incised delta front. Along incised areas, rapid deposition at the river mouth may have caused rapid loading and dewatering which, along with the steep foresets, tended to destabilize the sediments and trigger their collapse. Therefore downstream flows from river mouth to deeper water areas would have been a combination of sediment-laden river underflows and collapsed sediment from the mouth bar.

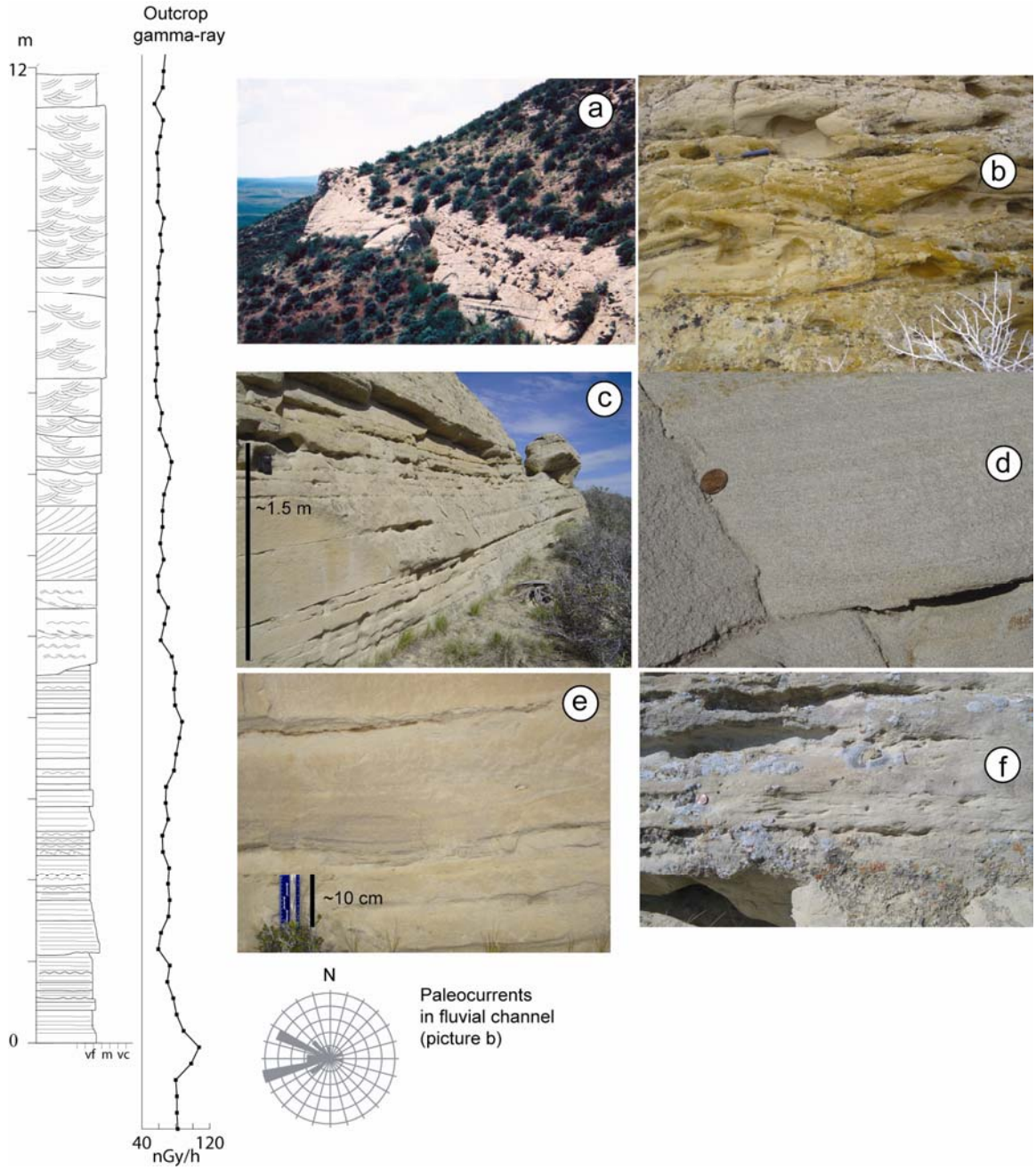

Figure 4.9: Fluvial channel and river-mouth facies associations. The former is represented by through cross beds in upper segment of the outcrop log and photo b. Photo (a) shows truncation-incision surface with foreset strata below and fluvial channel above (sandstone outcrop is ~10 m thick). Tabular beds (c) with flat lamination (d), shallow scours (e) and ripple cross lamination (f) in river mouth bar facies. Rose diagram indicates westward paleocurrents in fluvial channel

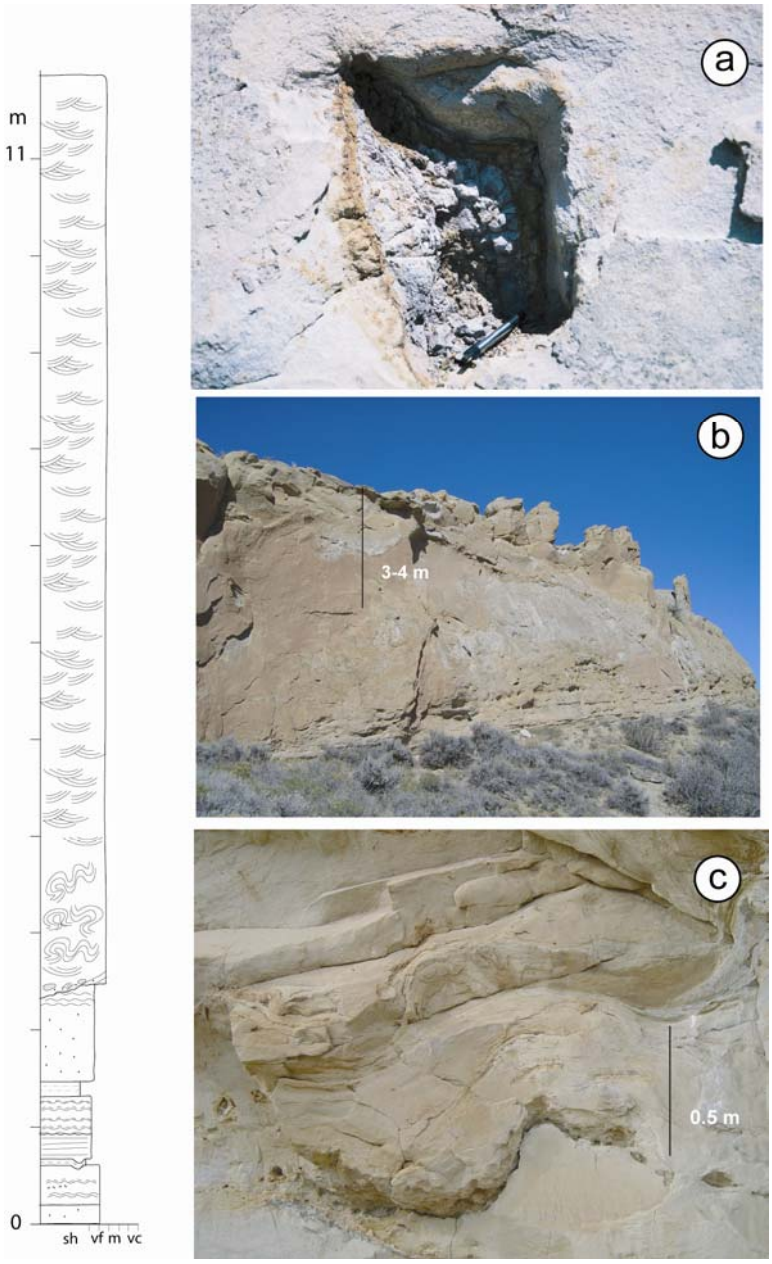

Figure 4.10: Characteristic features of the distal (at or near the shelf edge) segments of fluvial channel. Large pebble (a), highly incising basal surface (b) and slumped beds (c) toward the shelf edge.

Tidally-Influenced Delta-Front Facies Association

Description: This hetherolithic facies is present basinwards from the river mouth-bar facies, and is well exposed where the distributary channel facies is thickest and its basal surface cuts down deepest (Figures 4.11 and 4.16). It is composed of fine to medium-grained sandstone (<60 cm), but with numerous mudstone layers (typically < 10-20 cm). Beds are lenticular with lateral pinchouts over short distances. Sandstone beds exhibit 2D dunes with tangential bottom sets, sometimes ripple cross laminated. Foreset paleocurrents are mainly toward the E and NE; but foresets dipping toward the SW are clearly visible in some sets. Very thin beds (e.g. < ~3 cm) of mudstone commonly drape foresets, bottomsets and ripples, in the latter occasionally forming wavy, flaser and lenticular bedding. Some mudstone laminations look remarkably structureless and non-biouturbated. Locally present are shallow scours and small (<20 cm) load structures. Bioturbation abundance is low, though there are traces of *Planolites, Arenicolites, Chondrites, Conichnus* and *Thalassinoides*. At one horizon, burrows of the latter penetrate downward (< 3 cm) into shale from an overlying sandstone that also fills the burrows, defining thus the *Glossifungites* ichnofacies.

Toward the end reaches of the outcrop this facies is represented by sandstones that are very-fine grained sometimes rhythmically alternating with muddy and organic rich layers and laminations. Overall, these beds are organized into upward thickening and coarsening packages. Sedimentary structures include ripple cross lamination in cases grading upwards to sets of 2D dunes with bidirectional foresets.

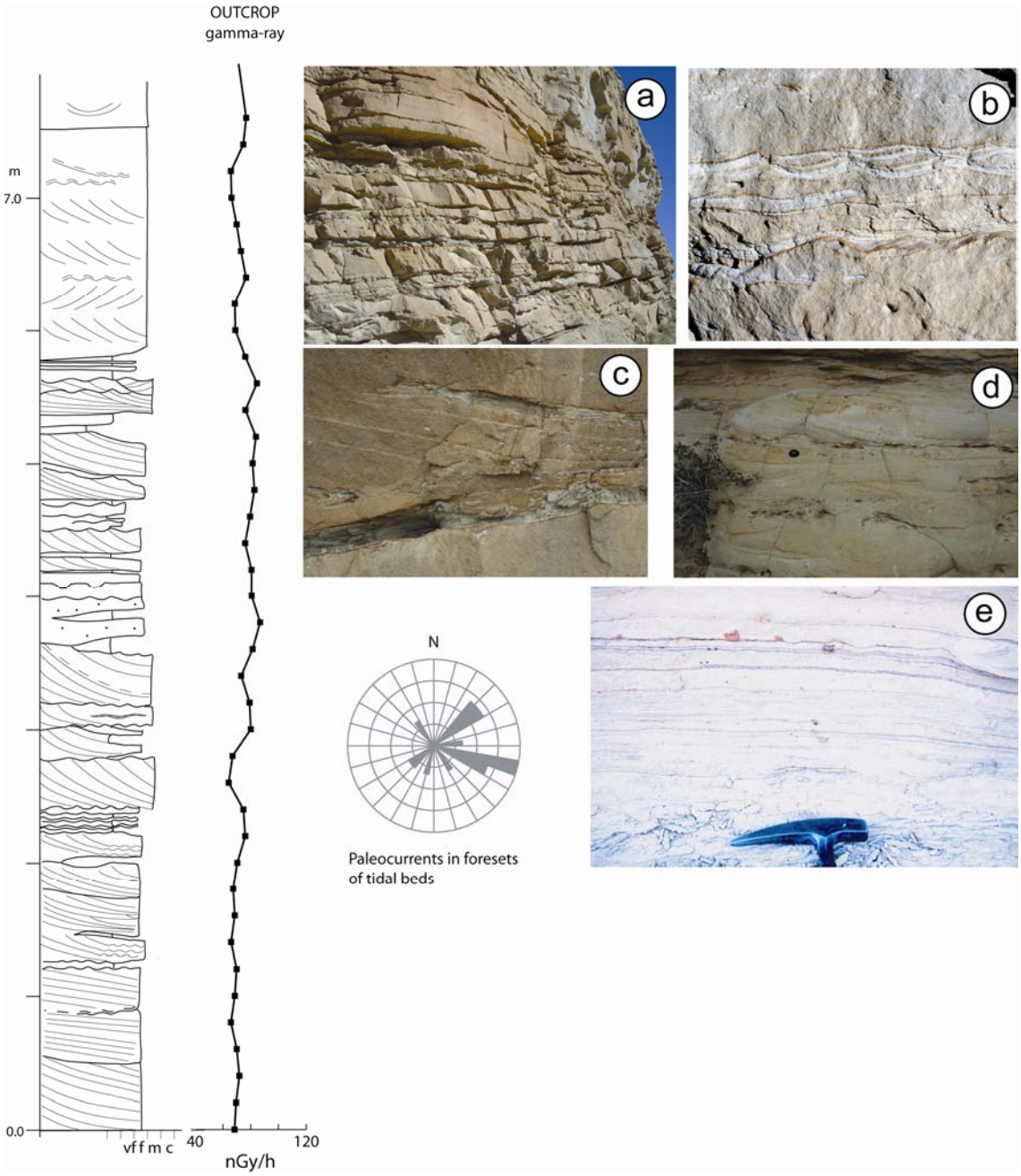

Figure 4.11: Tide-dominated shelf-edge delta facies association. Notice heterolithic bedding in the outcrop log and in photo (a). Wavy bedding (b), mud drapes in forests (c), bidirectional paleocurrents (d) and finer grained rhythmites (e) in more distal (or off-axis) portions of the delta. Rose diagram indicates bidirectional and landward oriented paleocurrents.

Interpretation: The inclined strata, vertical juxtaposition just below a fluvial channel, and short lateral transition to the river mouth-bar facies suggest that this facies represent delta front deposits. In addition, the heterolithic bedding, mudstone drapes, flaser, lenticular and wavy bedding and basin and landward oriented paleocurrents suggest that this delta front was strongly influenced by flood and ebb tidal currents. Examples of shelf-edge, tidally influenced deltas are rare (but see Cummings et al., 2006). My shelf-edge maps, complemented by those of Perman (1990), indicate the shelf-edge in this area was concave landwards, creating an embayment where confinement could have enhanced tidal currents. Also the thickening of the distributary channel above and the steep foresets in the river mouth bar facies may indicate an incised area, where tidal currents were amplified (e.g. see Cummings et al., 2006). The grain size fining of this facies in distal reaches indicates transition to a more basinward setting within the delta or to a site laterally removed from the main axis of tidal currents circulation.

Tidal Sand Bars Facies Association

Description: This facies consists of mostly fine (lower) grained sandstones with 2D dune sets. It lies above the distributary channel facies association on a relatively flat contact surface (Figure 4.12). Typically 30-40 cm thick, sets contain sigmoidal dunes with symmetric-ripple cross lamination in tangential bottom sets. Organic-rich laminations drape a few foresets and in some cases double mudstone drapes are present. Most paleocurrents from foresets are basinward oriented, but in a few cases we observe herringbone cross stratification. Thick ripple-cross-laminated intervals exist locally as well as irregular surfaces toward the top. Bioturbation is low.

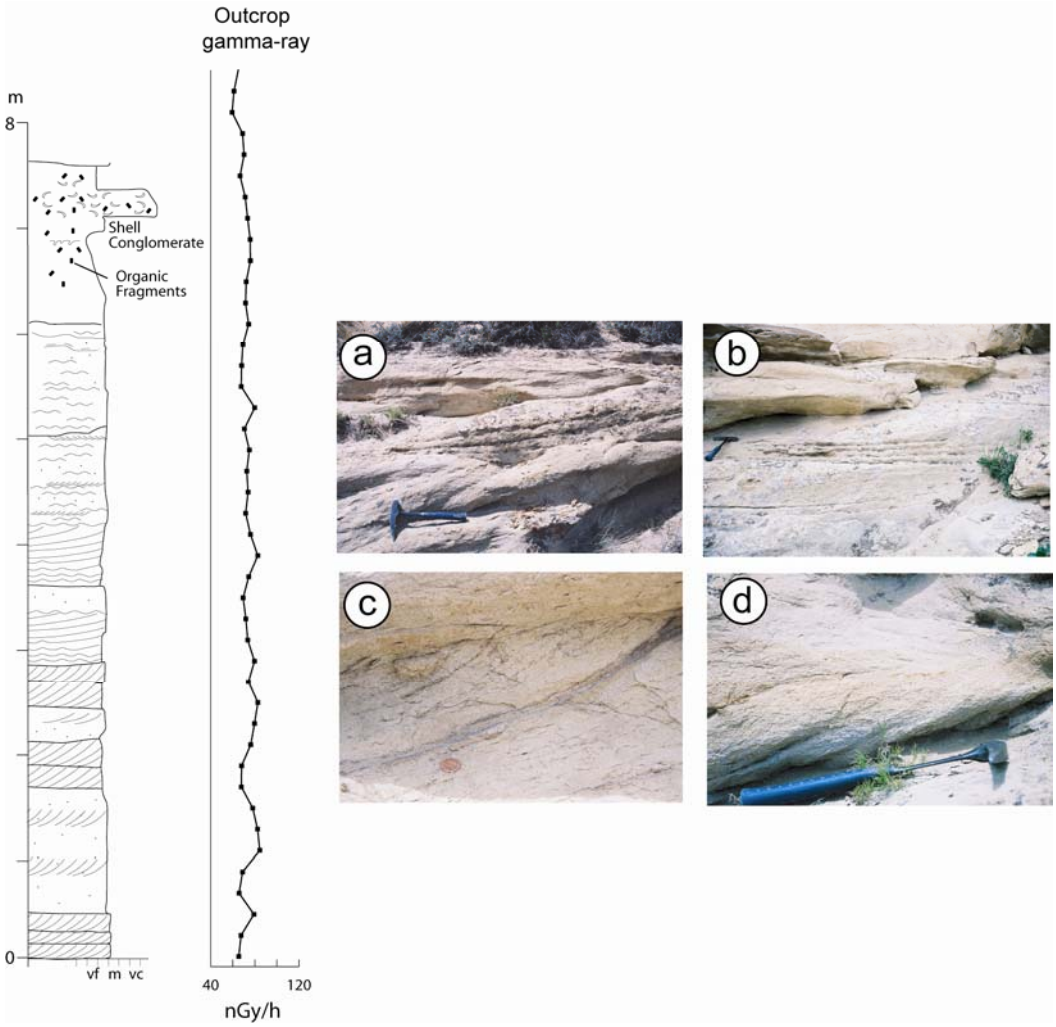

Figure 4.12: Tidal sand bars facies association. 2D dunes (a) with ripple cross laminated bottom sets (b), muddy drapes on foresets (c) and herringbone bedding (d). Notice shell conglomerate at the top of the facies succession on log.

Interpretation: The presence of mudstone drapes (albeit few) in foresets and bi-directional cross strata indicate that the formative flows for these facies were bi-directional and alternated with slack-water periods, strongly suggesting that the dunes of this facies were driven by tidal currents. In addition, the basal conformable contact with fluvial facies and close proximity to the shelf-edge suggests that the environment was at the interface between the ocean and the coastal plain. The lack of organization into upward thickening and coarsening trends, as well as the apparent lack of clinoform surfaces, tends to preclude a delta-front to shoreface interpretation. Tidal dunes and sand bars in an estuary is a likely interpretation. Brackish water in the estuary would have created stress environments, resulting in the low bioturbation (MacEachern et al., 2005).

Estuary Mouth Sandstones and Shell Conglomerates Facies Association

Description: This facies occupies a middle position within the succession and consists of very fine to fine sandstones, shell conglomerates and rare mudstone laminations (Figure 4.12). The ca. 7 m succession is organized into basal shell conglomerates (each <20 cm), a middle sandstone (< 2 m) and an upper clinoformed set (< 5 m) of beds. Basal conglomerates contain broken shells (including oysters), have irregular basal surfaces, are of variable thickness and laterally discontinuous and lenticular, very thin in distal areas. The middle sandstone exhibits wave ripples, irregular surfaces (every 20 cm or so), small-scale trough cross strata and, in distal areas, swaley-like cross-stratification. Trenching in the upper half of the middle sandstone shows structureless, very fine sandstone with small organic particles. The clinoformed set (beds < 40-80 cm) is mostly composed of very fine to fine-grained sandstones that thicken upwards and dip basinward at low angles. Few of these beds show discernable grading (either normal or reverse), or

vertical transitions from lower flat laminations evolving upwards to ripples followed by undulating bed tops capped by shale laminations. The uppermost sandstone (80 cm) in the clinoform set is completely bioturbated with numerous traces of *Ophiomorpha*. This bed marks a conformable transition to the estuary muds.

Interpretation: I interpret basal conglomerates as shell lags left by waves during transgression. This interpretation is consistent with the overlying wave rippled and through- and swaley-cross-stratified sands, which suggest wave influence in more shoreward settings, and so a landward migration of areas near the estuary mouth. So the basal conglomerates define a wave-ravinement surface (WRS). Upward thickening and basinward clinformed architecture in the upper set of beds indicates a regressive event punctuating transgression. Processes during this pulse of regression are difficult to interpret. Flat lamination evolving upward to ripple cross lamination in a few beds suggest tractive and bed load deposition and may be related to underflow river effluents. However the succession top does not show a fluvial channel making it hard to prove river domination. Instead the top is occupied by bioturbated sandstone with abundant *Ophiomorpha* and may be more indicative of a wave-dominated shoreline. In any case, the complete succession from the basal conglomerates through the clinoformed set demonstrates landward transit of estuary mouth areas.

Estuary Mud Facies Association

Description: This facies occurs toward the middle of the succession. It is < 6 m thick and composed of shale with a few siltstone layers, little bioturbation and with a persistent presence of scattered organic fragments. It conformably rests on the estuary mouth facies with a somewhat flat contact and gradationally transitions upward to overlying sandstone beds. The shale is easily traceable between outcrop sections.

Interpretation: The muddiness of this facies indicates deposition in a low energy environment. Candidates are an offshore setting or a muddy environment within the estuary. I prefer the latter, because the low bioturbation and persistence of organic particles is consistent with an estuary, whose proximal position is prone to receive organic matter and brackish water may preclude high and diverse bioturbation. This facies is in conformable contact and upward transition to sand-rich deposits, and suggests that these muds may sit at the distal end of the sands.

Tidally Influenced Bay Head Delta Facies Association

Description: This facies association occupies the upper outcrop segment and is largely covered, so it is mostly described from trenches (< 1 m width). It is composed of sandstones, most fine-grained (few very-fine and medium), and shales, generally < ~30 cm thick but reaching ~ 1 m at the top. Organic particles (< 3 mm) are present in a few layers. Bedding is heterolithic with poorly developed upward thickening and grain-size coarsening in bed sets. The basal of these sets is best developed, marking a clear conformable and gradational transition from underlying estuary muds. Laterally this set can be observed to pinch out over a short distance (several 10s m). Most sedimentary structures are ripple cross lamination, lenticular and flaser bedding and planar cross stratification with mud drapes (albeit few). Only in the basal set are there a few cases of normal and reverse grading in beds with flat laminations transitioning upward to ripples and to thin shale caps. Bioturbation is low with few examples of small sandy burrows of *Glussifungites*-like ichnofacies, and possible *Conichnus* and *Rosselia* traces.

Interpretation: The highly heterolithic lithology of this facies, the multiple examples of lenticular and flaser bedding and the foreset mud drapes indicates alternation of slack and faster moving water flows, which suggest tidal currents. In addition, the bed geometry

and stacking, as seen as in trenches, and the evidence for tidal processes make this facies similar to the tidally influenced delta front described above and I suggest this facies also represent deltaic deposition, but at the head of an estuary, in a bay-head delta.

Paleogeography, Coastal Processes and Deepwater Setting

Subsurface sandstone isopach maps and the outcrop facies associations indicate that a main river system existed from the coastline in this eastern reach of the basin margin (Figures 4.13, 4.14, 4.15 and 4.16). The rivers flowed to the W and SW probably from the Rawlins Uplift and Granite Mountains area. They delivered abundant sand to the ocean to judge from the thick, large-volume basin-floor sandstones linked to clinothem 10. Despite such sand abundance, however, there is no well-developed belt of wave-dominated coastal sandstone aligned along the shelf-edge as in clinoform 9. The wave regime at the coast here was clearly less dominant. This, together with the high degree of erosion observed at the outcrop, suggests that along the eastern reaches of the basin margin the shelf-edge was deeply and broadly incised by river channels that extended onto the slope. Through these incisions, rivers would have discharged their sandy load directly to the upper slope and from there, aided also by upper slope failure, turbidity currents would have transported sediment to deepwater areas to form a broad and sandy fan.

The rivers would no longer have been located at the shelf edge when the system evolved to an estuary. Estuary rivers discharge their load to the estuary head forming bayhead deltas, whereas in the middle and estuary mouth reaches tidal currents and/or waves deliver (from the sea) and rework sediments (Dalrymple et al., 1992). In the present study case, a mixed-energy, wave and tide interaction estuary has been documented. There are some parallels with the Holocene fill of the Gironde Estuary in southern France (Allen and Posamentier, 1993). As in the study succession, the Gironde has a fluvial base below tidal sands, that toward the estuary mouth, underlie tidal and wave reworked sandstones (estuary mouth sands). The upper segment of the estuary is

filled by estuary muds on which a tidally-influenced bay head delta (< ~17 m) regresses. Besides providing seaward sourced sediment to the estuary, waves and tides essentially shape the estuary geometry. Waves create a bar at the estuary mouth that partially disconnects the estuary from the open ocean. Tides can breach this bar and create tidal inlets and deltas, and further tidal incursion reworks fluvially and tidally derived sediments into tidal bars. These processes tend to trap much sediment in the estuary itself and therefore would at least partially shut down the delivery of sand to deepwater areas.

Sea Level

As documented above, the delta front to fluvial channel along the eastern basin margin is <18 m thick, whereas the highstand wave dominated deltas on the western basin margin are ca. 50 m thick, i.e. almost three times thicker. This strongly suggests that the progradation of the fluvial/tidal eastern deltas occurred in a significantly lower accommodation setting than that of the western wave deltas. In addition, the eastern deltas belong to a clinothem whose shelf-edge prograded extensively (~10 km) beyond the shelf edge of the previous clinoform and with a relatively flat shelf-edge trajectory. Based on this highly progradational and flat shelf-edge growth, Carvajal and Steel (2006) have indicated that relative sea-level was stable to falling during shelf-edge accretion; I further suggest here that the highly incised shelf-edge, the relatively thin delta fronts (< 7 m) and the late-stage estuarine system seen in outcrop, also favor a falling relative sea level. Accordingly, I interpret the strata of the eastern delta fronts as forced regressive deposits (Hunt and Tucker, 1992).

After the initial stage of relative sea level fall and vigorous shelf margin accretion, early rise of sea level caused aggradation of the fluvial channel feeders. During continued

rise of sea level the channel was infilled and filling of the estuary proceeded during transgression to culminate with highstand bay-head delta progradation.

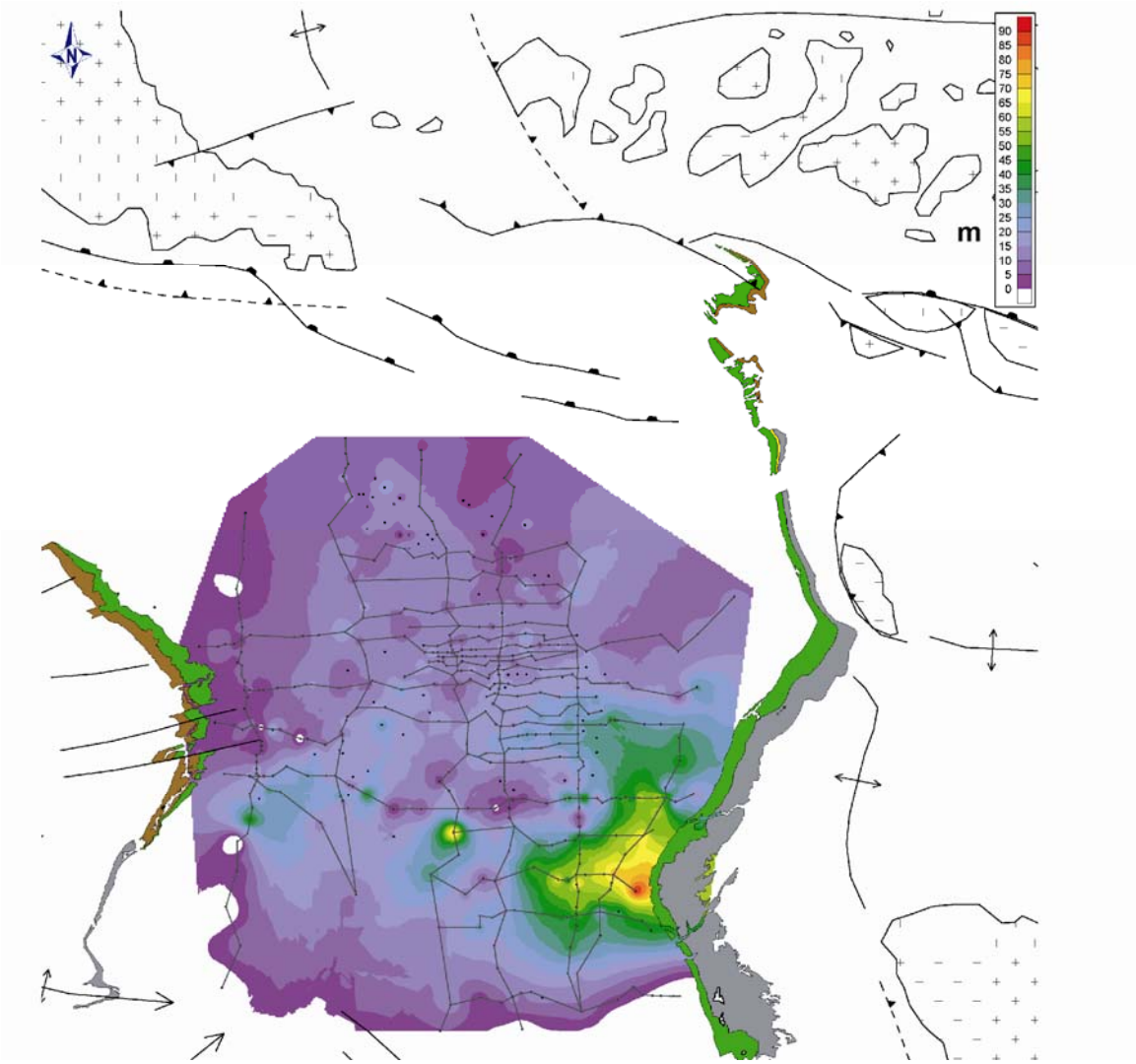

Figure 4.13: Sandstone isopach map for clinothem 10 (in meters).

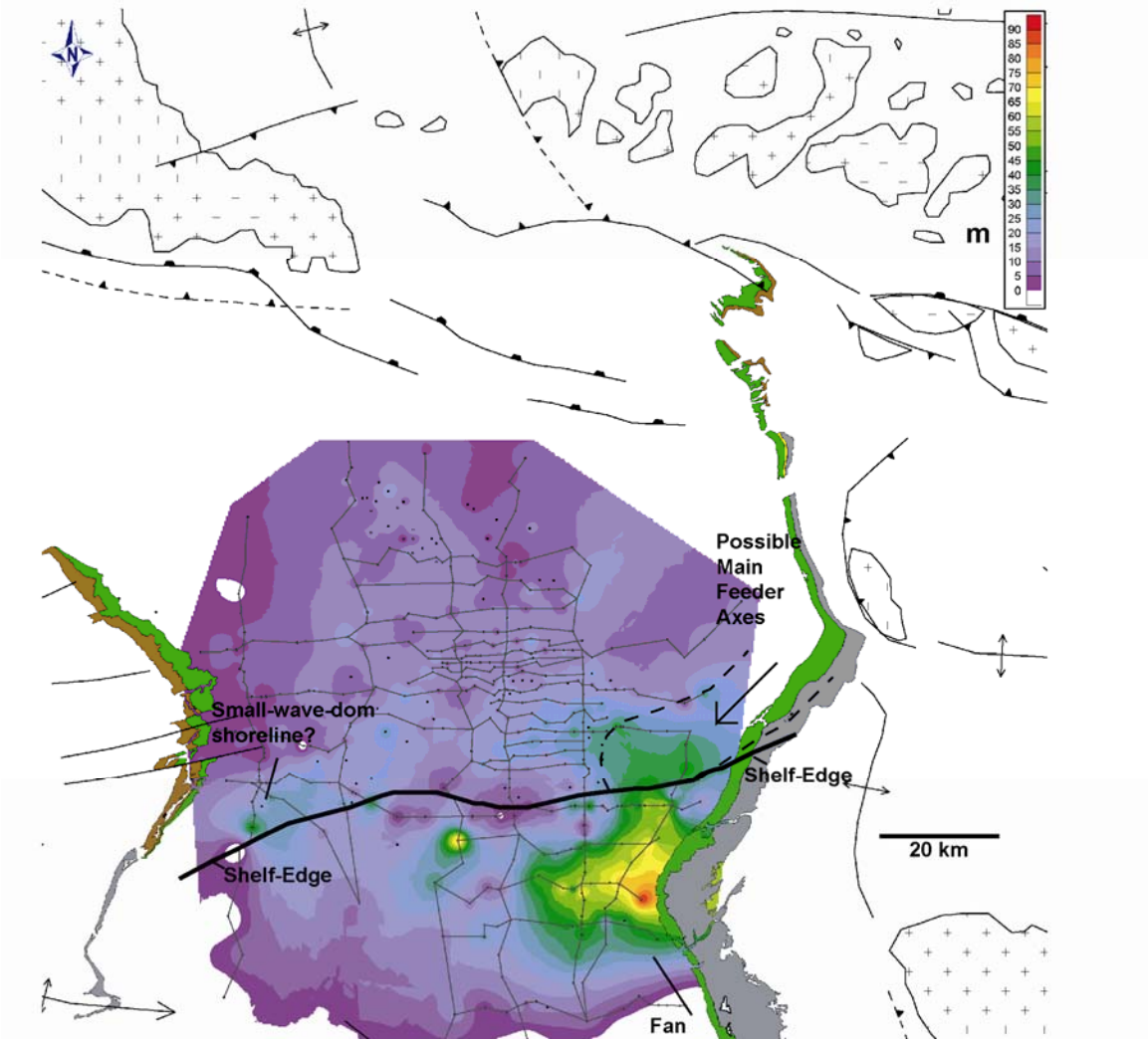

Figure 4.14: Interpreted sandstone isopach map for clinothem 10. Shelf-edge position towards the end of the cycle.

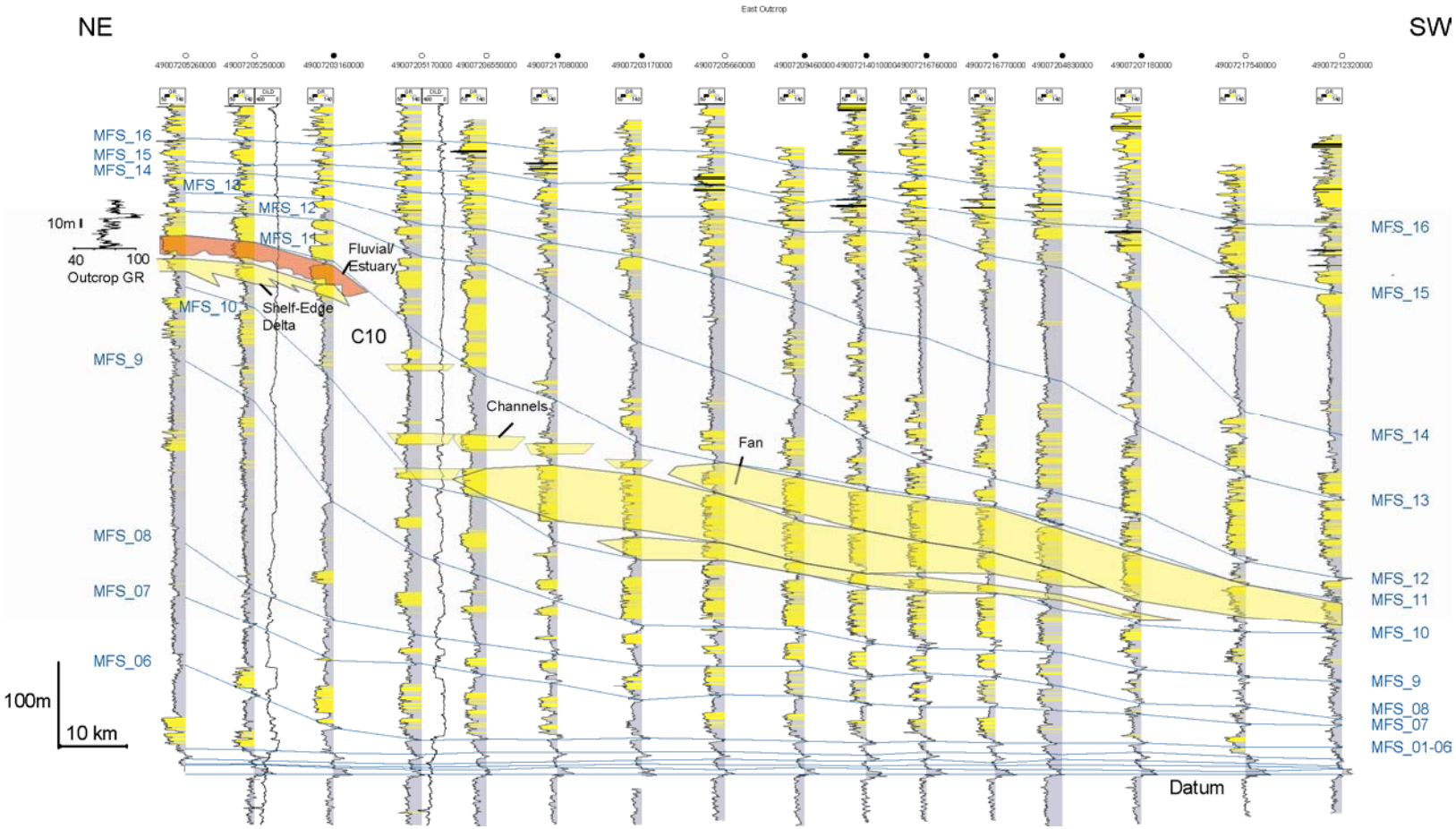

Figure 4.15: Outcrop deepwater linkage between shelf edge and deepwater fans in the eastern outcrop. Notice outcrop gamma-ray log on the left (see Figure 4.1 for location).

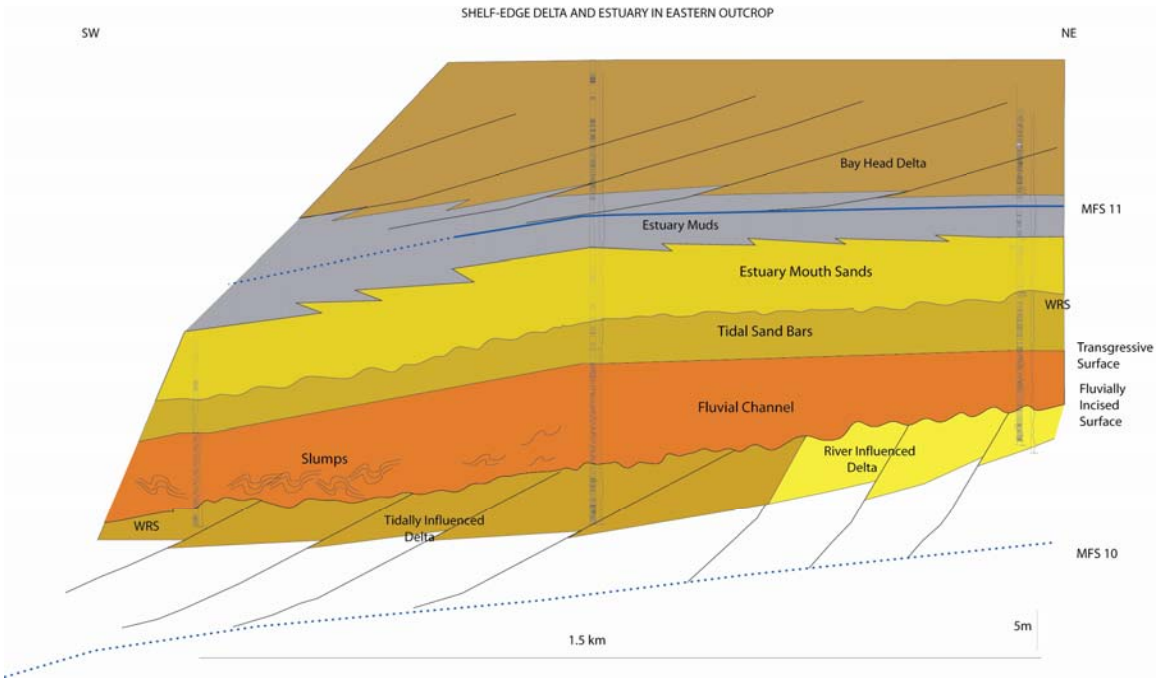

Figure 4.16: Shelf-edge delta and estuary succession as seen in outcrop in the eastern area (WRS = wave ravinement surface) (see Figure 4.1 for location).

DISCUSSION: HIGHSTAND VERSUS LOWSTAND REGIMES FOR SAND BYPASS TO DEEPWATER AREAS

High-Energy Wave Regime and Rivers during Sea Level Highstand

Role of Rivers

On a shelf margin with highstand, wave-dominated shelf-edge deltas linked down slope to two sandy basin-floor fans, the following question arises: what is the relative contribution of waves and rivers in the formation of the fans? The location of the fan directly downslope from shelf-edge river mouths and their lobe morphology strongly suggests that rivers played an important role on bypass (for instance, compare with Hueneme Fan in California Borderland (Normark et al., 1998) and the Rhone Neofan in France (Torres et al., 1997). Clearly the rivers supply much sediment for fan formation and common river scour of the substrate will create shelf-edge channeling and, further downslope, erosion by sediment gravity flows can create slope channels directly connecting mouth bars with the basin floor. Moreover the river itself may drive these flows by turbidite current ignition either from hyperpycnal flows (Mulder et al., 2003) or mouth bar collapse due to rapid loading. In this way semi-permanent conduits for sediment bypass can be maintained in front of the river mouth.

Role of Waves

On the other hand, waves have much less potential to create their own conduicts to the basin floor. For instance, the thick, shale-rich slope succession below the wave-dominated deltas of the western area contain only discrete occurrences of thin sandstone sheets and subsurface cross-sections also show a highly mud-prone slope (Figures 4.5, 4.6 and 4.8). So despite the strong wave domination at the shelf edge, there are few signs

that wave-triggered offshore flows (rip currents or storm surges) can bypass significant volumes of sand to deepwater. This is quite predictable because although waves can create offshore flows toward the slope, especially during storms (Dumas and Arnott, 2006), these flows seem to have an insignificant potential to channel the slope, so they travel downslope as unconfined flows tending to loose their momentum and deposit their load as thin sand sheets as documented in the outcrop. Deposition in deepwater below storm wave base will prevent further wave reworking of these sediments and they will remain on the slope. Waves themselves are apparently very efficient at reworking and storing coastal sand as elongate sandstone belts along the shelf-edge, but inefficient at triggering bypass to the slope and basin floor.

However once rivers initiate conduits to the basin floor, waves can become important suppliers of sediment to deepwater. As discussed, wave energy can induce a permanent alongshore sand drift on the coast and some of this drift can be captured at channel heads to be transferred either immediately or later to the basin floor (Michels et. al., 2003; Weber et al., 1997). It is worth noting that such alongshore drift can bring sand from distant places; for instance in the study case, some of the supply by the smaller western rivers was likely transported eastward by the alongshore drift, contributing not only to coastal building, but also to bypass through the main feeders. These means of sand transport are well known from the present highstand world. For instance, on the Bangladesh shelf, the 'Swatch of No Ground' is a canyon deeply incised into the Bengal shelf, directly connecting inner shelf areas with deepwater settings. During fair weather the canyon head receives mud from tidal currents and during storms it receives mud and sand (Michels et al., 2003). Weber et al. (1997) have documented that turbidity currents through the canyon have resulted in active growth of the Bengal Fan during both rising and highstand of sea level. Additional examples of coastal drift as a supplier to deepwater

via slope canyons have been described in the California Borderland (Piper and Normark, 2001). Here, for example, the small Dume Fan is thought to receive sand solely by longshore drift. I underline that, in these scenarios, the highstand delivery to deepwater seems to be possible ultimately due to river supply (e.g. Ganges and Brahmaputra in the Bangladesh shelf, or Santa Clara in southern California), the presence of inner-shelf to deepwater canyons (Bangladesh shelf) or narrow shelves (California).

In the absence of cross-shelf incisions or in the case of wide shelves, highstand delivery will be much more dependent on the development of highstand shelf-edge deltas. For such deltas, a high sediment supply, a modest rate of sea level rise and minimal alongshore sediment dispersal may result in these deltas achieving a shelf edge position. In turn, this would ensure a river supply to the coast and the generation of river channels at the shelf-edge that could connect to the basin floor through slope channels generated by sediment gravity flows. In addition, as in this study, the highstand shelf-edge deltas will tend to show some significant wave influence, because rising sea level during regression tends to create open and cuspate coasts (Porębski and Steel, 2006). These waves commonly generate alongshore sand drifts to build extensive sand belts along the shelf-edge (see also Galloway, 2001). On one hand these waves and drifts decrease the available sediment volume for bypass as much sediment is trapped at the shelf-edge, but on the other hand they may bring sand from distant places and make it available for bypass. Longshore drift can also deflect river mouths which may influence the path of delivery to deepwater. The highstand shelf-edge coast and sediment delivery to the slope can therefore be quite complex, resulting from the interaction of rivers and waves; with the latter by no means least important. From a hydrocarbon exploration point of view this ‘highstand’ configuration may be attractive, because it creates potential

reservoirs in fluvial feeders, in wave-dominated shelf-edge sand belts, in the slope channels and on the basin floor.

River and Tide-Influenced Shelf-Edge Deltas during Sea Level Lowstand

Role of Rivers and Stratigraphic Implications

Fluvial-tide interaction in deltas at the shelf edge during sea level lowstand present a contrasting picture to the above for the delivery of sand to deepwater. As in highstand delivery, the outcrop demonstrates that rivers were important for sediment delivery and bypass. In this case, however, falling sea level accentuates their importance, because it induces deeper and more focused (albeit broad in places) river erosion of the shelf edge, creating more effective bypass conduits for either hyperpynal flows or mouth bar failures. In addition, the indented coasts created by this erosion and low sea level would tend to reduce the potential for both high wave energy along the coast and wave driven alongshore drift. Therefore sand volume retention by waves at the shelf edge is less significant and more of the sediment budget is available for bypass.

I postulate that such bypass happens by increments during the fall of sea level rather than concentrated mainly at the time of lowest sea level or maximum regression. This is likely because the fluvial delta-front facies in themselves suggest bypass, but do not occupy a position of maximum regression. As deltas approach the shelf edge, bypass may start as soon as the delta toe connects with the shelf edge (or earlier). At this time, the slope break between the delta plain and front is near the shelf edge and from here the slope extends downward to the basin floor. Hyperpycnal flows or mouth bar failure have thus the potential to ignite turbidity currents that may channel the slope and reach the

basin floor. Continued delta progradation will further accrete the shelf margin and also bypass sands to deepwater, albeit not simultaneously. Moreover continued progradation will maintain the basinward propagation of the erosional surface resulting from river scour of delta fronts. At the time of maximum regression, this surface will not correlate with the base of sands on the basin floor, which would have started to accumulate some time earlier. This has an important stratigraphic implication, because some researchers use this surface as a sequence boundary (Van Wagoner et al., 1990); a reasonable use based on the surface's prominent erosional character on the topset. Nonetheless the surface at the base of the basin floor fan would be diachronous. Not only do the outlined outcrop and conceptual analysis suggest such diachronoeity, but also shelf edge to deepwater cross sections in the study basin and in others places point to the onset of fan formation prior to the time of maximum shelf-edge progradation (Johannessen and Steel, 2005).

Role of Tides

Besides the diminished wave influence and strong fluvial drive, the studied lowstand delivery system also demonstrates the importance of tidal influence on the shelf-edge deltas. Few descriptions exist of tidal-influenced deltas at the shelf edge (see one of them in Cummings and others, 2006). In our case study, tidal and fluvial facies are present and important as a mixed-energy component in the same deltaic regression. Porębski and Steel (2006) have suggested, that as sea level falls, differential erosion causes coastal morphology to become irregular, providing local indentations where confinement can enhance tidal currents. Bird-foot delta architecture in fluvial dominated deltas would produce a more segmented coast. In the study case, the high degree of erosion exhibited by the shelf edge is consistent with a more indented or embayed coast.

In addition, our maps of the shelf edge and those of Perman (1990) document that at this time the eastern basin margin area may have been embayed, facilitating the amplification of tidal currents.

The role that tides may play in the delivery of sand to deepwater areas has been less explored. In some ancient cases and at present, there is convincing evidence pointing to tidal currents in deepwater, especially in canyons (see Shepard, 1976; Shepard et al., 1979 and Shanmugan, 2003). Bottom currents in many modern canyons show up- and down-canyon flow directions (e.g. Congo, Santa Monica, Monterrey, Rio Balsas, Wilmington canyons, etc.) at times with the periodicity of daily tidal cycles (e.g. Hueneme Canyon) and with velocities commonly in the range of 25-50 cm/s, but reaching even 70-75 cm/s, i.e. velocities able to transport even coarse sand. In our study case, paleocurrents are dominated by flood tides (Figures 4.11) and so they would have had a limited potential to transport sediment down the slope to the basin floor. In addition, the sandstone architecture on the basin floor is lobate (Figures 4.14 and 4.15), more consistent with deposition from un-confined turbidity currents. I acknowledge however that in other cases, ebb currents may dominate tidal flows and therefore tides could be more important in bringing sand to deepwater areas through canyons. Such importance will be enhanced if tides are able to transport sand from distant places, thereby increasing the budget of sand for bypass.

In summary, lowstand delivery in the study case was characterized by a strong fluvial drive and well developed tidal influence. River-induced processes such as shelf-edge erosion, hyperpycnal flows, and mouth bar failure due to rapid loading seem to be the most important mechanisms on the generation of turbidity currents to bypass sand to deepwater areas. In addition, coastal morphology may provide indentations or local embayment in which tidal currents are amplified and dominate delta front sedimentation.

Regarding sand bypass, the role of tides could potentially be significant especially in ebb dominated settings and in cases where tides can bring sediment from more distant areas along the coast.

CONCLUSIONS

Sedimentary facies analysis performed on opposite sites of the Washakie-Great Divide basin of southern Wyoming, demonstrates two sharply distinct shelf-edge settings: 1) on the western basin margin, storm-wave dominated shelf-edge deltas aggraded and prograded into the basin during sea level highstand. Under continued sea level rise during transgression, the setting evolved into a tidally influenced sandy estuary and this in turn to a swamp where coal and plant rich shales accumulated. Toward the top of the succession wave influenced highstand progradation resumed and very restricted paths of east-flowing river appeared; 2) on the eastern basin margin, river and tidally influenced shelf-edge deltas show a strongly progradational and incised character developed under falling sea level. Subsequent early rise of sea level and transgression resulted on a mixed, tidal-wave estuary.

Correlation of the shelf-edge deltas to their coeval deepwater and coastal environments helps to characterize the highstand and lowstand shelf-edge coasts and their modes of sediment delivery to deepwater. In the highstand scenario, river and wave influence on the deltas results in extensive shelf-edge coastal building and significant bypass of sand to the basin floor. Most likely through hyperpycnal flows and mouth bar failure, rivers supply large volumes of sediment for bypass. Also river channeling of the shelf edge generates upslope bypass conduits that turbidity currents seem to extend to deepwater by channeling the slope. In contrast, waves in themselves (for instance through rip-up currents, offshore-directed surges, etc.) apparently bypass insignificant sand volumes. However waves can induce strong alongshore drift that vigorously builds the

coast. Naturally, retention of this sand along the coast tends to decrease the total sand volumes available for bypass, but this reduction may be compensated by sand potentially sourced from distant areas and brought to canyon heads by alongshore drift. In addition, drift strength was high enough compared with riverine outflow to create an asymmetric coastal distribution of sand with sandier areas up-drift with respect to river mouths. Moreover, these rivers may be deflected in the drift direction; an important deflection because turbidity channels will follow mouth bars down-slope and create fan lobes elongated in the deflection direction.

The described combination of river and wave-drift mode of coast building and bypass may be characteristic of highstand shelf-edge deltas. In a shelf-edge coast, a high sea level at highstand and the increased water depth due to rapid deepening toward the slope will tend to reduce the dissipation of waves by shoaling and breaking, and therefore open ocean swales will more fully impact the coast. Development of a sandy highstand shelf-edge coast and deepwater setting, however, probably requires a high sediment supply. The high supply is necessary not only for bypass and for coastal accretion but also to sustain delta progradation to the shelf edge during rising sea level. In moderately wide to wide shelves (few to several 10's of km), for such progradation, supply requirements may be reduced if rate of sea level rise is small or there is minimum sediment dispersal along shore or a combination of these variables. However once deltas are at the shelf-edge, significant coastal accretion and bypass may not both take place with a small supply. Examples from Spitsbergen suggest that if the supply is low, only the coast is accreted but by small amounts of progradation.

In contrast, in the sea level lowstand scenario, river and tidal processes coexist in the deltas. A seemingly diminished wave power (or overwhelming by rivers and tides) tends to trap smaller sand volumes along the coast. More of the sand budget is funneled

toward the slope and basin floor. Such funneling is achieved by rivers that tend to create deeper, wider and probably more numerous bypass conduits at the shelf edge. River-induced mouth-bar failure and hyperpycnal flows can ignite into turbidity currents and, through slope channeling, extend these conduits to the basin floor. In addition, fluvial domination during sea-level fall will tend to produce more bird-foot delta lobe geometries which, with more prominent and numerous incisions, can create an irregular and indented coast. Consequently, tidal currents may be amplified in confined coastal segments and such amplification can leave a strong tidal signature on the shelf-edge deltas. Although not documented in this study, these currents could bring sand from distal places and transport it to deepwater by continued tidal amplification through confinement in slope channels as documented in many modern canyons. In our study case, dominance of flood tides indicates that tides probably did not contribute greatly to down-canyon bypass; instead the fan lobe-geometry points to deposition from the expansion of unconfined turbidity flows on the basin floor. Even if tides do bring much sand to the canyons, it is quite likely that these sediments may be incorporated into subsequent turbidity flows and loose both their tidal architecture and signatures. In any case, rivers seem to be driving the shelf-edge processes at lowstand, facilitating and enhancing bypass to deepwater areas.

CHAPTER 5: SEDIMENT SUPPLY, BASIN FILL ARCHITECTURE, AND DEEPWATER SANDS: INSIGHTS FROM MARGIN ACCRETION RATES

ABSTRACT

Despite the obvious importance of sediment supply for studies of shelf-margin architecture and on the potential of margins to contain and by-pass deepwater sands, the role of supply in such studies has received very limited attention. This probably reflects the strong emphasis given to sea level, however high sediment flux can be critically important for the occurrence of deepwater sands, not least on Greenhouse or rapidly subsiding margins where the impact of sea-level fall may be insufficient to drive sediment delivery out across the shelf into deepwater areas. I suggest a methodology for inferring high or low sediment supply rates on margins, based on estimates of shelf-edge accretion rates. There are two broad types of shelf margin, based on structural style, water depth and proneness to sediment failure. *Moderately deep-water (<1000 m water depth) margins* produce clinoforms 100s of m high and can prograde and aggrade at rates up to 61 km/my and 270 m/my, respectively. On these margins, rates of progradation of several 10s km/my suggest supply domination, a term also used to denote the abundant and recurrent dispersal of large volumes of sediment into the basin. High supply is especially important for producing deepwater sand accumulation at relative sea-level highstand. In contrast, low rates of shelf-edge progradation (<10 km/my) on these same margins, where significant accumulation of sand can be seen to occur on the slope and basin floor, implies a deepwater delivery that is less recurrent and abundant, and that probably involves emplacement at lowstand of relative sea level. These trends indicate that for moderately deep margins, sediment supply (and not sea level) is the key limiting

factor on shelf-margin accretion rate, clinoform topset width, and volume of sand bypassed to deepwater; supply, as indicated by progradation rate, can therefore be used to predict relative sand volumes bypassed to deepwater areas. *Very deep water (>1000 m water depth) margins*, in contrast, create much higher but more complex clinoforms, and tend to show lower maximum progradation and higher maximum aggradation rates (up to 37 km/my and up to 2500 m/my respectively). These margins aggrade faster and prograde slower because they are fronted by much deeper water, and because they subside faster, and are prone to large-scale, growth-fault development and large-scale mass failure. This mass failure tendency, the scale of these margins and some scarcity of data, however, make it difficult to correlate their accretion rates with supply and delivery of sand to deepwater areas.

INTRODUCTION

From a first principles viewpoint, there is no doubt that sediment supply is a major external control on shelf-margin architecture and on a margin's potential to produce deepwater sandstones. The so-called accommodation/supply (A/S) ratio (Schlager, 1993) explicitly acknowledges the importance of supply, as do flume experiments and numerical and forward models (Paola, 2000). Studies of modern river-delta systems have also highlighted supply and quantified it in terms of climate and tectonics (e.g. see Milliman and Syvitski, 1992; Hovius, 1998; Syvitski et al., 2003) and in terms of its impact on shelf-transit times (Burgess and Hovius, 1998; Muto and Steel, 2002). However, in the study of ancient shelf margins, and perhaps in stratigraphic studies in general the role of sediment supply has received limited attention (see exceptions in Galloway, 2001; Carvajal and Steel, 2006). Part of this oversight is, of course, the difficulty of quantifying supply (generally through sediment volumes) as this requires representative data coverage, good preservation of depositional systems and an

acceptable methodology (e.g. for a discussion see Liu and Galloway, 1997). Nonetheless, there has been some over-emphasis on sea level in efforts to predict the delivery and formation of sandy deepwater deposits (e.g. see Posamentier et al., 1988; Posamentier and Allen, 1999) despite the likelihood that supply 1) can be the key driver for shelf-margin progradation and delivery of sand to deepwater areas even during periods of rising sea level (Kolla and Perlmutter, 1993; Burgess and Hovius, 1998; Pinous et al., 2001; Muto and Steel, 2002; Carvajal and Steel, 2006), and 2) may also predict sediment bypass to deepwater areas, as the present data suggest.

In this paper, I explore the driving role that sediment supply may play in the accretion of ancient shelf margins and the potential for supply signatures that may reflect the likely volumes of by-passed, deepwater sand. I attempt to develop a proxy by which to read supply, based on the aggradation and progradation rates of ancient shelf margins. Results indicate that in progradational margins of low to moderate water depth (<1000 m), accretion rates tend to correlate with sediment supply, and that increasing rates of progradation imply increased volumes of deepwater sand. Furthermore, it seems that supply is the key limiting variable controlling the volume of sand bypassed to the slope and basin floor in these basins. Very deep-water margins, in contrast, show a different pattern of behavior, as shown below.

SELECTED MARGINS

Twelve shelf margins have been selected to evaluate the role of supply on their architecture and deepwater sand content. A supply proxy is developed using different basin types, each with enough data to determine accretion rates with reasonable certainty (Figure 1). Accretion rate refers to both the aggradation and progradation rate of the shelf margin measured at the shelf edge. Examples are included from foreland, intermontane, rift and piggy-back basins, as well as passive margins, and from very deep (>1000 m) and

moderately deepwater (<1000 m) shelf margins. In so doing I follow Swift and Thorne (1991) in emphasizing that the shelf-slope-basin clinoform morphology is a characteristic feature of most basins, not only on continental margins, provided the water is deep enough. However, it is quickly apparent there are significant differences between moderately and very deep-water margins and so we analyze them separately. The study intervals range from Jurassic through present. Some margins have a long history spanning several 10s my (e.g. Gulf of Mexico, Orinoco Margin) and accretion rates for different time intervals have been calculated for these margins. In addition to using published data from the margins, I have recent experience with databases in the Maastrichtian Lewis-Fox Hills margin (Wyoming, USA) (Carvajal and Steel, 2006), and links to researchers working in the Eocene Spitsbergen margin (Norway) (e.g. see Plink-Björklund et al., 2001; Mellere et al., 2002; Plink-Björklund and Steel, 2002, 2004; Petter and Steel, 2006) as well as in the Eocene Porcupine (offshore Ireland) (Johannessen and Steel, 2005) and the Paleogene-present Orinoco margins (Sydow et al., 2003). The Lewis-Fox Hills and Spitsbergen/Porcupine margins had <1000 m water depth and represent contrasting end member examples of high and low sediment supply systems, respectively. The impact of this on the margin's production of deepwater deposits will be explored further.

Direct measurements of shelf-edge progradation and shelf aggradation rates were made on cross-sections and maps between horizons bounding 3rd-order time intervals (i.e. ca 1 my or greater). This is the time resolution available in most basins and is appropriate for this study because I seek to characterize the supply at time intervals that will produce economic volumes of deepwater sand from an industry viewpoint. In *shelf-edge maps*, I have generally used data on the maximum progradation distance of the shelf-edge in the dip direction of the feeding fairway system. In *cross-sections*, I have used data, as far as

possible, from those transects oriented along the direction of basin infilling, i.e., along the direction of steepest clinoform gradients. At the scale of shelf margins and 3rd-order architecture, rates obtained from an adequately oriented cross-section are fairly representative of significant distances (10's of km) along strike. This is because the along-strike change in geometry, progradation and aggradation of the shelf-edge occurs over distances of several tens of kilometers as shown from shelf-edge or isopach maps in NW Borneo, Gulf of Mexico, Orinoco and Lewis margins. Therefore a carefully-chosen cross-section on the margin is likely to be representative of a significant area along strike. Shelf margin architecture tends to change gradually along strike (in contrast to along-strike shoreline changes that may occur over short distances), in part because it results from allogenic forcing acting sub-regionally and on relatively long time scales. It is when smaller-scale shelf-margin elements (e.g. precise location of deltas, channels, estuaries, etc.) are investigated that an enhanced 3-D coverage of the shelf margin is absolutely necessary. Aggradation rates were measured at the outermost shelf, and within growth-fault compartments in margins where these features were present.

In this review I focus on margins in which rivers and deltas are the main supply agents for shelf-margin growth, and I have not included margin growth where sediment has been delivered purely by waves or tides on the outermost shelf (Boyd et al., 2006), or by outer-shelf oceanic currents (Lu et al., 2003) or by shelf incisions from distant inner shelf areas (Weber et al., 1997).

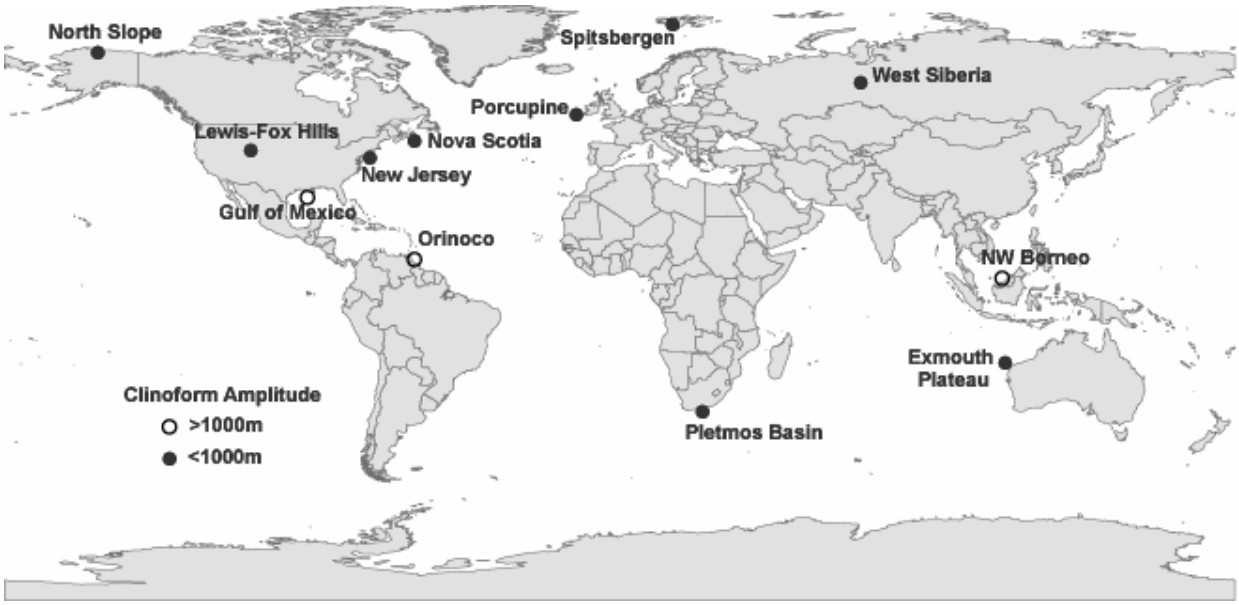

Figure 5.1: Location of study margins. New Jersey and Nova Scotia were included in the low-amplitude margins (<1000 m) because the study clinoforms were of this height during their respective times.

SHELF MARGIN AGGRADATION AND PROGRADATION RATES

Accretion rates show a wide range of variation on the selected margins (Table 5.1, Figure 5.1) depending on sediment supply rate, basinal water depth, presence/absence of large growth faults in the outer shelf to shelf-edge area, and architecture. Progradation and aggradation rates range from <1 to 61 km/my and from a few meters to 1000s m/my respectively. Interestingly, margins can exhibit either a high progradational or high aggradational rate but apparently not both, i.e., none of the studied margins is able to prograde at a high rate (e.g. > 50 km/my) and aggrade at a high rate (e.g. > 2000 m/my). It remains to be seen whether margins fed by extremely high-supply fluvial systems (e.g the Bramaphutra and Ganges Rivers) can show high rates of both progradation and

aggradation. I note that there are clear and interesting differences between margins with clinoform amplitude > 1000 m and those < 1000 m, and I refer to these as low-to-moderately deep-water and very deep-water margins, respectively.

Margins fronted by clinoform amplitudes > 1000 m.

On these margins (Gulf of Mexico, Orinoco, and Borneo margins; Table 1), progradation rates tend to be low to moderate (between 7 and 30.5 km/my), whereas aggradation rates tend to be extremely high (100's to 1000's m/my). The accretion of such margins into water of great depth (1000's of meters of water) explains the low to moderate progradation rate. Maintenance of progradation at a high rate on such deepwater margins would require much greater volumes of sediment than are available.

In addition, these margins tend to exhibit elements akin to the faulted and erosional margins of Hedberg (1970) and Ross et al. (1994), or destructional slope systems of Galloway (1998). Faulting typically includes large growth faults on the outer-shelf to shelf-edge area (e.g. GOM, Orinoco and Borneo), probably induced by a high sediment supply and rapid compaction of shales. These faults may locally have throws that are one third to half of the clinoform amplitude. For instance, clinoform amplitude in the NW Borneo and Orinoco margins (Columbus Basin) reach ~2700 and ~4000 m respectively, and the throws on shelf-edge growth faults may be ~1000 m and ~2500 m respectively. These growth faults trap thick packages of sediment (e.g. thousands of meters thick in the Columbus Basin of the Orinoco margin) increasing the outer shelf-aggradation rate and decreasing the sediment budget available for progradation. For instance, during the Pleistocene, in the extensively growth-faulted Columbus Basin of the Orinoco Margin (Wood, 2000; Sydow et al., 2003), aggradation rates reach peak values (~2500 m/my) whereas progradation rates remain rather low (~15 m/my). Just east of the Columbus Basin along the Orinoco Margin in the Plataforma Deltana of Venezuela,

extensive growth faulting is absent and progradation rates significantly increase (~35 km/my) whereas aggradation rates decrease (~1000 m/my). Thus the trapping of large sediment volumes results in high aggradation rates, in turn a signature of greater accommodation space on the outer shelf because of the higher rates of tectonic subsidence. Such enhanced subsidence naturally tends to raise relative sea level, making it more difficult for eustasy-driven sea-level falls to have enough impact to generate a fall of relative sea level below the shelf-edge (to trigger deepwater sand bypass at lowstand). These falls below the shelf edge will be easier to achieve during Ice-house times with large-amplitude, high-frequency eustatic changes, but become more difficult to attain during Greenhouse conditions when amplitude and possibly frequency of eustatic sea-level change is believed to be much smaller.

Erosional or destructional processes (e.g. slumps) may result from the collapse of substantial segments of the shelf margin in response to slope readjustment (Ross et al., 1994; Galloway, 1998) to maintain equilibrium with prevalent regime variables (e.g. supply, water depth, etc.) or from tectonic activity due to seismicity, tilting and salt/mud mobilization. Such catastrophic removal of sediment on a margin decreases the progradational rate, and can even cause sub-regional shelf-edge retrogradation, for example, as occurred during the early Pliocene in the northern Gulf of Mexico (Galloway et al., 2000). Mass failure may be quite common in these margins, thus obscuring the calculation of accretion rates.

Shelf margins fronted by clinoform amplitudes <1000 m water depth

In these margins (North Slope, Lewis, Porcupine, Spitsbergen, West Siberia, NW Australia, South Africa, New Jersey and Nova Scotia), progradation rates vary from < 1 km/my (New Jersey) to ~61 km/my (West Siberia) and aggradation rates are < 270 m/my. Whereas progradation rates reach high values, aggradation rates remain

characteristically low. Clearly the reduced water-depth (space) in front of these margins favored increased rates of shelf-edge progradation. In addition, these margins tend to lack large-scale outer-shelf to shelf-edge growth faults that trap local, but large volumes of sediment. Consequently, more of the sediment budget was used for progradation. These margins exhibit elements more akin to the 'progradational' (Hedberg, 1970; Ross et al., 1994) or 'constructional' (Galloway, 1998) shelf margin categories; they tend to exhibit obvious patterns of clinoform progradation in which large-scale slope failure was a less common process. Therefore on these margins accretion rates will tend to reflect more closely the original rate of shelf margin building and therefore, probably more closely reflect the supply rate.

Table 5.1: Aggradation and progradation rates for different shelf margins*

Shelf Margin	Age	Aggradation (m)	Progradation Distance (km)	Time (my)	Aggradation Rate (m/my)	Progradation Rate (km/my)	Reference
Lewis-Fox Hills Wyoming	Late Cretaceous	>480	>86	1.8	267	47.8	Carvajal & Steel, (2006)
West Siberia	Early Cretaceous	1000	550	9.0	111	61.1	Pinous et al., (2001)
Spitsbergen Norway	Early Eocene	1150	30	6.0	192	5.0	Johannessen & Steel, (2005)
Porcupine Basin Ireland	Early Eocene	400	30	4-5	80-100	6.7	Johannessen & Steel, (2005)
North Slope Alaska	Early to Late Cretaceous	~1000	152	10.0	100	15.6	McMillen,, (1991)
Exmouth Plateau NW Australia	Early Cretaceous	610	>57	6	102	9.5	Erskine & Vail, (1988)
Pletmos Basin South Africa	Early Cretaceous	500	60	4.4	113	14	Brink et al., (1993)
Nova Scotia					20	5	Pers. Comm. J. Gelberg.
New Jersey	Middle Miocene	48	58	3.5	13.7	16.5	Steckler et al., 1999
New Jersey	Lower Miocene	A few meters	22	7.4	<~1-2 m	3	Steckler et al., 1999
New Jersey	Oligocene	38	5.8	9.5	0.4	0.6	Steckler et al., 1999
Orinoco Margin Columbus Basin	Pleistocene to present	4400	29	1.8	2450 (higher at times)	15.6	Sydow et al., 2003; Wood, 2000
Orinoco Margin Plat. Deltana	Pleistocene	1500	60	1.6	935	37.5	Di Croce et al., (1999)

Shelf Margin	Age	Aggradation (m)	Progradation Distance (km)	Time (my)	Aggradation Rate (m/my)	Progradation Rate (km/my)	Reference
Orinoco Margin Plat. Deltana	Pliocene	2000	60	3.5	550	18	Di Croce et al., (1999)
Orinoco Margin E Venezuela Bas.	Upper Miocene	1200	200	6	200	33	Di Croce et al., (1999)
Orinoco Margin E Venezuela Bas.	Middle Miocene	2000	60	5	400	10	Di Croce et al., (1999)
Orinoco Margin E Venezuela Bas.	Lower Miocene	2000	75	7	280	7.5	Di Croce et al., (1999)
Gulf of Mexico Louisiana Coast	Middle to Late Miocene	2.500 – 3000	89	5..8	463-555	15.3	Galloway et al., (2000); Wu & Galloway, (2002)
Gulf of Mexico Texas Coast	Oligocene (Frio)		143	8.5	600-700	16.8	Galloway & Williams, (1991); Galloway et al., (2000)
Gulf of Mexico Texas Coast	Eocene (Queen City)		31	2.8	600-1450	11	Galloway & Williams, (1991); Galloway et al., (2000)
Gulf of Mexico Texas Coast	Eocene (U. Wilcox)		25	5.5	100-300	4.5	Galloway & Williams, (1991); Galloway et al., (2000)
Gulf of Mexico Texas Coast	Paleocene (L. Wilcox)		74	4.6	500-600	16	Galloway & Williams, (1991); Galloway et al., (2000)
Borneo Bar-Ch Deltas	Pleistocene	2300-1700	7-20	1.7	1350-1000	4.1-11.8	Saller & Blake, (2003)
Borneo Bar-Ch Deltas	Pliocene	2000-1700	30-20	3.7	540-459	10-3.2	Saller & Blake, (2003)
Borneo Bar-Ch Deltas	Late Miocene		20-40	5.7		3.5-7	Saller & Blake, (2003)

*Accretion distance and aggradation measured in shelf-edge maps and cross-sections. All measures un-decompacted except for New Jersey Margin, and Gulf of Mexico in the Paleocene, Eocene and Oligocene whose progradation rates are directly provided in Galloway and Willimas (1991) (i.e. there is no need to measure progradation). Some uncertainties may arise from cross-sections orientations, lack of depth-converted seismic data and limited aerial coverage. Dating is reasonably good for all margins except for the North Slope (which may lead to errors in accretion and aggradation rates). In the Orinoco and New Jersey margin more than one period was chosen to represent variability. For the Gulf of Mexico, time interval is during high rate of progradation.

Accretion rates and basin fill architecture

The variable rates of progradation and aggradation show that clinoforms filled the basin in very different ways in the moderately deep-water and very deep-water margins (Figure 5.3). Depending on clinoform-slope gradient, the slope width from the shelf edge to base of slope on a moderately-deep shelf margin will typically be <30 km, whereas in a very deep-water margin it will be up to 100's of km (e.g. >200 km in the Columbus Basin). Therefore the slope width in the moderately deep basin is within the potential

progradational range of that system, and so the space below the shelf-edge on the slope can be commonly filled within a few hundred ky in rapidly prograding margins and around 1 My in slowly prograding margins. For instance, the slowly prograding Porcupine and Spitsbergen margins have clinoform amplitudes of 250-400 m (un-decompacted) and slope angles of 2-4^{o}. On these margins, an average clinoform of 325 m amplitude and 3^{o} slope will have a width of ~ 6 km, i.e., close to the range of average progradation rate for these margins (5-7 km/my), and so will be able to fill the accommodation below the shelf-edge within ~ 1 my. As a consequence, these systems have the potential to build extensive topsets at a high rate. For instance the West Siberia margin built a 550 km wide shelf in 9 my (Pinous et al., 2001). In contrast, the Gulf of Mexico margin platform width is ~ 360 km for the entire Cenozoic (~65 my). On the other hand, the 100s km long slopes in very deep-water margins require several millions years (in cases > 10 my) to fill the slope space, this together with the high aggradation rate results in a more aggradational style of clinoform growth. Therefore, the progradational basin filling style, so typical of the descriptions of shelf margins, is likely to occur on low to moderately deep margins.

Smaller margins are not scaled-versions of large margins

The geometric differences in the way clinoforms fill the basin (resulting from their distinct progradation rates and clinoform dimensions), and the different structural style and tendency to mass failure indicate that the smaller margins are different than the larger margins. This is the case despite both having the characteristic shelf-slope-basin-floor morphology and both being able to develop growth faulting, mass failure and

changing accretion rates. Nonetheless, the moderately deep margins are not simply scaled-down versions of the larger margins (Figure 5.3).

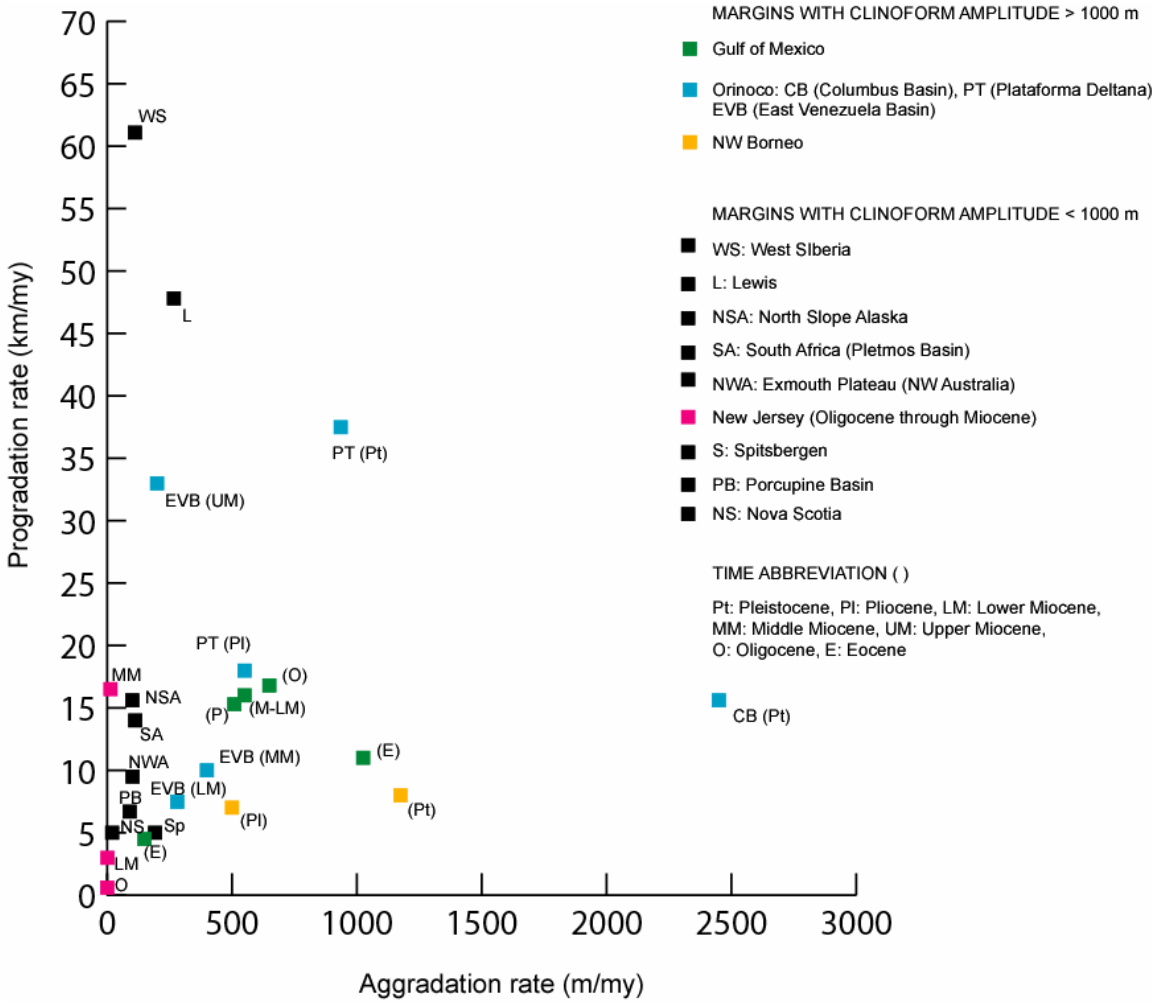

Figure 5.2: Progradaton and aggradation rates in the study margins.

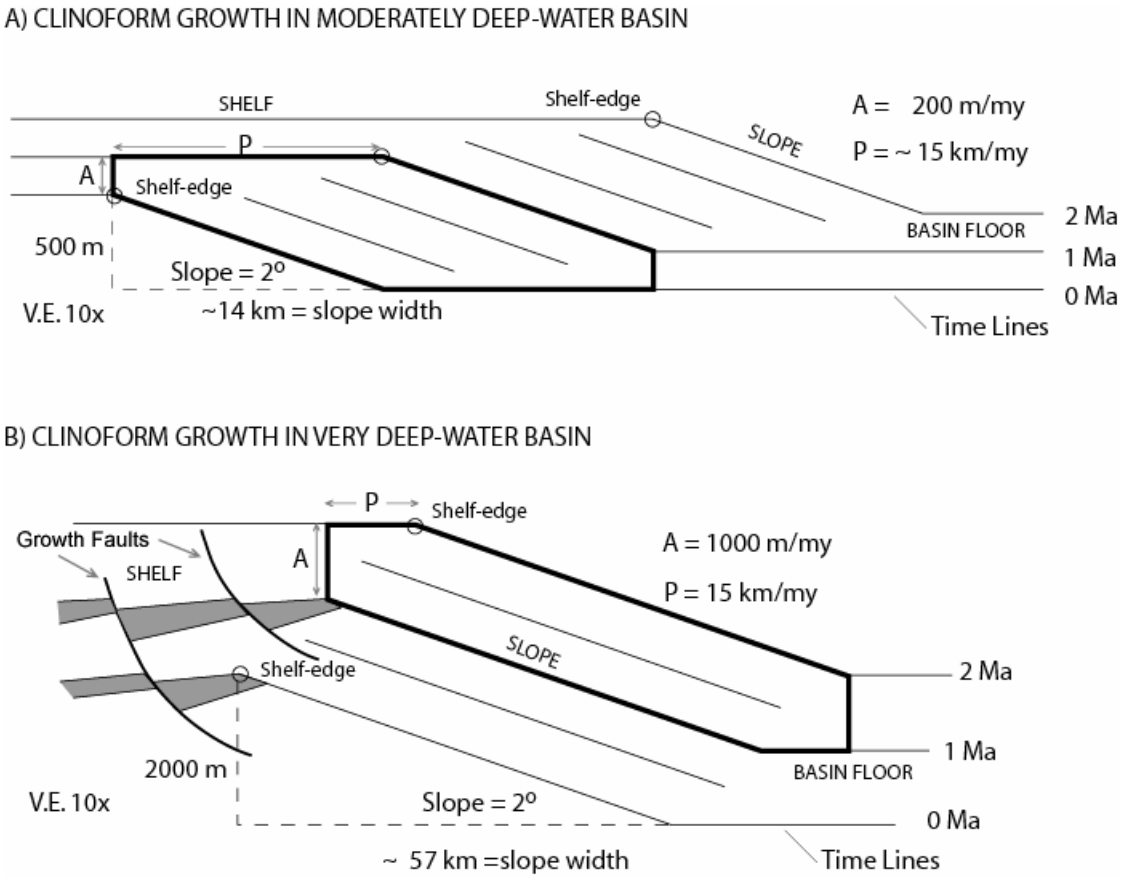

Figure 5.3: Schematic representation of basin fill architecture in moderately deep and very deep-water margins. Both cartoons are at the same vertical exaggeration (but they have different dimensions), so the different geometries of the basin fill can be appreciated. Notice that filling in the moderately deep margin (even in cases of slow progradation) is more progradational than in a very deep margin.

DO AGGRADATION AND PROGRADATION RATES REFLECT HIGH/LOW SEDIMENT SUPPLY?

The rate at which a shelf margin progrades and aggrades is a direct result of the volume of sediment supplied, relative sea level changes, and basin dimensions, particularly clinoform amplitude. Basinal processes (e.g. waves, tides, river influence) may cause some along-strike variability, but storm waves are usually the dominant

element along shelf-edge areas during highstand conditions because of exposure to oceanic swell (Porebski & Steel. 2006). Process variability is usually much greater along shorelines (e.g., Bhattacharya, 2006), and morphology change is usually, therefore, much greater along shorelines than along shelf margins. For margins of similar clinoform amplitude and sea level regime, therefore, accretion rates should show some degree of correlation with sediment supply; increasing accretion rates should be linked to increasing supply at least along the segment of the margin under consideration.

Margins with clinoform amplitude < 1000 m

On these margins, higher progradation rates correlate reasonably well with sediment volume as estimated simply from infill dimensions. For instance, the rapidly prograding clinoforms (61.1 km/my) of the West Siberia margin filled a basin whose area was some 100,000's of km^2 (although total basin area reaches ~ 2 x 10^6 km^2) and built an extensive shelf platform at least ~550 km wide during about 9 my (Pinous et al., 2001). In the Lewis-Fox Hills margin (> 48 km/my progradation rate), the basin area filled by the clinoforms was of the order of 10,000's km^2 and built a platform greater than 100 km wide. In contrast, the slowly accreting margins in the Central Basin (Spitsbergen), Pletmos Basin (South Africa), Porcupine Basin (offshore Ireland) filled basinal areas of only some 100's km^2 and built platforms typically < 60 km wide. These slowly accreting margins remained active for a time interval shorter than the West Siberia margin, but even if their life had been longer they would not have reached (other variables remaining the same) the infill dimensions of West Siberia; the supplied sediment volumes in West Siberia were simply very large. Notice also that the duration of the Lewis-Fox Hills margin building was < 2 my, i.e., a shorter life span than all the other margins, but its

infill dimensions are still greater than those of the slowly accreting margins. Thus, in the study cases high rates of progradation correlate with high volumes of supplied sediment and vice versa.

This trend seems to occur also within a single basin. For example, increasing rates of progradation and aggradation on the New Jersey margin correlate with increased rates of sediment supply. Steckler et al. (1999) calculated rates of sediment supply from the Eocene through middle Miocene and determined that supply increased from a few m^2/y (area units because a cross section was used by Steckler and others) in the Eocene to about 40 m^2/y in the Middle Miocene. Accordingly, the increasing rates of supply correlate with increasing rates of shelf margin accretion. For instance, during the Oligocene, Steckler et al. (1999) calculated that supply was 1.5 m^2/y and the shelf margin prograded at a rate < 1 km/my and aggraded at a rate < 4 m/m.y. In the Early Miocene, supply rose to ca. 5 m^2/y, and the shelf margin progradation rate increased to 3 km/m.y. and the aggradation rate slightly decreased to 1-2 m/m.y. indicating that the increase in supply resulted in increasing progradation rate. During the Middle Miocene, supply increased to rates typically between 10-40 m^2/y and progradation rates increased to 16-17 km/my and average aggradation rates were greater than 10 m/my Thus on this margin, it is clear that increases in supply correlate with increases in accretion rate, although the analysis does not take into account the volume of sediment that may have bypassed the clinoform entirely. Calculations of supply by Steckler et al. (1999) and our measures of progradation and aggradation rates were done using one cross-section.

The above examples suggest that high/low end members for progradation rates reflect larger/smaller volumes of sediment supplied to the outer shelf, when comparing basins of low to moderate clinoform amplitude (< 1000 m) and low aggradation rates (i.e. Spitsbergen, Porcupine, Lewis-Fox Hills and West Siberia) or rates within the same basin

(e.g. New Jersey). However, it seems likely that there will be cases where a higher progradation rate does not closely reflect a higher volume of supplied sediment, notably where 1) much sediment has bypassed to deepwater areas, in which case the supply increase would be underestimated, 2) the higher progradation rate results from slight changes in other variables (e.g., fall of sea level) despite similar clinoform amplitude and 3) there is greater than normal lateral variability along the shelf margin, and off-axis data transects underestimate the supply, or accretion caused by high rates of longshore feeding reflect far distant river supply.

To resolve this problem I suggest referring collectively to these margins as 'supply dominated', expanding on the supply-domination concept from regime theory (Swift and Thorne, 1991). Although the regime concept was chiefly applied to shelf systems, the regime variables can also be used for the edge of the shelf platform. The variables include sediment supply and caliber, sea level and dispersal system (e.g., frequency and power of waves, tides, river currents and sediment-density flows). In supply-dominated shelf regimes, sediment supply outpaces accommodation and the dispersal of sediment produces a clear pattern of progradation. Supply domination does not necessarily imply a larger volume of sediment; two shelves may be supply dominated but the sediment budget maybe quite different depending on sea level and basin processes. We thus suggest referring to supply-dominated margins as those that show high progradation rates, typically several tens of km/my This designation also eliminates the need to calculate absolute values of sediment supply.

Margins with water depths > 1000 m

The large scale of these margins, their relative lack of published data and their wide range of complicating slope features (e.g. mass failures, large growth faults, salt and mud diapirs, etc) make it very difficult to evaluate whether accretion rates correlate with

supply. Data from the Gulf of Mexico seem to suggest that accretion rate may, at times, correlate with volume of sediment delivered to *deltaic and shorezone systems on the shelf*. For instance, Galloway (2001) obtained relatively large volumes (3.5-8 x 10^4 km^3/my) of sediment in deltaic and shorezone systems during the growth of the Upper Paleocene (Lower Wilcox), the Oligocene (Frio-Vicksburg) and Upper Miocene shelf margins. During these periods progradation rates were between 15 and 17 km/my and aggradation rates between 450 and 700 m/my (decompacted). In contrast, for the Lower and Middle Eocene (Upper Wilcox and Queen City respectively) the volumes of sediment in deltaic and shore zone systems were smaller (< 1 x 10^4 km^3/my) as was their progradation rates (< 4.5 and 11 km/my respectively). The aggradation rate was also smaller (100-300 m/my) for the Upper Eocene, but higher for the Middle Eocene (600-1450 m/my) probably reflecting that during Queen City times (Middle Eocene) there was much retention and storage of most of the sediment budget on the shelf without much bypass to the basin floor. Therefore, there seems to be a crude relationship between progradation rate and volume of sediment in deltaic and shorezones; high rates (15-17 km/my) are linked to higher volumes. Whether these relate to total volume is hard to determine, because an important problem in this analysis is that sediment volumes do not consider the fraction of sediment bypassed to the deepwater slope and basin floor, which can be substantial on these margins.

ACCRETION RATES AND DEEPWATER SEDIMENTATION

The Importance of Shelf-Edge Deltas

The selected margins indicate that shelf-edge deltas and associated strandplains are the principal drivers of shelf-margin accretion, especially in supply-dominated margins with several 10s km/my of progradation (Porębski and Steel, 2003). Other

processes may also prograde the shelf margin, but they are less common. For example, in the Miocene Canterbury Basin, offshore New Zealand, contour currents are interpreted to have caused shelf margin accretion but with progradation rates < 2-3 km/my (or even retrogradation at times) (Lu et al., 2003). The Eocene Queen City depisode (Galloway et al., 1991; Galloway et al., 2000) in the Gulf of Mexico did not develop shelf-edge deltas and its progradation rate is relatively small (~ 10 km/my) and restricted to a small area in the basin. Similarly, during the Pliocene and Pleistocene in the NW Borneo margin, deltas appeared to have been restricted mostly to the inner and outer shelf and consequently the margin experienced low progradation rates (5-10 km/my) (Saller and Blake, 2003). In addition, accreted deposits tended to be muddy in these latter cases. In contrast, the Lewis-Fox Hills and West Siberia margins and generally most of the other margins show that shelf-edge progradation occurred chiefly through shelf-edge deltas and their along-strike strandplains. A high shelf-margin progradation rate therefore generally implies the recurrent arrival of deltas at the shelf edge, and the retention/maintenance of these deltas at an outer shelf location for longer times, with only short regressive-transgressive transits close to the shelf edge. As delivery systems, these shelf-edge deltas naturally increase the potential to bypass sediment to deepwater areas.

Margins with water depths < 1000 m

There are sharp differences between rapidly and slowly prograding margins (Figures 5.4, 5.5, 5.6, 5.7 and 5.8). A common theme on the West Siberia and Fox Hills margins is the recurrent and abundant delivery of sand to deepwater fans. In West Siberia, Pinuous et al. (2001) has interpreted 16 clinoformed sequences and in most of them abundant sandstones are present on the slope and basin floor. Common intervening shales separating deepwater sandstones suggest to Pinuous et al. (2001) that delivery

continued even during higher frequency cycles (possibly fourth to fifth order). These sandbodies frequently reach thicknesses greater than 100 m. In the lowstand systems tract (not including the prograding wedge) of one of these sequences (~0.6-0.7 my duration), maps of the basin floor and slope sandy deposits show an area of a few 1000s of km^2 (Pinous et al., 1999) (Figure 5.5). In West Siberia, the amount of deepwater sand in both the slope and basin floor is notably linked to shelf-edge deltas interpreted as lowstand prograding features; i.e. sands that were bypassed to the basin floor when sea level was not falling, but at stillstand or rising slowly (Pinous et al., 1999). It is also notable that sand was also bypassed to deepwater areas, albeit in apparently very small volumes, during transgression. Similarly in the Lewis margin, this study indicate that all of the 5^{th}- and 4^{th}-order shelf sequences generated sand-prone deepwater deposits (Carvajal and Steel, 2006). Basin-floor sandbodies in the Lewis-Fox Hills margin reach maximum thickness between 52 and 121 m and have areas ranging between 1387-2580 km^2, quite extensive for fans of 4^{th} to 5^{th} order. Slope sandstones in the Lewis form channel belts, sometimes reaching 10s of km of width. Furthermore, the Lewis-Fox Hills delivery took place during both lowstand and highstand sea-level conditions in 4th to 5th order cycles as indicated by the presence of fans in rising and flatter clinoform trajectories linked to shelf-edge deltas. Thus, signatures of supply domination include recurrent (i.e., frequently in sequences of ~100-350ky duration) and abundant delivery of sand to deepwater either at lowstand or highstand, as well as high progradation rates (Figure 5.9).

These characteristics contrast with those observed in slowly prograding margins (Figures 5.6, 5.7 and 5.8). For instance, the Spitsbergen and Porcupine Basin fans are less than 50-60 m thick. Fan area in the Porcupine basin is < 100 km^2 and in Spitsbergen maximum fan length (along the exposed cross-section) < 10 km (Figure 4). In the slowly accreting Nova Scotia margin the deepwater setting is relatively muddy and exploration

for large sandy fans has been fairly unsuccessful. Fan area in the Pletmos Basin is ca.150 km^2 and if the "slope fan" is included it may reach ~300 km^2 (Brink et al., 1993). Notice that in the Pletmos margin (progradation rate ~14 km/my), sand bypass to deepwater areas was recurrent (i.e., fans frequently occur in high-order sequences), but fans are smaller than in the Lewis and West Siberia margins, though larger than in the Porcupine basin (Figure 5.8). Also, in the North Slope margin (progradation rate = 15 km/my) sand bypass was recurrent, but unfortunately here the poor dating impedes determination of sequence order; and so it is quite possible that high-frequency regressive-transgressive shelf cycles may commonly alternate between deepwater sand delivery and non-delivery. Similarly in the New Jersey margin, reported fan thickness is 15-75m (Greenlee et al., 1992). The area of these fans is not provided, but isochron maps of 3^{rd} order sequences (Poulsen et al., 1998) suggest that they are probably not much greater than a few 10's of km^2. It should be stressed, however, that fans reported by Greenlee et al. (1992) belong to sequences of typically >1 my duration, and 4^{th}- to 5^{th}-order fan dimensions are not given. For instance, as described above 4^{th} to 5^{th} order fans in the Lewis are <120 thick and < 2,500 km^2, but at the 3^{rd} -order scale they would reach thickness and areas of several 100's m and 1000's km^2 respectively. In addition, most of the sand bypass to deepwater areas in these slowly-prograding margins has been interpreted to take place at sea-level lowstand. This is confirmed by the case of clinoform 17 in Spitsbergen which shows highstand shelf-edge deltas but no associated deepwater sands (Steel et al., in review). The low supply rates would have been unable to compete with rising sea-level at highstand to deliver deepwater sands. Consequently, falling sea level seems to be required to drive the delivery of sand to deepwater areas in these slowly accreting margins. Porębski and Steel (Porębski and Steel, 2006) referred to the delivery deltas in

such cases as accommodation-driven deltas, in contrast to the supply-driven ones that are able to deliver at highstands.

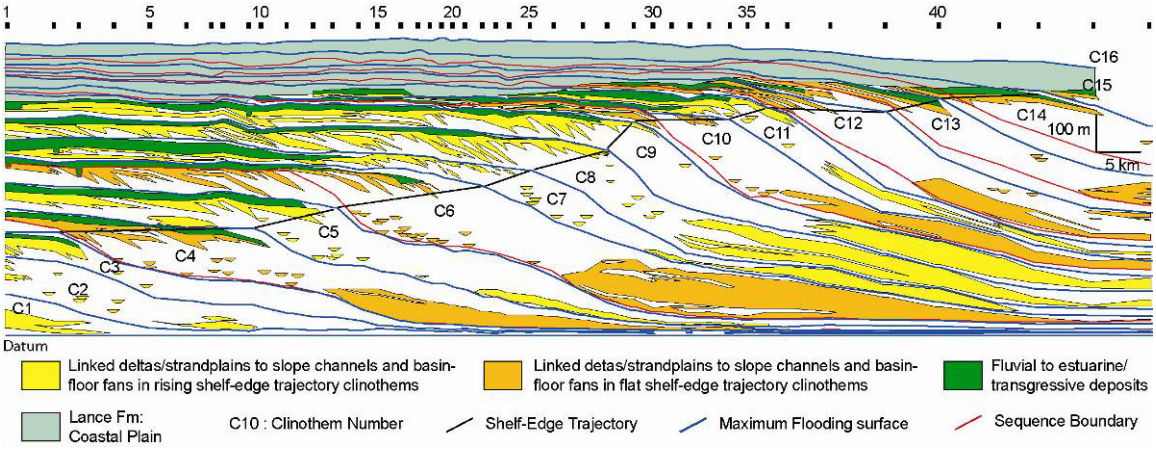

Figure 5.4: Accretion in the Lewis-Fox Hills Shelf Margin (from Carvajal and Steel, 2006).

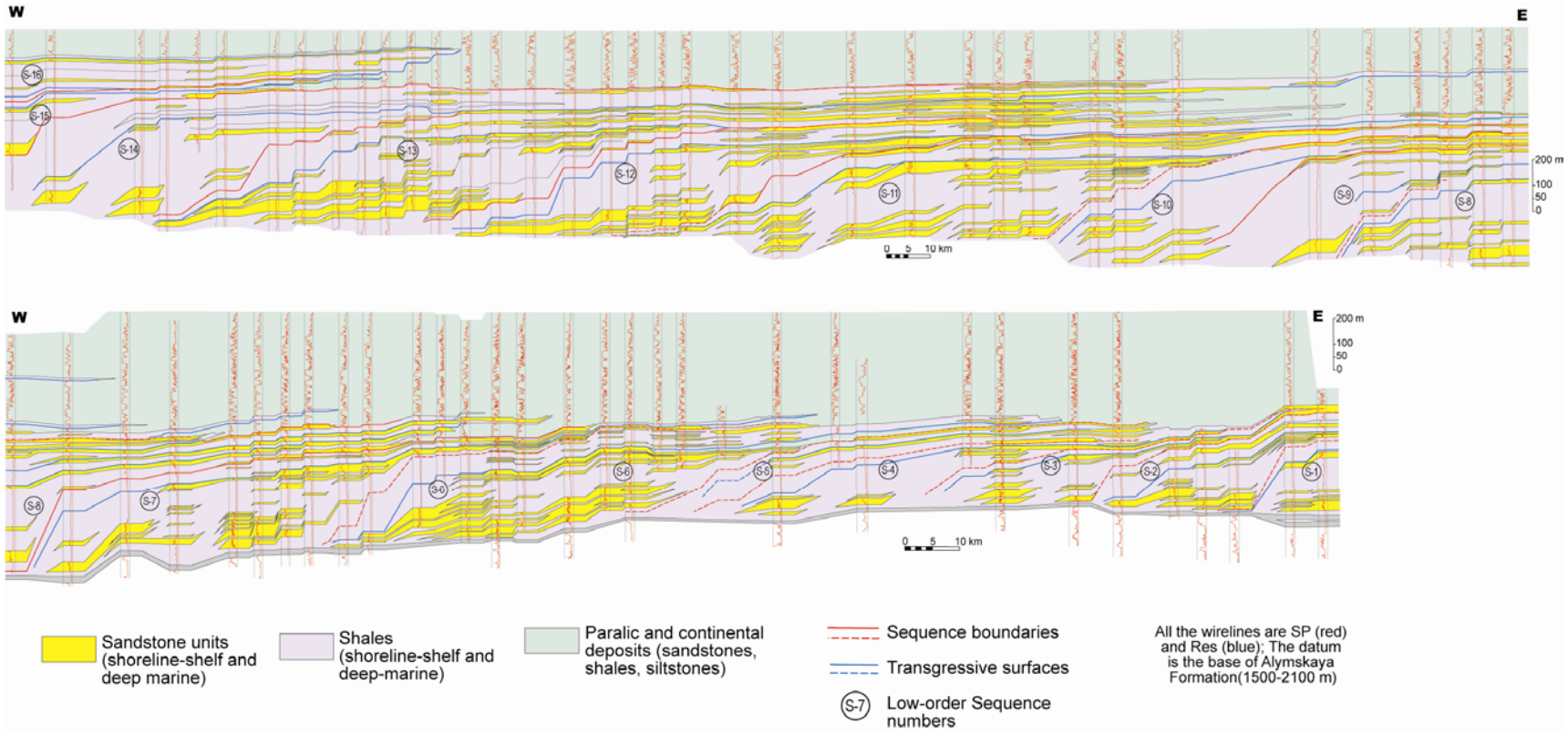

Figure 5.5: Accretion in the West Siberia Margin. As in the Lewis, notice the abundant and recurrent delivery of sand in this highly prograding shelf margin (from Pinouos et al. 2001).

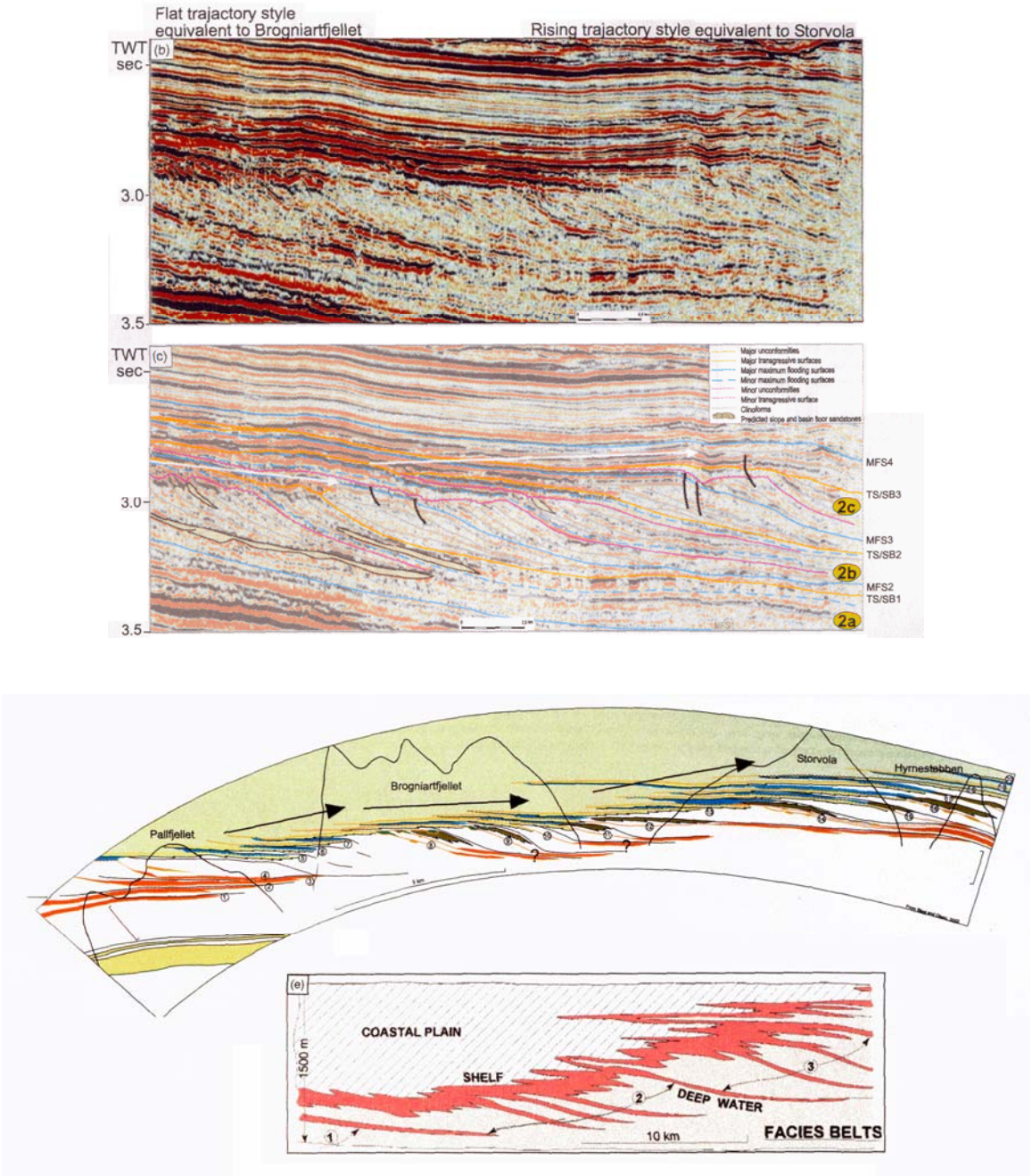

Figure 5.6: Porcupine (top) and Spitsbergen (below) shelf margins. Delivery in these margins with low progradation rates seems to be less frequent, in smaller volumes and more driven by accommodation (Johannessen and Steel, 2005).

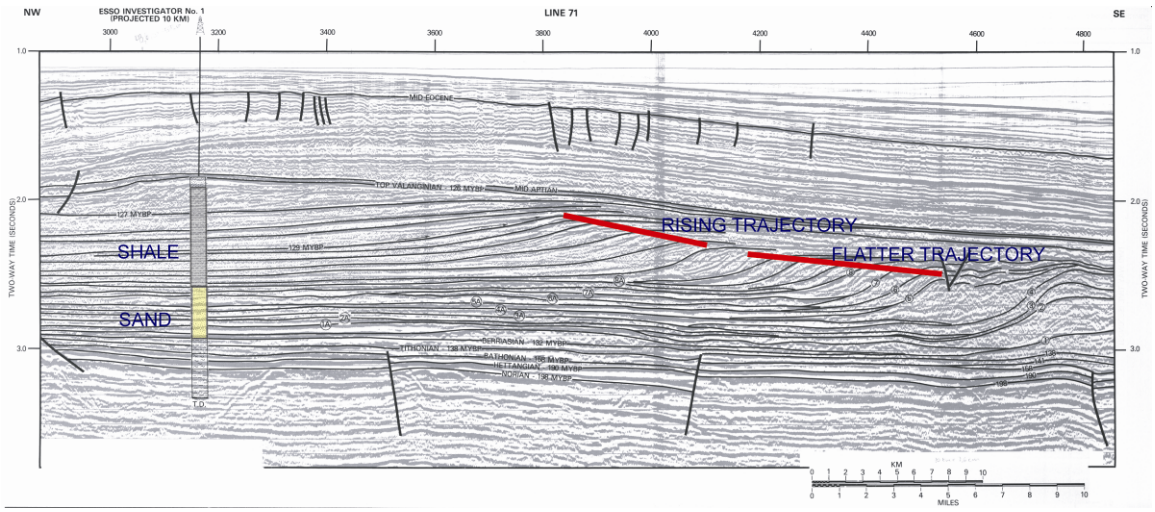

Figure 5.7: NW Australia margin. Notice that in this slowly accreting margin delivery is also constrained to clinoforms with flatter shelf-edge trajectories (from Erskine and Vail, 1988).

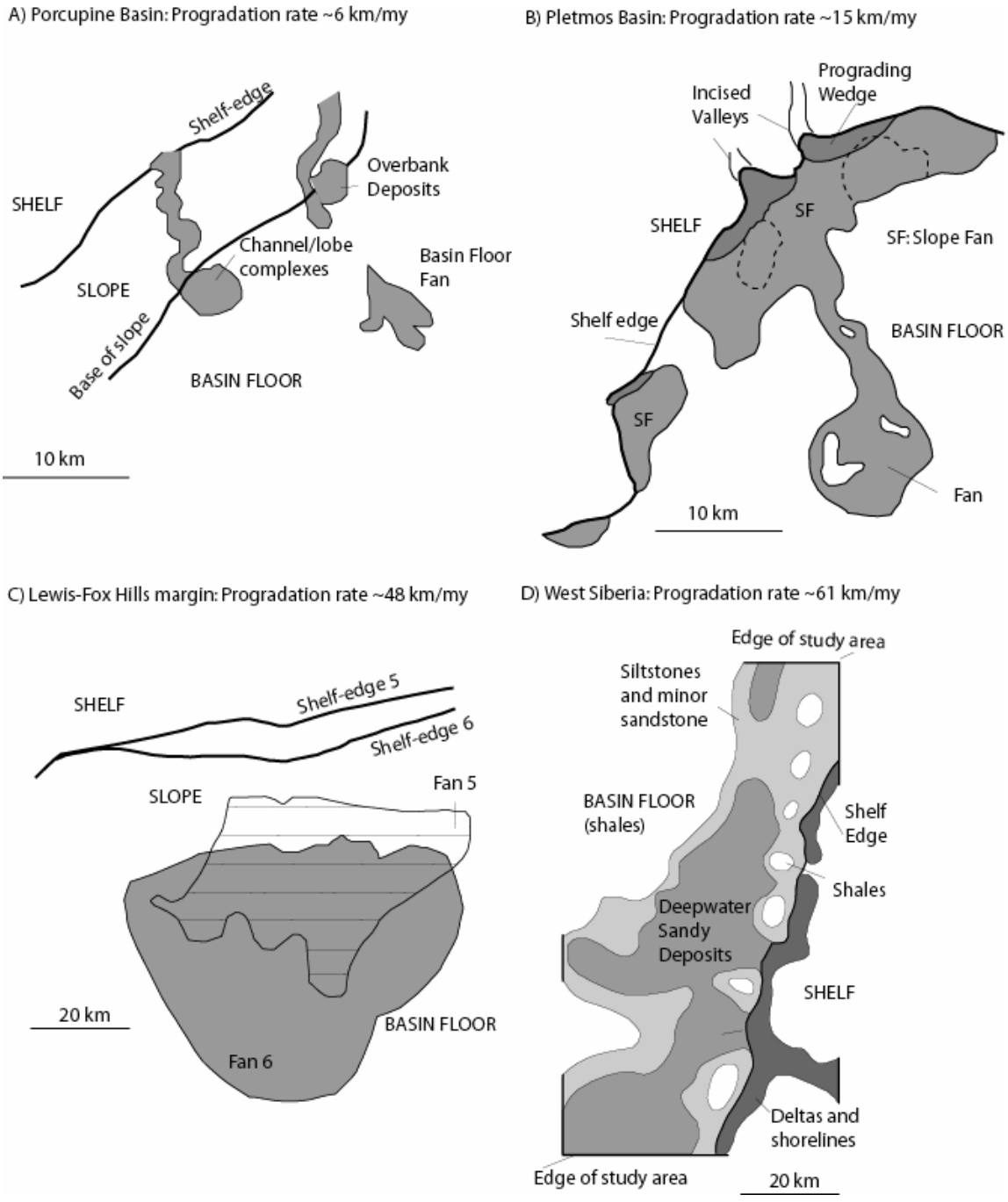

Figure 5.8: Comparison of deepwater systems and progradation rates for the Porcupine, Pletmos Basin, Lewis and West Siberia margins. Notice the significant increase in the area (which is accompanied by increases in deepwater sandstone thickness as well) of sandy deepwater deposits as progradation rate and sediment supply increases (see Table 1 for references).

Sediment supply as limiting factor

Increasing rates of progradation seem to be linked to increasing frequency and more abundant delivery of sand to deepwater areas and an enhanced potential to form highstand fans. These trends are easily explained by, and should be a natural result of, a greater sediment volume or supply domination on the shelf margin. However, emphasis on sea level has caused the scientific community to overlook these patterns. Furthermore, this analysis raises the hypothesis that sediment supply is really the primary variable limiting the delivery of sand to deepwater areas. This possibility is heightened if we take into account the fact that the high supply systems, the Lewis-Fox Hills and West Siberia margins, developed during greenhouse times, i.e. when eustatic sea-level changes are generally considered to be low to moderate (a few tens of meters at most). Thus, at these times high-frequency and high-amplitude sea level falls, and their driving role to trigger sand bypass to deepwater areas, are presumably of limited importance. Forward modeling (Burgess and Steel, in review) does suggest that sediment volume (for a given clinoform amplitude) represents the primary factor limiting shelf-margin topset width, i.e., in Burgess and Steel's forward models, topset width increases linearly with sediment supply, whereas it shows minor variations (under constant supply) for typical eustatically driven sea-level amplitude changes (25, 50 and 100 m) superimposed on average subsidence trends. Increasing sediment transport efficiency led to an enhanced sea-level influence on topset width, but still sediment supply remained the primary control. If a similar trend exists for deepwater sediments, as our observations suggest, then future research addressing the problem of sediment production volume and transfer to marine settings may significantly improve prediction of basin-floor sands.

Implications for Exploration

This analysis suggests that a high progradation rate and linked high supply will tend to reduce the risk of finding a basin floor without sandy fan reservoirs. In addition, when the supply is high, the greater area of the reservoirs will make it easier to target them. In contrast, a low supply shelf margin, albeit allowing the bypass of sand caused by a relative sea level fall, will generate smaller fan reservoirs that are more difficult to target (Figure 5.9). Although these trends are clear for the study margins, more testing of these hypotheses is needed.

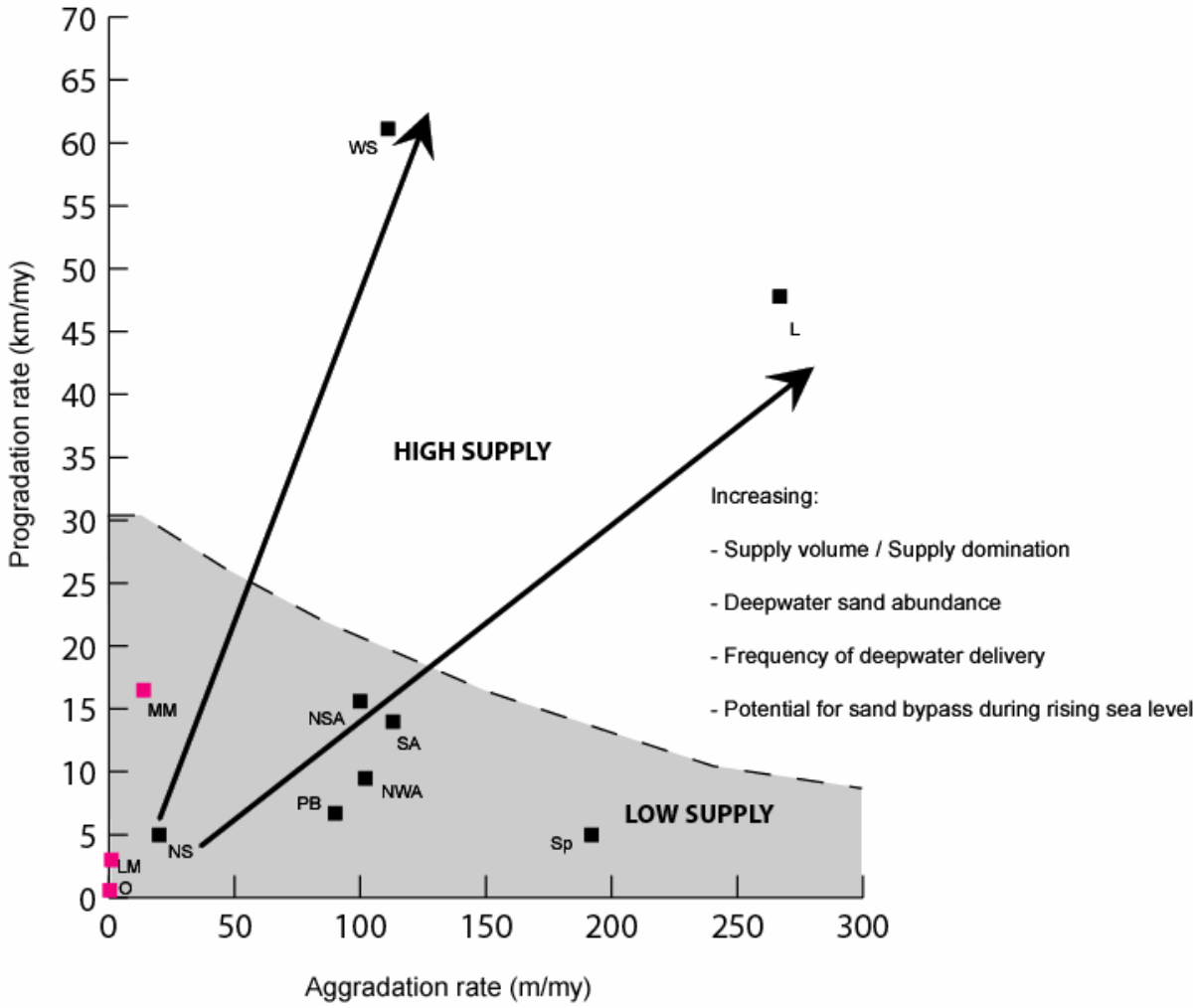

Figure 5.9: Accretion rates and their relationship to inferred sediment supply volume and deepwater sandstones for margins with clinoform amplitudes <1000m. See Figure 5.2 for margins legend.

Margins with water depths > 1000 m

The relative lack of data on these margins (except for the Gulf of Mexico) and their greater tendency to slope failure complicates prediction of deepwater sediment bypass from accretion rates. In the Gulf of Mexico basin, all the study intervals except

the Queen City depisode contain abundant deepwater deposits (Feng, 1995; Galloway et al., 2000). This tells us that progradation rates as low as 4.5 km/my and as high as 17 km/my, accompanied by aggradation rates of 100's m/my may generate significant deepwater sands. Interestingly, the Queen City depisode has the highest range of aggradation rates (600-1450 m/my; the only one >1000 m/my) and does not contain basin-floor fans. However in the Columbus Basin, the Pleistocene Orinoco margin stacking is also quite aggradational (~2500 m/my), but shelf-edge to slope failure has led to the bypass of sediment to deepwater areas (Moscardelli et al., 2006) and at least one modern fan presently exists on the Orinoco basin floor (the "Orinoco Fan"). Shelf-margin collapse can be quite severe and involve large volumes of sediment. For instance, during the Pliocene, shelf-edge collapse through several 10's of kms along north-east Gulf of Mexico led to ~24 km of shelf-edge retrogradation. Such collapse resulted in the formation of sand-rich fans on the basin floor which may contain an even greater sediment volume than the fans formed from construction or progradation of the shelf-edge in the adjacent and contemporaneous NW Gulf basin floor. The NW Borneo margin also shows low progradation rates (5-10 km/my) and relatively high aggradation (500-1250 m/my) and is chiefly built by deltas that did not reach the shelf edge, resulting in a muddy shelf-edge and slope and significant storage of sediment in growth-fault compartments. However, turbidites have been found in outer neritic to bathyal depths and it is postulated that sand may have been bypassed to deepwater areas at sea-level lowstand (Koopman and Schreurs, 1996; Saller and Blake, 2003), though the quantity of sand is unknown. Thus, progradation and aggradation rates may be misleading in these large, failure-prone margins.

CONCLUSIONS

Shelf margin accretion rates show a wide range of variation across moderately deep-water and very deep-water basins. In the former case, progradation and aggradation rates are <61 km/my and <270 m/my, respectively, whereas in the latter case, they are <~37 km/my (generally <20 km/my) and <~2.5 m/my, respectively. In very deep- water basins, the trapping of large volumes of sediment by growth faults on the outer shelf and near shelf edge evidently decreases slope progradation rates and increases shelf aggradation rates.

Moderately deep margins are not simply scaled down versions of larger margins; they tend to show a more progradational architecture and they are much less prone to develop large-scale growth faulting and to catastrophic sub-regional failure. These characteristics cause the accretion rates on these margins to more closely reflect the sediment-supply rate into the basin.

In the selected moderately deep margins (< 1000 m water depth), a sharp contrast exists between slowly and rapidly prograding margins. Slowly prograding margins (<10 km/my) tend to produce small volumes of sediment in the basin and a delivery of sand to deepwater that is: a) less recurrent, b) volumetrically smaller and c) emplaced chiefly at lowstand. Rapidly prograding margins (several 10's km/my) show greater volumes of sediment in the basin and a delivery of sand to deepwater that is: a) recurrent (i.e., it occurs during most 4^{th}-5^{th} order cycles), b) abundant (i.e., 4^{th}-order fan thickness several 10s m and area ~ few 1000s km^2) and 3) can occur at lowstand and highstand in 4^{th}-5^{th} order cycles. I consider these last features typical signatures of what I term supply-dominated margins.

These trends suggest that sediment supply (not sea level) is the key limiting variable controlling the bypass of sand to deepwater areas; i.e. the larger the supply, the

larger the shelf-margin in general and the larger the volumes of sediment in the slope and basin floor. This seems a logical result, but probably has been overlooked due to over-emphasis on sea-level change to predict deepwater sands.

In very deep-water margins a paucity of data, very large architectural dimensions and greater tendency for shelf-edge failure makes it difficult to relate accretion rates to sediment volumes and deepwater sands. For instance, it is common on these margins that shelf-edge retrogradation through catastrophic failure may lead to deepwater sands.

CHAPTER 6: CONCLUSION

Detailed conclusions are presented in each chapter; here I summarize the main contribution of my dissertation. The key results emphasize the driving role of sediment supply in rapid shelf-margin building and deepwater sand emplacement. On the study margin, supply was able to outpace shelf accommodation even at times of high and strongly rising sea level. At these times, clinoforms developed a more aggradational architecture with relatively thick and marine-influenced topsets formed in response to basin deepening due to rapid subsidence. The high supply and subsidence are interpreted to have resulted from crustal loading and significant erosion during prominent Laramide thrust-driven mountain uplift. Despite the rising relative sea level, the high supply drove deltas to the shelf-edge where they developed strong wave and river influence. This resulted in extensive coastal sand belts at the shelf margin, and bypass of significant volumes of sand to deepwater areas. In contrast, during times of stable to very low rates of sea-level rise, the basin developed more progradational clinoforms with more terrestrial and generally thinner topsets. More of the sediment was funneled to the basin floor and shelf-edge deltas were under strong river and tidal influence. Stable or even falling sea level resulted from decreased or zero basin subsidence, interpreted to have resulted from decreasing uplift, tectonic quiescence or possibly slight tectonic rebound in the basin. The Lewis-Fox Hills margin is considered supply-dominated, a term to denote moderately deep shelf margins (< 1000 m) that prograde at high rates (several tens of kms/my) and deliver sand to deepwater areas recurrently and in large volumes even at sea level highstand.

APPENDIX

The appendix is in a DVD and is composed of two parts. The first part contains a set of 21 cross sections (File: "Cross Sections" in DVD) to illustrate the basin scale correlation of maximum flooding surfaces and surfaces separating regressive and transgressive compartments in the topset. Also in north-south cross sections is shown the division of the topset and slope. A map is included with the location of the cross sections.

The second part (File: Isopach Maps in DVD) contains the isopach maps for sandstone, shale and coal. These maps were created from the same grids used in Petra for volume calculation. For each clinothem or cycle a map is provided for the referred lithologies in the topset, regressive-topset, slope and basin-floor compartments. Each map also shows the polygons for the topset and basin floor. The basinward boundary of the topset is placed at approximately the shelf-edge position at the end of the cycle.

The DVD is available from the author (ccarvajal@chevron.com or ccarvaj@yahoo.com) or from the Walter Geology Library at the University of Texas at Austin:

MAILING ADDRESS:
Walter Geology Library, GEO 4.202, S5438
The University of Texas at Austin
Austin, TX 78712-1101

PHONE
voice: +1 (512) 495-4680
fax: +1 (512) 495-4102
EMAIL: georequests@lib.utexas.edu

REFERENCES

Allen, G.P., and Posamentier, H.W., 1993, Sequence stratigraphy and facies model of an incised valley fill: the Gironde estuary, France: Journal of Sedimentary Petrology, v. 63, p. 378-391.

Almon, W.R., Dawson, W.C., Sutton, S.J., Ethridge, F.G., and Castelblanco, B., 2001, Sequence stratigraphy, petrophysical variation, and sealing capacity in deepwater shales, Upper Cretaceous Lewis Shale, south-central Wyoming, *in* Crockett, F., and Stilwell, D.P., eds., Wyoming gas resources and technology: Wyoming Geological Association Guidebook 52, p. 163-182.

—, 2002, Sequence stratigraphy, facies variation and petrophysical properties in deepwater shales, Upper Cretaceous Lewis Shale, south-central Wyoming, *in* Dutton, S.P., Ruppel, S.C., and Hentz, T.F., eds., 52nd annual convention of the Gulf Coast Association of Geological Societies, Volume 52: New Orleans, LA, United States, Gulf Coast Association of Geological Societies, p. 1041-1053.

Asquith, D.O., 1970, Depositional topography and major marine environments, Late Cretaceous, Wyoming: American Association of Petroleum Geologists Bulletin, v. 54, p. 1184-1224.

Beaumont, C., 1981, Foreland basins: Geophysical Journal of the Royal Astronomical Society, v. 65, p. 291-329.

Berg, R.R., 1962, Mountain flank thrusting in Rocky Mountain foreland, Wyoming and Colorado: Bulletin of the American Association of Petroleum Geologists, v. 46, p. 2019-2032.

Bhattacharya, J.P., and Giosan, L., 2003, Wave-influenced deltas: geomorphological implications for facies reconstruction: Sedimentology, v. 50, p. 187-210.

Blackstone, D.L., Jr., 1991, Tectonic relationships of the southeastern Wind River Range, southwestern Sweetwater Uplift, and Rawlins Uplift, Wyoming, Report of Investigations, Volume 47: United States, Geological Survey of Wyoming : Laramie, WY, United States.

Bohacs, K., and Suter, J., 1997, Sequence stratigraphic distribution of coaly rocks: fundamental controls and paralic examples: Bulletin of the American Association of Petroleum Geologists, v. 81, p. 1612-1639.

Boyd, R., Ruming, K., Sandstrom, M., and Schroder-Adams, C., 2006, Highstand sand transport to deep water by longshore transport, tidal and gravity processes, *in* Kneller, B.C., McCaffrey, B., Martinsen, O., and Posamentier, H.W., eds., External controls on deepwater depositional systems -climate, sea-level and sediment flux: London, SEPM-GSL conference, p. 17.

Brink, G.J., Keenan, J.H.G., and Brown, L.F., Jr., 1993, Deposition of fourth-order, post-rift sequences and sequence sets, Lower Cretaceous (Lower Valanginian to Lower Aptian), Pletmos Basin, southern offshore, South Africa, *in* Weimer, P., and Posamentier, H.W., eds., Siliciclastic sequence stratigraphy -recent developments and applications: American Association of Petroleum Geologists Memoir 58, p. 43-69.

Brown, W.G., 1988, Deformational style of Laramide uplifts in the Wyoming foreland, *in* Schmidt, C.J., and Perry, W.J., Jr. [editor], eds., Memoir - Geological Society of America: Geological Society of America (GSA) Memoir 171, p. 1-25.

Burgess, P.M., and Hovius, N., 1998, Rates of delta progradation during highstands; consequences for timing of deposition in deep-marine systems: Journal of the Geological Society of London, v. 155, Part 2, p. 217-222.

Burgess, P.M., and Steel, R.J., in review, Stratigraphic forward modeling of delta auto-retreat and clinoform topset width: implications for controls on topset width and timing of formation of shelf-edge deltas, SEPM Special Publication.

Carvajal, C.R., and Steel, R.J., 2006, Thick turbidite successions from supply-dominated shelves during sea-level highstand: Geology, v. 34, p. 665-668 doi 10.1130/G22505.1.

Connor, C.W., 1992, The Lance Formation; petrography and stratigraphy, Powder River basin and nearby basins, Wyoming and Montana: U. S. Geological Survey Bulletin B 1917-I, 17 p.

Cross, T.A., and Lessenger, M.A., 1998, Sediment volume partitioning: rationale for stratigraphic model evaluation and high-resolution stratigraphic correlation, *in* Gradstein, F., Sandvik, K., and Milton, N., eds., Sequence stratigraphy: Concepts and applications: Norwegian Petroleum Society Special Publication 8, p. 171-195.

Cummings, D.I., Arnott, R.W.C., and Hart, B.S., 2006, Tidal signatures in a shelf-margin delta: Geology, v. 34, p. 249-252.

Dalrymple, R.W., Zaitlin, B.A., and Boyd, R., 1992, Estuarine facies models: conceptual basis and stratigraphic implications: Journal of Sedimentary Petrology, p. 1130-1146.

Damuth, J.E., Flood, R.D., Kowsmann, R.O., Belderson, R.H., and Gorini, M.A., 1988, Anatomy and growth pattern of Amazon deep-sea fan as revealed by long-range side-scan sonar (GLORIA) and high-resolution seismic studies: American Association of Petroleum Geologists Bulletin, v. 72, p. 885-911.

DeCelles, P.G., 1994, Late Cretaceous-Paleocene synorogenic sedimentation and kinematic histroy of the Sevier thurst belt, northeast Utah and southwest Wyoming: Geological Society of America Bulletin, v. 106, p. 32-56.

—, 2004, Late Jurassic to Eocene Evolution of the Cordilleran Thrust Belt and Foreland Basin System, Western U.S.A.: American Journal of Science, v. 304, p. 105-168.

Dettman, D.L., and Lohmann, K.C., 2000, Oxygen isotope evidence for high-altitude snow in the Laramide Rocky Mountains of North America during the Late Cretaceous and Paleogene: Geology, v. 28, p. 243-246.

Di Croce, J., Bally, A.W., and Vail, P., 1999, Sequence stratigraphy of the eastern Venezuelan Basin, *in* Mann, P., ed., Sedimentary Basins of the World: Elsevier 4, p. 419-476.

Dickinson, W.R., Klute, M.A., Hayes, M.J., Janecke, S.U., Lundin, E.R., McKittrick, M.A., and Olivares, M.D., 1988, Paleogeographic and paleotectonic setting of Laramide sedimentary basins in the central Rocky Mountain region: Geological Society of America Bulletin, p. 1023-1039.

Dumas, S., and Arnott, R.W.C., 2006, Origin of hummocky and swaley cross-stratification--The controlling influence of unidirectional current strength and aggradation rate: Geology, v. 34, p. 1073-1076.
Erskine, R.D., and Vail, P.R., 1988, Seismic stratigraphy of the Exmouth Plateau, *in* Bally, A.W., ed., Atlas of seismic stratigraphy.: American Association of Petroleum Geologists AAPG Studies in Geology 27, Vol. 2, p. 163-173.
Feng, J., 1995, Post mid-Cretaceous seismic stratigraphy and depositional history, deep Gulf of Mexico: Austin, TX United States, PhD dissertation, The University of Texas at Austin.
Flemings, P.B., Jordan, T.E., and Reynolds, S., 1986, Flexural analysis of two broken foreland basins; late Cenozoic Bermejo Basin and early Cenozoic Green River basin (Abstract): AAPG Bulletin, v. 70, p. 591.
Flood, R.D., and Piper, D.J.W., 1997, Amazon Fan sedimentation; the relationship to equatorial climate change, continental denudation, and sea-level fluctuations: Proceedings of the Ocean Drilling Program, Scientific Results, v. 155, p. 653-675.
Frey, R.W., and Pemberton, G.S., 1984, Trace fossil facies models, *in* Walker, R.G., ed., Volume Facies Models: Geoscience Canada, Reprint Series, Geological Association of Canada, p. 189-207.
Galloway, W.E., 1975, Process framework for describing the morphologic and stratigraphic evolution of deltaic depositional systems, *in* Broussard, M.L., ed., Deltas, Models for Exploration, Houston Geological Society, Houston, p. 87-98.
—, 1989, Genetic stratigraphic sequences in basin analysis; I, Architecture and genesis of flooding-surface bounded depositional units: American Association of Petroleum Geologists Bulletin, v. 73, p. 125-142.
—, 1998, Siliciclastic Slope and Base-of-Slope Depositional Systems: Component Facies, Stratigraphic Architecture and Classification: American Association of Petroleum Geologists Bulletin, v. 82, p. 569-595.
—, 2001, Cenozoic evolution of sediment accumulation in deltaic and shore-zone depositional systems, northern Gulf of Mexico Basin: Marine and Petroleum Geology, v. 18, p. 1031-1040.
Galloway, W.E., Dingus, W.F., and Paige, R.E., 1991, Seismic and depositional facies of Paleocene-Eocene Wilcox Group submarine canyon fills, Northwest Gulf Coast, U.S.A, *in* Weimer, P., and Link, M.H., eds., Seismic facies and sedimentary processes of submarine fans and turbidite systems: New York, NY, US, Springer-Verlag, p. 247-271.
Galloway, W.E., Ganey-Curry, P.E., Xiang, L., and Buffler, R.T., 2000, Cenozoic depositional history of the Gulf of Mexico basin: American Association of Petroleum Geologists Bulletin, v. 84, p. 1743-1774.
Galloway, W.E., and Hobbay, D.K., 1996, Terrigenous Clastic Depositional Systems, Springer International : Berlin, Federal Republic of Germany, 489 p.
Galloway, W.E., and Williams, T.A., 1991, Sediment accumulation rates in time and space: Paleogene genetic stratigraphic sequences of the northwestern Gulf of Mexico basin: Geology, v. 19, p. 986-989.

Gill, J.R., and Cobban, W.A., 1973, Stratigraphy and geologic history of the Montana Group and equivalent rocks, Montana, Wyoming, and North and South Dakota: U. S. Geological Survey Professional Paper P 0776, 37 p.
Gill, J.R., Merewether, E.A., and Cobban, W.A., 1970, Stratigraphy and nomenclature of some Upper Cretaceous and lower Tertiary rocks in south-central Wyoming: U. S. Geological Survey Professional Paper 667, 53 p.
Giosan, L., and Bhattacharya, J.P., 2005, New directions in deltaic studies, *in* Giosan, L., and Bhattacharya, J.P., eds., River Deltas-Concepts, Models and Examples: Special Publication 83: Tulsa, OK United States, Society for Sedimentary Geology (SEPM), p. 3-10.
Greenlee, S.M., Devlin, W.J., Miller, K.G., Mountain, G.S., and Flemings, P.B., 1992, Integrated sequence stratigraphy of Neogene deposits, New Jersey continental shelf and slope: Comparison with the Exxon model: Geological Society of America Bulletin, v. 104, p. 1403-1411.
Hagen, E.S., Shuster, M.W., and Furlong, K.P., 1985, Tectonic loading and subsidence of intermontane basins; Wyoming foreland province: Geology, v. 13, p. 585-588.
Hanson, W.B., Vega, V., and Cox, D., 2004, Structural geology, seismic imaging and genesis of the giant Jonah Gas Field, Wyoming, USA, *in* Robinson, J.W., and Shanley, K.W., eds., Jonah Field: Case Study of a Thight-Gas Fluvial Reservoir: AAPG Studies in Geology 52, p. 21-35.
Harms, J.C., Southard, J.B., and Walker, R.G., 1982, Structures and Sequences in Clastic Rocks: Short Course, Society of Economic Paleontologists and Mineralogists, p.??
Hedberg, H.D., 1970, Continental margins from viewpoint of the petroleum geologist: American Association of Petroleum Geologists Bulletin, v. 54, p. 3-43.
Heller, P.L., Angevine, C.L., Winslow, N., S., and Paola, C., 1988, Two-Phase Stratigraphic Model of Foreland-Basin Sequences: Geology, v. 16, p. 501-504.
Hettinger, R.D., and Roberts, L.N.R., 2005, Lewis total petroleum system of the Southwestern Wyoming Province, Wyoming, Colorado, and Utah: U. S. Geological Survey Digital Data Series: Petroleum systems and geologic assessment of oil and gas in the Southwestern Wyoming Province, Wyoming, Colorado, and Utah Report # DDS-0069-D, 39 p.
Hovius, N., 1998, Controls on sediment supply by large rivers, *in* Shanley, K.W., and McCabe, P.J., eds., Relative role of eustasy, climate and tectonism in continental rocks: SEPM Special Publication 59, p. 3-16.
Hunt, D., and Tucker, M.E., 1992, Stranded parasequences and the forced regressive wedge systems tract; deposition during base-level fall: Sedimentary Geology, v. 81, p. 1-9.
Ito, M., and Masuda, F., 1988, Late Cenozoic deep-sea to fan-delta sedimentation in an arc-arc collision zone, central Honshu, Japan; sedimentary response to varying plate-tectonic regime, *in* Nemec, W., and Steel, R.J., eds., Fan deltas; sedimentology and tectonic settings: Glasgow, United Kingdom, Blackie and Son, p. 400-418.
Johannessen, E.P., and Steel, R.J., 2005, Clinoforms and their exploration significance for deepwater sands: Basin Research, v. 17, p. 521-550.

Johnson, R.C., Finn, T.M., and Roberts, S.B., 2004, Regional stratigraphic setting of the Maastrichtian rocks in the Central Rocky Mountain region, *in* Robinson, J.W., and Shanley, K.W., eds., Jonah Field; case study of a tight-gas fluvial reservoir: American Association of Petroleum Geologists : Tulsa, OK, United States AAPG Studies in Geology 52, p. 21.

Jordan, T.E., 1981, Thrust loads and foreland basin evolution, Cretaceous, western United States: AAPG Bulletin, v. 65, p. 2506-2520.

Kauffman, E.G., Sageman, B.B., Kirkland, J.I., Elder, W.P., Harries, P.J., and Villamil, T., 1993, Molluscan biostratigraphy of the Cretaceous Western Interior Basin, North America, *in* Caldwell, W.G.E., and Kauffman, E.G., eds., Evolution of the Western Interior Basin: Geological Association of Canada Special Paper 39, p. 397-424.

Kneller, B.C., and Buckee, C., 2000, The structure and fuild mechanics of turbidity currents: a review of some recent studies and their geological implications: Sedimentology, v. 47, p. 62-94.

Kolla, V., and Perlmutter, M.A., 1993, Timing of turbidite sedimentation on the Mississippi Fan: AAPG Bulletin, v. 77, p. 1129-1141.

Koopman, A., and Schreurs, J., 1996, Onshore lithostratigraphy, *in* Sandal, S.T., ed., The geology and hydrocarbon resources of Negara Brunei Darussalam: Brunei Darussalam, Brunei Shell, p. 97-102.

Land, C.B., Jr., 1972, Stratigraphy of Fox Hills Sandstone and associated formations, Rock Springs Uplift and Wamsutter Arch Area, Sweetwater County, Wyoming; a shoreline-estuary sandstone model for the late Cretaceous: Quarterly of the Colorado School of Mines, v. 67, p. 1-69.

Liu, X., and Galloway, W.E., 1993, Sediment accumulation rate: problems and new approach, *in* Armentrout, J.M., Bloch, R.B., Olson, H.C., and Perkins, B.F., eds., Rates of geological processes-tectonics, sedimentation, eustasy and climate, implications of hydrocarbon exploration: Proceedings of the Fourteenth Annual Research Conference, Gulf Coast Section SEPM, p. 101-107.

—, 1997, Quantitative Determination of Tertiary Sediment Supply to the North Sea Basin: American Association of Petroleum Geologists Bulletin, v. 81, p. 1482-1509.

Love, J.D., and Christiansen, A.C., 1985, Geologic Map of Wyoming: U.S. Geological Survey (in cooperation with The Geological Survery of Wyoming, Laramie), Reston, Virginia, United States, scale 1: 500,000, 3 sheets.

Lu, H., Fulthorpe, C.S., and Mann, P., 2003, Three-dimensional architecture of shelf-building sediment drifts in the offshore Canterbury Basin, New Zealand: Marine Geology, v. 193, p. 19-57.

MacEachern, J.A., Bann, K.L., Bhattacharya, J.P., and Howell, C.D.J., 2005, Ichnology of deltas: Organism responses to the dynamic interplay of rivers, waves, storms, and tides, *in* Bhattacharya, J.P., and Giosan, L., eds., River Deltas-Concepts, Models, and Examples: SEPM Society for Sedimentary Geology Special Publication 83, p. 49-85.

MacLeod, M.K., 1981, The Pacific Creek Anticline; buckling above a basement thrust fault: Contributions to Geology (University of Wyoming), v. 19, p. 143-160.

McMillen, K.M., 1991, Seismic stratigraphy of Lower Cretaceous foreland basin submarine fans in the North Slope, Alaska, *in* Weimer, P., and Link, M.H., eds., Seismic facies and sedimentary processes of submarine fans and turbidite systems: New York, United States, Springer-Verlag, p. 289-302.

McMillen, K.M., and Winn, R.D., Jr., 1991, Seismic facies of shelf, slope,and submarine fan environments of the Lewis Shale, Upper Cretaceous, Wyoming, *in* Weimer, P., and Link, M.H., eds., Seismic facies and sedimentary processes of submarine fans and turbidite systems: New York, United States, Springer-Verlag, p. 273-287.

Mellere, D., Plink-Bjorklund, P., and Steel, R., 2002, Anatomy of shelf deltas at the edge of a prograding Eocene shelf margin, Spitsbergen: Sedimentology, v. 49, p. 1181-1206.

Michels, K.H., Suckow, A., Breitzke, M., Kudrass, H.R., and Kottke, 2003, Sediment transport in the shelf canyon "Swatch of No Ground" (Bay of Bengal): Deep-Sea Research. Part II: Topical Studies in Oceanography, v. 50, p. 1003-1022.

Miller, K.G., Barrera, E., Olsson, R.K., Sugarman, P.J., and Savin, S.M., 1999, Does ice drive early Maastrichtian eustasy?: Geology, v. 27, p. 783-786.

Miller, K.G., Sugarman, P.J., Browning, J.V., Kominz, M.A., Olsson, R.K., Feigenson, M.D., and Hernandez, J.C., 2004, Upper Cretaceous sequences and sea-level history, New Jersey coastal plain: Geological Society of America Bulletin, v. 116, p. 368-393.

Miller, K.G., Wright, J.D., and Browning, J.V., 2005, Visions of ice sheets in a greenhouse world: Marine Geology, v. 217, p. 215-231.

Milliman, J.D., and Meade, R.H., 1983, World-wide delivery of river sediment to the oceans: Journal of Geology, v. 91, p. 1-21.

Milliman, J.D., and Syvitski, J.P.M., 1992, Geomorphic/tectonic control of sediment discharge to the ocean: the importance of small mountainous rivers: The Journal of Geology, v. 100, p. 525-544.

Moscardelli, L., Wood, L., and Mann, P., 2006, Mass-trasnport complexes and associated porcesses in the offshore area of Trinidad and Venezuela: American Association of Petroleum Geologists Bulletin, v. 90, p. 1059-1088.

Mulder, T., and Syvitski, J.P.M., 1996, Climatic and morphologic relationships of rivers; implications of sea-level fluctuations on river loads: Journal of Geology, v. 104, p. 509-523.

Mulder, T., Syvitski, J.P.M., Migeon, S., Faugeres, J.-C., and Savoye, B., 2003, Marine hyperpycnal flows; initiation, behavior and related deposits; a review: Marine and Petroleum Geology, v. 20, p. 861-882.

Muto, T., and Steel, R.J., 2002, In defense of shelf-edge delta development during falling and lowstand of relative sea level: Journal of Geology, v. 110, p. 421-436.

Mutti, E., 1985, Turbidite systems and their relations to depositional sequences, *in* Zuffa, G.G., ed., Provenance of arenites: NATO ASI Series. Series C: Mathematical and Physical Sciences 148, D. Reidel Publishing Company, Dordrecht-Boston, p. 65-93.

Nio, S.-D., and Yang, C.-S., 1991, Diagnostic attributes of clastic tidal deposits: a review, *in* Smith, D.G., Reinson, G.E., Zaitlin, B.A., and Rahmani, R.A., eds., Volume

Clastic Tidal Sedimentology: Memoir, Canadian Society of Petroleum Geologists, p. 3-28.
Normark, W.R., Piper, D.J.W., and Hiscott, R.N., 1998, Sea level controls on the textural characteristics and depositional architecture of the Hueneme and associated submarine fan systems, Santa Monica Basin, California: Sedimentology, v. 45, p. 53-70.
Paola, C., 2000, Quantitative models of sedimentary basin infilling: Sedimentology, v. 47, p. 121-178.
Perman, R., Chambers, 1990, Depositional history of the Maastrichtian Lewis Shale in south-central Wyoming: deltaic and interdeltaic, marginal marine through deep-water marine, environments: The American Association of Petroleum Geologists Bulletin, p. 1695-1717.
Petter, A., and Steel, R.J., 2006, Hyperpycnal flow variability and slope organization on an Eocene shelf margin, Central Basin, Spitsbergen: AAPG Bulletin, p. in press.
Pinet, P., and Souriau, M., 1988, Continental erosion and large-scale relief: Tectonics, v. 7, p. 563-582.
Pinous, O.V., Karogodin, Y.N., Ershov, S.V., and Sahagian, D.L., 1999, Sequence stratigraphy, facies and sea level change of the Hauterivian productive complex, Priobskoe Oil Field (West Siberia): American Association of Petroleum Geologists Bulletin, v. 83, p. 972-989.
Pinous, O.V., Levchuk, M.A., and Sahagian, D.L., 2001, Regional synthesis of the productive Neocomian complex of West Siberia; sequence stratigraphic framework: AAPG Bulletin, v. 85, p. 1713-1730.
Piper, D.J.W., and Normark, W.R., 2001, Sandy fans; from Amazon to Hueneme and beyond: AAPG Bulletin, v. 85, p. 1407-1438.
Pirmez, C., Pratsen, L.F., and Steckler, M.S., 1998, Clinoform development by advective diffusion of suspended sediment: modelling and comparison to natural systems: Journal of Geophysical Research, p. 24,141-24,157.
Plink-Björklund, P., Mellere, D., and Steel, R.J., 2001, Turbidite variability and architecture of sand-prone, deep-water slopes: Eocene clinoforms in the Central Basin, Spitsbergen: Journal of Sedimentary Research, p. 895-912.
Plink-Björklund, P., and Steel, R.J., 2002, Sea-level fall below the shelf edge without basin-floor fans: Geology, p. 115-118.
—, 2004, Initiation of turbidity currents; outcrop evidence for Eocene hyperpycnal flow turbidites: Sedimentary Geology, v. 165, p. 29-52.
—, 2005, Deltas on falling-stage and lowstand shelf marigns, the Eocene Central Basin of Spitsbergen: Importance of sediment supply, *in* Giosan, L., and Bhattacharya, J.P., eds., River Deltas-Concepts, Models and Examples: Society for Sedimentary Geology (SEPM) Special Publication 83, p. 179-206.
Porębski, S.J., and Steel, R.J., 2003, Shelf-margin deltas; their stratigraphic significance and relation to deepwater sands: Earth-Science Reviews, v. 62, p. 283-326.
—, 2006, Deltas and sea-level change: Journal of Sedimentary Research, v. 76, p. 390-403.
Posamentier, H.W., and Allen, G.P., 1999, Siliciclastic Sequence Stratigraphy - Concepts and Applications, *in* Dalrymple, R.W., ed., Concepts in Sedimentology and

Paleontology, Volume 7: Tulsa, Oklahoma, United States, SEPM (Society for Sedimentary Geology), p. 204.
Posamentier, H.W., Jervey, M.T., and Vail, P.R., 1988, Eustatic controls on clastic deposition; I, Conceptual framework, *in* Wilgus, C.K., Hastings, B.S., Ross, C.A., Posamentier, H.W., Van Wagoner, J., and Kendall, C.G.S.C., eds., Sea-level changes; an integrated approach: Society for Sedimentary Geology (SEPM) Special Publication 42, p. 109-124.
Posamentier, H.W., and Vail, P.R., 1988, Eustatic controls on clastic deposition; II, Sequence and systems tract models, *in* Wilgus, C.K., Hastings, B.S., Ross, C.A., Posamentier, H.W., Van Wagoner, J., and Kendall, C.G.S.C., eds., Sea-level changes; an integrated approach: Society for Sedimentary Geology (SEPM) Special Publication 42, p. 125-154.
Poulsen, C.J., Flemings, P.B., Robinson, R.A.J., and Metzger, J.M., 1998, Three-dimensional stratigraphic evolution of the Miocene Baltimore Canyon region: Implications for eustatic interpretations and the systems tract model: Geological Society of America Bulletin, v. 110, p. 1105-1122.
Pyles, D., and Slatt, R., 2000, A high-frequency sequence stratigraphic framework for shallow through deep-water deposits of the Lewis Shale and Fox Hills Sandstone, Great Divide and Washakie basins, Wyoming, *in* Weimer, P., Slatt, R.M., Coleman, J., Rosen, N.C., Bouma, H.C., Styzen, M.J., and Lawrence, D.T., eds., Deep-water Reservoirs of the World (CD-ROM): Gulf Coast Section Society for Sedimentary Geology (GCSSEPM) 20th Annual Research Conference (Houston), p. 836-861.
Pyles, D., and Slatt, R.M., 2002, Almond, Lewis, Fox Hills and Lance Systems in the Greater Green River Basin Wyoming, *in* Steel, R.J., Crabaugh, J., Carvajal, C., Slatt, R.M., Pyles, D., and Olson, M., eds., Introduction to the Lance, Fox Hills, and Lewis Formations on the eastern margin of the Great Divide and Washakie basins: Rocky Mountain Section American Association of Petroleum Geologists (RMS-AAPG) Annual Meeting (Laramie), Fieldtrip #1 Guidebook, p. 1-46.
Reynolds, M.W., 1976, Influence of recurrent Laramide structural growth on sedimentation and petroleum accumulation, Lost Soldier area, Wyoming: AAPG Bulletin, v. 60, p. 12-33.
Rich, J.L., 1951, Three critical environments of deposition and criteria for recognition of rocks deposited in each of them: Geological Society of America Bulletin, v. 62, p. 1-20.
Ross, C.A., Halliwell, B.A., May, J.A., Watts, D.E., and Syvitski, J.P.M., 1994, Slope Readjustment: A new model for the development of submarine fans and aprons: Geology, v. 22, p. 511-514.
Ross, W.C., Watts, D.E., and May, J.A., 1995, Insights from stratigraphic modeling; mud-limited versus sand-limited depositional systems: AAPG Bulletin, v. 79, p. 231-258.
Saller, A., and Blake, G., 2003, Sequence stratigraphy and syndepositional tectonics of Upper Miocene and Pliocene deltaic sediments, offshore Brunei Darussalam, *in* Sidi, F.H., Nummedal, D., Imbert, P., Darman, H., and Posamentier, H.W., eds., Tropical deltas of Southeast Asia; sedimentology, stratigraphy, and petroleum

geology: Society for Sedimentary Geology (SEPM) Special Publication 76, p. 219-234.
Schlager, W., 1993, Accommodation and supply -a dual control on stratigraphic sequences: Sedimentary Geology, v. 86, p. 111-136.
Shuster, M.W., and Steidtmann, J.R., 1988, Tectonic and sedimentary evolution of the northern Green River basin, western Wyoming, *in* J., C., and Perry, W.J., Jr. , eds., Interaction of the Rocky Mountain Foreland and the Cordilleran thrust belt: Geological Society of America (GSA) Memoir 171, p. 515.
Steel, R.J., Carvajal, C., Petter, A., and Uroza, C., in review, The Growth of Shelves and Shelf Margins, SEPM Special Publication.
Steidtmann, J.R., 1993, The Cretaceous foreland basin and its sedimentary record, *in* Snoke, A.W., Steidtmann, J.R., and Roberts, S.M., eds., Volume Geology of Wyoming: Memoir, Geological Survey of Wyoming, p. 250-271.
Steidtmann, J.R., and Middleton, L.T., 1991, Fault chronology and uplift history of the southern Wind River Range, Wyoming; implications for Laramide and post-Laramide deformation in the Rocky Mountain foreland: Geological Society of America Bulletin, v. 103, p. 472-485.
Swift, D.J.P., and Thorne, J.A., 1991, Sedimentation on continental margins, 1: a general model for shelf sedimentation, *in* Swift, D.J.P., Oertel, G.F., Tillman, R.W., and Thorne, J.A., eds., Volume Shelf Sand and Sandstone Bodies; Geometry, Facies and Sequence Stratigraphy: Special Publication, International Association of Sedimentologists, p. 3-31.
Sydow, J., Finneran, J., and Bowman, A.P., 2003, Stacked shelf-edge delta reservoirs of the Columbus Basin, Trinidad, West Indies, *in* Roberts, H.H., Rosen, N.C., Fillon, R.H., and Anderson, J.B., eds., Shelf margin deltas and linked down slope petroleum systems (CD-ROM): Gulf Coast Section Society for Sedimentary Geology (GCSSEPM) 23rd Annual Research Conference (Houston), p. 441-465.
Syvitski, J.P.M., Peckham, S.D., Hilberman, R., and Mulder, T., 2003, Predicting the terrestrial flux of sediment to the global ocean; a planetary perspective: Sedimentary Geology, v. 162, p. 5-24.
Syvitski, J.P.M., Weaver, S.B., Nittrouer, C.A., Trincardi, F., and Canals, M., 2004, Strate formation on European Margins: Oceanography, v. 17, p. 14-15.
Torres, J., Droz, L., Savoye, B., Terentieva, E., Cochonat, P., Kenyon, N.H., and Canals, M., 1997, Deep-sea avulsion and morphosedimentary evolution of the Rhone fan valley and neofan during the late Quaternary (north-western Mediterranean Sea): Sedimentology, v. 44, p. 457-477.
Upchurch, G.R., Jr., and Wolfe, J.A., 1993, Cretaceous vegetation of the Western Interior and adjacent regions of North America, *in* Caldwell, W.G.E., and Kauffman, E.G., eds., Evolution of the Western Interior Basin: Geological Association of Canada : Toronto, ON, Canada Special Paper 39, p. 243-281.
Vail, P.R., Hardenbol, J., and Todd, R.G., 1984, Jurassic unconformities, chronostratigraphy, and sea-evel changes from seismic stratigraphy, *in* Schlee, J.S., ed., Volume Inter-Regional Unconformities and Hydrocarbon Exploration: Memoir, American Association of Petroleum Geologists, p. 129-144.

Vail, P.R., Mitchum, R.M., Jr., and Thompson, S., III, 1977, Seismic stratigraphy and global changes of sea level; Part 3, Relative changes of sea level from coastal onlap, *in* Payton, C.E., ed., Seismic stratigraphy; applications to hydrocarbon exploration: American Association of Petroleum Geologists Memoir 26, p. 63-31.

Van Horn, M.D., and Shannon, L.T., 1989, Hay reservoir field; a submarine fan gas reservoir within the Lewis Shale, Sweetwater County, Wyoming, *in* Eisert, J.L., ed., Gas resources of Wyoming: Wyoming Geological Association Guidebook 40, p. 155-180.

Van Wagoner, J.C., Mitchum, R.M., Campion, K.M., and Rahmanian, V.D., 1990, Siliciclastic Sequence Stratigraphy in Well Logs, Cores, and Outcrops: Methods in Exploration Series, American Association of Petroleum Geologists, p. 55.

Walker, R.G., 1984, Shelf and shallow marine sands, *in* Walker, R.G., ed., Volume Facies Models: Geoscience Canada Reprint Series, Geological Association of Canada, p. 141-169.

Weber, M.E., Wiedicke, M.H., Kudrass, H.R., Huebscher, C., and Erlenkeuser, H., 1997, Active growth of the Bengal Fan during sea-level rise and highstand: Geology, v. 25, p. 315-318.

Weimer, R.J., 1961a, Spatial dimensions of Upper Cretaceous Sandstones, Rocky Mountain Area.

—, 1961b, Uppermost Cretaceous rocks in central and southern Wyoming, and northwest Colorado, *in* Wiloth, G.J., ed., Volume Symposium on Late Cretaceous rocks: Annual Field Conference Guidebook, Wyoming Geological Association, p. 17-28.

Willis, J.J., and Brown, W.G., 1993, Structural interpretations of the Rocky Mountain foreland; past, present, and future, *in* Stroock, B., and Andrew, S., eds., Wyoming Geological Association jubilee anniversary field conference: Wyoming Geological Association Guidebook 44, p. 95-120.

Winn, R., D., Jr., Bishop, M., G., and Gardener, P., S., 1985, Lewis Shale, south-sentral Wyoming: shelf, delta front, and turbidite sedimentation, *in* Nelson, G., E., ed., Volume The Cretaceous Geology of Wyoming: Annual Field Conference Guidebook, Wyoming Geological Association, p. 113-130.

Winn, R.D., Jr., Bishop, M.G., and Gardner, P.S., 1987, Shallow-water and sub-storm-base deposition of Lewis Shale in Cretaceous Western Interior seaway, south-central Wyoming: American Association of Petroleum Geologists Bulletin, v. 71, p. 859-881.

Wolfe, J.A., and Upchurch, G.R., Jr., 1987, North American nonmarine climates and vegetation during the Late Cretaceous: Palaeogeography, Palaeoclimatology, Palaeoecology, v. 61, p. 33-77.

Wood, L., 2000, Chronostratigraphy and tectnostratigraphy of the Columbus Basin, eastern offshore Trinidad: American Association of Petroleum Geologists Bulletin, v. 84, p. 1905-1928.

Wu, X., and Galloway, W.E., 2002, Upper Miocene depositional history of the central Gulf of Mexico Basin, *in* Dutton, S.P., Ruppel, S.C., and Hentz, T.F.e., eds., Transactions - Gulf Coast Association of Geological Societies, Volume 52: Austin, TX United States, Gulf Coast Association of Geological Societies, p. 1019-1030.

Yoshida, S., Steel, R. J., and Dalrymple, R. W., 2007 (in press), Changes in depositional processes -an ingredient in a new generation of sequence-stratigraphic models: Journal of Sedimentary Research, vol. 77, DOI: 10.2110/jsr.2007.048.

VITA

Cristian Carvajal was born in 1971, in the town of Curicó, Chile, as the first son of Carlos Gilberto Carvajal Amaya and Delfina del Carmen Gamboa Jofre. Cristian attended Elementary School at the Escuela E-21 in Curicó and High School in the Liceos of Curicó and San Bernardo. Cristian went on to study Geology at the Universidad de Chile where he was awarded the Geologist degree with a maximum distinction. After some time working as an ore deposits explorationist in the Andes Mountains, Cristian went back to college to obtain a Masters Degree at Loma Linda University in California, where he investigated the Sedimentology and Stratigraphy of shallow water deposits in coastal Perú. Upon completion of this degree he moved to the University of Wyoming to begin studies toward a Ph.D., completed at the University of Texas at Austin.

Permanent address: 7777 Greenbriar St. Apt. 2063, Houston TX 77030.

This dissertation was typed by Cristian Carvajal.